THE EFFECTS OF MECHANICAL STRETCH ON VASCULAR CELLS *IN VITRO* : STUDIES OF GROWTH AND PROTO-ONCOGENE EXPRESSION USING A NEW CELL-STRETCHING APPARATUS.

by

Maureen Rose Deehan

A thesis submitted to the University of Glasgow for the degree of Doctor of Philosophy

Faculty of Medicine, University of Glasgow

Department of Medicine & Therapeutics,
Gardiner Institute,
Western Infirmary,
Glasgow G11 6NT.

Submitted July 1994

ProQuest LLC.
789 East Eisenhower Parkway
P.O. Box 1346
Ann Arbor, MI 48106 – 1346

TABLE OF CONTENTS

LIST OF FIGURES

LIST OF PHOTOGRAPHIC PLATES

ACKNOWLEDGEMENTS

Special thanks to my supervisor Dr. Fiona Lyall for her encouragement and source of ideas throughout the project and to Fiona Boswell for her invaluable technical assistance. I am also very grateful to William Brown for his important role in the design of the stretching apparatus, Alec Smith from the Department of Physiology, University of Glasgow and Tom Neil and his staff from the Department of Physics & Astronomy, University of Glasgow for their involvement in the construction of the cell stretching systems. Much time and effort was contributed by Dr. R. Fraser who proof read the thesis, for this I am extremely grateful. Thanks also to Dr. J. A. T. Dow , Department of Cell Biology, University of Glasgow, for his advice in the initial design of the system and for his photography skills.

While working in the MRC Blood Pressure Unit the staff showed me considerable help and kindness, I would like to thank them for this. I especially wish to express my thanks to Professor A.F. Lever for making the facilities of the unit available to me.

My thanks also to Dr Gordon McInnes and Dr. Dai Davies from the Department of Medicine and Therapeutics, for their support and financial contributions to the project. I am also grateful to the Greater Glasgow Health board who provided additional funding for the project.

I wish also to express my thanks to the following persons for their assistance in various aspects of this project:
Ian Ramsden and his staff from the Department of Medical Illustration, University of Glasgow, for their excellent illustrations. Dr. S. Chettibi, Department of Cell Biology, University of Glasgow for his help in cell measurements and photography. Kate Howie, Department of Medicine and Therapeutics, University of Glasgow, for her statistical advice. Professor Ian A. Greer for making the facilities of the Department of Obstetrics & Gynaecology, Royal Infirmary, available for part of the experimental work of this thesis.

Sincere thanks to my parents, brothers and sister who have been a vital source of support and understanding throughout my studies. Finally, extra special thanks to my husband Joe who provided me with the necessary faith and encouragement which I required in the writing of this thesis.

SUMMARY

Vascular hypertrophy has been identified as an important process in the development of essential hypertension. At present, the nature by which hemodynamic forces contribute to this process is poorly understood. To address the role of a hemodynamic component, the effect of a stretching force on vascular smooth muscle and endothelial cell function, was investigated.

This project involved the development of an *in vitro* cell stretching system which satisfied the essential criteria of a sterile, cell culture system. An initial proto-type was developed which vertically displaced cells grown on flexible membranes, by means of a vacuum. The surface area of the base of the dish was increased in response to suction and hence the cells attached to the base of the dish stretched. A non-uniform stretch of limited range was achieved using this system.

The second proto-type developed involved growing cells on silicone sheeting, mounted on a frame. Cells attached to the sheeting were stretched by increasing the length of the silicone. Due to the design of the system a fixed stretch within the range of 0-20% was achieved.

20% stretch stimulated *c-fos* mRNA expression and increased phosphoinositide turnover, in vsmc. However, 20% stretch did not induce *c-jun* or *c-myc* mRNA expression in vsmc. Mechanical stretch increased vsmc growth, although did not reach statistical significance. Endothelial cell studies showed that *c-fos* and *c-jun* mRNA expression was increased in response to 20% stretch.

The results of these studies suggest that mechanical stretch may be an important stimulus, for the activation of signalling mechanisms, involved in vascular smooth muscle and endothelial cell growth. Therefore, such a force may play an important role in the development of vascular hypertrophy.

ABBREVIATIONS

ACTH	adrenocorticotrophic hormone
ANG I	angiotensin I
ANG II	angiotensin II
ACE	angiotensin converting enzyme
AC	adenylate cyclase
ACA	adenylate cyclase activity
AlF^{4-}	aluminium fluoride
ADP	adenosine diphosphate
ADPase	adenosine diphosphatase
ANP	atrial natriuretic peptide
ATP	adenosine triphosphate
ATPase	adenosine triphosphatase
AVP	vasopressin
Ca^{2+}	calcium ion(s)
$[Ca^{2+}]$	calcium ion concentration
$[Ca^{2+}]_i$	intracellular calcium ion concentration
CAT	chloramphenicol acetyltransferase
CO	cardiac output
Cl^-	chloride ion(s)
cAMP	adenosine 3', 5'-cyclic monophosphate
cDNA	complementary DNA
cGMP	guanosine 3', 5'-cyclic monophosphate
CO_2	carbon dioxide
$[CO_2]$	carbon dioxide concentration
CTP	deoxy (5-^{3}H) cytidine 5'-triphosphate ammonium salt
dATP	deoxy adenosine triphosphate

dGTP	deoxy guanosine triphosphate
dTTP	deoxy thymidine triphosphate
DAG	diacylglycerol
ddH_2O	deionised distilled water
dH_2O	distilled water
DBP	diastolic blood pressure
DMEM	Dulbecco's modified Eagle medium
DNA	deoxyribonucleic acid
ECM	extracellular matrix
EDTA	diaminoethanetetra-acetic acid-disodium salt
EGF	epidermal growth factor
FCS	foetal calf serum
FGF	fibroblast growth factor
Fos	*c-fos* protein
GDP	guanosine diphosphate
G protein	guanine nucleotide-binding protein
GTP	guanosine triphosphate
$[^3H]$	tritiated
HBG	Hanks' balanced salt solution with bovine serum albumin and glucose
HBSS	Hanks' balanced salt solution
HBGF	heparin binding growth factor
HDL	high density lipoprotein
HS	horse serum
IBMX	3-isobutyl-1-methylxanthine
IGF	insulin like growth factor
IGF-I	insulin like growth factor I
IGF-II	insulin like growth factor II

IL	interleukin
IP	inositol monophosphate
IP_2	inositol diphosphate
IP_3	inositol 1, 4, 5 trisphosphate
IP_4	inositol tetraphosphate
Jun	*c-jun* protein
LDL	low density lipoprotein
LVH	left ventricular hypertrophy
MOPS	2-[N-Morpholino] ethane-sulphonic acid
MPF	mitosis phase promoting factor
mRNA	messenger ribonucleic acid
Na^+	sodium ion(s)
NO	nitric oxide
PAI-1	plasminogen activator inhibitor-1
PBS	phosphate buffered saline
PC	phosphatidyl choline
PDGF	platelet derived growth factor
K^+	potassium ion(s)
PGE_2	prostaglandin E_2
PGI_2	prostacyclin
PIP_2	phosphatidyl inositol 4,5 bisphosphate
PKC	protein kinase C
PLC	phospholipase C
PLD	phospholipase D
PS	phosphatidyl serine
PTHrP	parathyroid hormone related protein
PVE	premature ventricular excitation
RAS	renin angiotensin system
RNA	ribonucleic acid

SBP	systolic blood pressure
SHR	spontaneously hypertensive rat
smc	smooth muscle cell(s)
SSC	sodium saline citrate
TE	Tris/EDTA electrophoresis buffer
TGF β	transforming growth factor β
tPA	tissue plasminogen activator
TPR	total peripheral resistance
TRE	12-O-tetradecanoylphorbol-13-acetate response element
VLDL	very low density lipoprotein
vsmc	vascular smooth muscle cell(s)
WKY	Wistar-Kyoto

CHAPTER ONE

INTRODUCTION

1.1 Blood pressure and hypertension

1.1.1 Blood pressure

Blood circulates under pressure in a closed vascular system. This pressure is the resultant of cardiac output (CO) and the total peripheral resistance (TPR). CO is expressed as the volume of blood ejected from the left ventricle per minute. TPR takes into account the phasic changes in pressure during the cardiac cycle in relation to the elasticity and geometry of the large arteries, the inertial and viscous properties of the blood and the resistance to flow posed by small muscular arteries and arterioles.

The pressure within the vessels when the heart rythmically contracts is termed systolic blood pressure (SBP) and diastolic blood pressure (DBP) that which exists during the relaxation period. A normal range of values for systolic and diastolic pressures are 110-130/65-80 mmHg (i.e systolic/diastolic).

Blood pressure is regulated by many factors of neural, endocrine and renal origin [1]. Vasomotor nerves belonging to the autonomic nervous system and baroreceptors which are pressure-sensitive receptors located at strategic points in the arterial side of the circulation, can influence blood pressure. Deviations from a previously stable level of blood pressure affect these baroreceptors and elicit reflexes influencing the activity of the heart and blood vessels, so as to compensate for the deviation, such that blood pressure tends to return to its initial level. Humoral factors such as carbon dioxide concentration ($[CO_2]$), pH, adrenal medulla catecholamines, adrenal cortical hormones and vasopressin (AVP) also play a role in blood pressure regulation. A rise in $[CO_2]$ in the circulation dilates peripheral blood vessels and decreases blood pressure. A fall in pH also leads to a reduction in blood pressure by impairing the responsiveness of the blood vessel to noradrenaline and other vasoconstrictors. The catecholamine, adrenaline, increases SBP and decreases DBP. In conditions of adrenocortical insufficiency, the permeability of the capillaries is increased, an impaired responsiveness of blood vessels to noradrenaline exists and thus blood pressure is lowered. The posterior pituitary hormone AVP causes constriction of blood vessels and hence an increased pressure. Prostaglandins of the E series cause

a decrease in TPR and thus reduce blood pressure. The prostaglandin inhibitor indomethacin increases TPR in normotensive humans [2], which supports the role of prostaglandins in blood pressure control. Nitric oxide (NO) and endothelin, both derived from the endothelium of the vessel wall are known to have contrasting effects on blood pressure. NO relaxes blood vessels and decreases blood pressure, whereas endothelin raises blood pressure by potentiating constriction. Angiotensin II (ANG II), the function of which will be discussed in greater detail in section 1.3.1.3, exerts a direct vasoconstrictor action which leads to an elevation in blood pressure. In addition ANG II, releases aldosterone which results in salt and water retention with a rise in extracellular fluid volume and circulating blood volume. This results in an increased CO.

Under normal situations of stress or increased physical activity blood pressure rises. However, if the blood pressure remains persistently elevated above 140/90 mm Hg, the patient is classified as hypertensive.

1.1.2 Hypertension

Hypertension or high systemic arterial blood pressure may be divided into two groups: secondary hypertension in which the elevation of blood pressure is a consequence of another disorder or can be assigned to a clearly identifiable cause, and essential (primary) hypertension in which the underlying cause is not known.

1.1.2.1 Secondary hypertension

Many causes of secondary hypertension have been identified. Among these are renovascular disease where stenosis or arteriosclerosis restrict blood flow to one or both kidneys. Frequently, correction of the lesion results in amelioration of hypertension. Glomerulonephritis, an inflammatory disease of the glomerulus potentiates hypertension. A variety of hormone-secreting tumours also raise blood pressure. These include adrenal medullary chromaffin tumours secreting catecholamines, aldosterone- and cortisol-secreting tumours of the

adrenal cortex and renin-secreting tumours of the kidney. Adrenocorticotrophic hormone- (ACTH) secreting tumours of the anterior pituitary excessively stimulate cortisol secretion containing hypertension. Finally, a series of inborn errors of corticosteroid biosynthesis and metabolism are associated with hypertension.

Hypertension can result as an effect of drugs including sympathomimetic amines, monoamine oxidase inhibitors, thyroid hormones, or oral contraceptives. The sympathomimetic amine ephidrine is given in the treatment of asthma. However, this drug acts on α-adrenoceptors in the blood vessel to produce a rise in blood pressure. The monoamine oxidase inhibitor pargyline is used as an antihypertensive agent because it inhibits the catabolism of catecholamines. However, the interaction of these agents with sympathomimetic amines can induce a severe hypertensive response. The thyroid hormone, thyroxine produces an increase in SBP and heart rate. There is a risk of development of hypertension or exacerbation of existing hypertension from oral contraceptives.

Unfortunately, these known causes of hypertension represent only a small proportion of cases.

1.1.2.2 Essential hypertension

Environmental and genetic factors play important roles in the development of essential hypertension.

Batumen [3] discovered that lead was the probable cause of essential hypertension in industrial workers. Increased salt intake, saturated fat and cholesterol, physical inactivity, increased intake of calories, obesity and stress have all been suggested to be factors which could potentiate coronary heart disease (Singh et al. [4]). Smoking is also known to be an important risk factor in the development of essential hypertension.

When these are accounted for it appears that a large proportion of the phenotypic variation observed in blood pressure is genetically determined [5]. The variation in blood pressure appears to be accounted for by the sum of the variation in many genes, indicating that blood pressure is inherited as a polygenic trait. The nature of the genes responsible for the variability in blood pressure has not been elucidated although recombinant DNA technology is currently being

applied to provide a better understanding of the role of genetic factors in hypertension .

Hypertensive patients are more likely to develop ischaemic heart disease and cerebrovascular disease (stroke). Because these risks are closely related to blood pressure and because blood pressure is abnormally increased in 15% of the adult population, hypertension is an important disorder.

1.1.2.3 Changes in vascular structure

In hypertension, changes in the vascular structure of the heart and vessels are evident. Left ventricular hypertrophy (LVH) occurs as a response of the heart to an increased workload. Meerson [6] summarised the development of LVH as a progression through 3 stages; hyperfunction, adaptive hypertrophy and ultimately failure. The actual shape of the adapting ventricular chamber depends on the nature of the hemodynamic overload. With pressure overload alone, blood is ejected against an increasing TPR (increased afterload) which causes the chamber to develop a concentric hypertrophy. Concentric hypertrophy is characterised by an increase in the thickness of the walls of the organ,with no enlargement and with diminished capacity (see Figure 1). With volume overload, an excessive venous return encourages the hypertrophy to adopt an eccentric morphology (see Figure 1), where hypertrophy of the organ occurs with a dilation of it's cavity [7]. Two factors which can account for the variability of LVH other than overload are age and race [8]. With advanced age, the hypertrophic response to either volume or pressure overload is attenuated. There is a greater prevalence of hypertension in blacks than whites.

The media of the rat aorta subjected to increased intraluminal pressure had a greater diameter, thickness and cross-sectional area than the media of normotensive animals [9, 10]. The increase in thickness was due to smooth muscle cell (smc) hypertrophy and/or hyperplasia. In the vascular beds of rats [11] and rabbits [12], hypertension increases the uptake of tritiated thymidine (a measurement of cell growth) in smc, strongly suggesting that vascular changes in the vessel wall occur in response to hypertension.

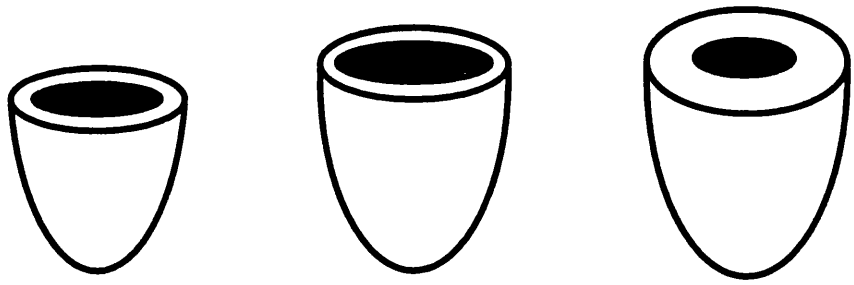

Figure 1 Left ventricular hypertrophy.

If the thickness of the wall relative to the radius of the chamber does not increase proportionately, the volume of the chamber is increased and eccentric LVH occurs. However, if both relative wall thickness and left ventricular mass increase concentric LVH occurs.

1.2 Vascular hypertrophy

The above evidence suggests that a relationship exists between pressure and hypertrophy. To study this relationship, it is necessary to begin by analysing the process of vascular hypertrophy.

Vascular hypertrophy can be defined as an increase in the size of the components of the blood vessel wall. Vascular hypertrophy is a common finding in resistance vessels in human and experimental hypertension. These changes could result from:

(1) An increase in individual smc size, known as hypertrophy [13, 14].

(2) Depending on the site of the vessel, an increase in the cell number, defined as hyperplasia [13, 15]. Yamori et al. [16] observed an increased growth rate of vsmc prepared from an experimental model of hypertension known as the spontaneously hypertensive rat (SHR), when compared to those of the control, normotensive Wistar-Kyoto (WKY) strain.

(3) Increases of collagen [17] and myosin [18]. An increase in myosin content renders the vessel more responsive to vasoconstrictior agents. As a result of increased collagen content the vessel becomes stiffer [19].

(4) Remodelling (See Figure 2). This involves a redistribution of vascular material to produce an increased media:lumen ratio, with no change in media mass, but a reduced lumen diameter (Figure 2c). In human essential hypertension, an increased media:lumen ratio has been observed in the vessels from hypertensive patients. However, the media volume per unit length was unchanged [20]. This suggested that the number of cells was the same and that the increased media:lumen ratio was due to remodelling.

1.2.1 Folkow's amplifier

The positive feedback mechanism in Figure 3 illustrates the proposed relationship which exists betwen vascular hypertrophy and pressure.

It is known that blood vessels are hypertrophic in established hypertension, that increased pressure causes hypertrophy and that hypertrophy can increase resistance thereby raising blood pressure. These events have been linked by Folkow [21] (Figure 3). He proposed

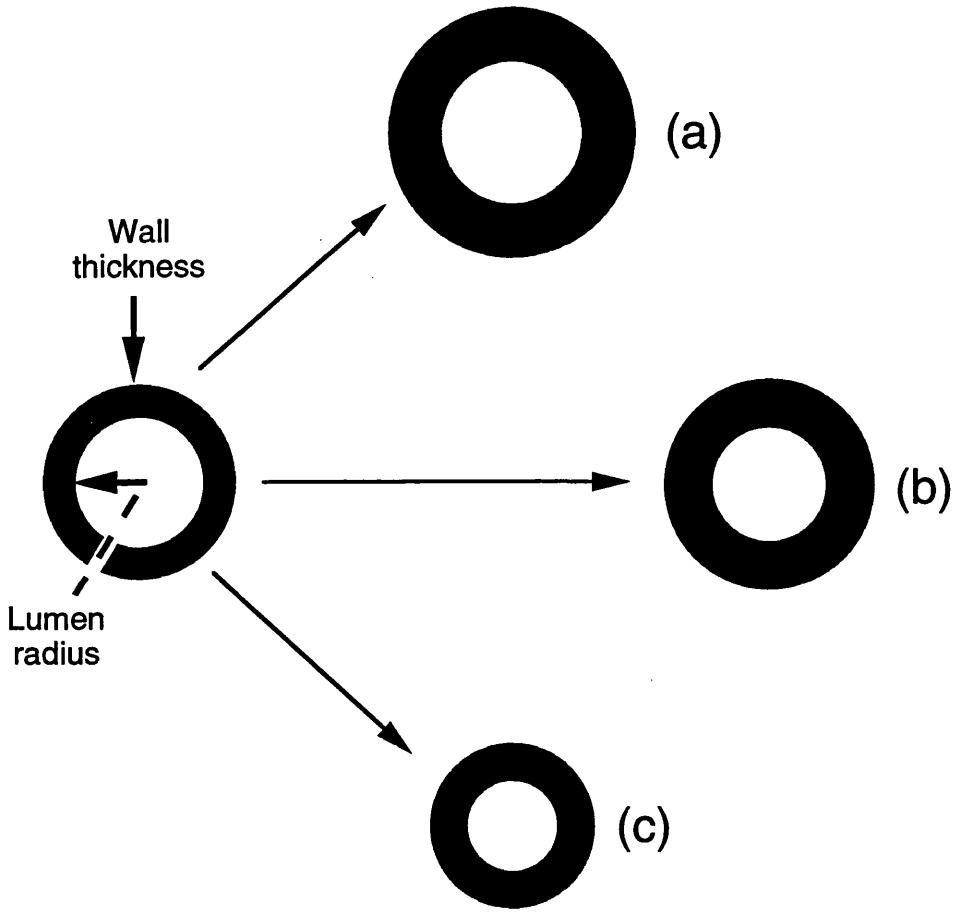

Figure 2 Structural changes of arteries.

The media cross section of a control vessel is illustrated on the left. The various ways in which the media lumen ratio can be increased are shown on the right.

(a) When material is added to the outer surface of the vessel an increase in media thickness occurs.

(b) When material is added to the inner surface of the vessel the radius of the lumen decreases.

(c) Remodelling. When rearrangement of the existing material occurs.

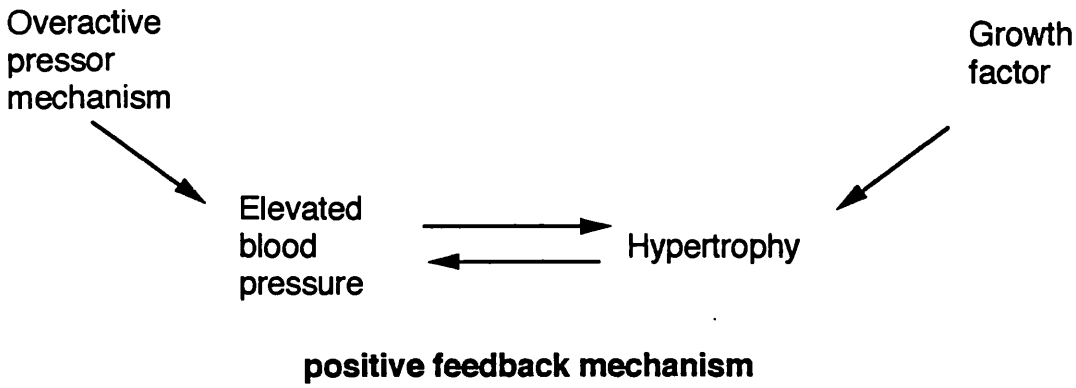

Figure 3 The mechanisms by which a pressor agent and a growth factor can independently contribute to the development of vascular hypertrophy.

that minor overactivity of a pressor mechanism could raise blood pressure slightly. The result of this continued overactivity is to cause hypertrophy with further increases in blood pressure, through the positive feedback process. Thus a sustained rise of pressure could result from a very small pressor signal. This information has identified the importance of a hemodynamic component in producing elevated blood pressure. However, vascular hypertrophy sometimes precedes the rise of blood pressure observed in hypertension [22, 23]. To explain this latter observation, a second component must play a role in elevating blood pressure independently of the pressure component. Furthermore pressure has been shown to be unchanged or slightly elevated in the venous system and in the right side of the heart in hypertension [24, 25], but hypertrophy develops in the veins of patients with hypertension and in the veins and pulmonary artery of hypertensive rats [26, 27]. In the SHR, proof exists that hypertrophy either precedes the rise of blood pressure or occurs when blood pressure is only slightly raised [28, 29]. To explain these observations, Lever [30] postulated that the second mechanism is a trophic factor which could produce elevated blood pressure by hypertrophy, independently of pressure. Two possible trophic factors are noradrenaline and ANG II, both of which have been shown to stimulate the growth of vascular smooth muscle cells (vsmc) *in vitro* [31, 32, 33].

1.3 Non-hemodynamic mechanisms

There are many theories on the pathogenesis of hypertension. The cause(s) of essential hypertension is not known and even where causes of secondary hypertension are known, there is disagreement on the mechanism by which arterial pressure is raised. However, it is clear from the literature that both hemodynamic and non-hemodynamic factors contribute to the development of vascular hypertrophy. The following section reviews the literature which discusses the importance of these 2 components.

In recent years, two factors have emerged as important nonhemodynamic agents in the development and reversal of ventricular hypertrophy, namely growth promoting substances and pharmacological agents. In the past, only the renin-angiotensin (RAS) and adrenergic nervous systems were believed to participate

independently, or in association with hemodynamic changes in the hypertrophic process. It is now known that other naturally occurring humoral and vasoactive agents including growth factors participate in vascular and myocardial cell protein synthesis and growth.

1.3.1 Growth factors

Growth factors are agents which stimulate cell division. Examples are platelet-derived growth factor (PDGF), insulin-like growth factor (IGF), fibroblast growth factor (FGF), epidermal growth factor (EGF), transforming growth factor β (TGFβ) and heparin-binding growth factor type one (HBGF-1). This will be discussed in greater detail in section 1.3.1.4. The growth promoting agents considered in this section are proto-oncogenes.

1.3.1.1 Proto-oncogenes

Proto-oncogenes are the cellular homologues of oncogenes carried by retroviruses. Because oncogenes were shown to be involved in conditions of abnormal growth, this led to the idea that proto-oncogenes may be involved in cell growth. Since then, it has become apparent that oncogenes are normal eukaryotic genes which have undergone a structural mutation, as a consequence of retroviral infection. A portion of the host's DNA has become incorporated with the viral genome and through a process of mutation, a new set of genes have been produced. Proto-oncogenes encode vital regulators of normal mitosis and cell growth. The involvement of proto-oncogenes in hypertension has been studied by looking at the effect of the pressor peptide, ANG II (see section 1.3.1.3) on proto-oncogene expression, in vsmc. Addition of ANG II to smc in culture, stimulated expression of the proto-oncogenes *c-myc, c-fos* and *c-jun* [34, 35, 36, 37]. The proto-oncogene *c-myc* has also been identified as playing a role in T cell and myeloid cell death [38, 39]. Thus the involvement of proto-oncogenes in cell growth is well established.

Nomenclature

There is an accepted nomenclature which is used when discussing proto-oncogenes. The proto-oncogenes which are the normal **c**ellular homologues of the gene are prefixed by **c**, e.g *c-fos.* The **v**iral oncogene is prefixed by **v**, e.g *v-fos.* Both the cellular and viral genes are written in italics. When discussing the protein products of proto-oncogenes, e.g that of *c-fos* , the prefix and the italics are dropped and the protein is written as Fos.

Regulation of transcription

The protein products of the proto-oncogenes *c-fos*, *c-myc*, and*c-jun* exist within the nucleus, where their primary role is to regulate gene expression, by modulating the process of transcription.

The protein products of the proto-oncogenes *c-fos* (Fos) and *c-jun* (Jun) interact with each other to form a heterodimeric transcription factor, via the formation of a leucine zipper [40], as shown in Figure 4. The leucine zipper domain is an α-helical structure composed of leucine residues spaced seven amino acids apart. This structure promotes dimerisation. The Fos/Jun heterodimer binds with high affinity and specificity to DNA elements of the 12-O-tetradecanoylphorbol-13-acetate response element (TRE) consensus sequence, a basic sequence derived from a large set of observed similar sequences. TRE was first identified as a phorbol ester-inducible promoter element, and the binding site for the transcription factor, AP-1 [41, 42, 43]. Much evidence has indicated that the expression of *c-fos* and *c-jun* are rapidly induced by a number of external stimuli and that the Fos/Jun complex then turns on the expression of late response genes containing AP-1 sites [44].

c-myc has been implicated in controlling both proliferation and differentiation in various cell types [45]. Increased expression of *c-myc* resulted in an increase in the rate of proliferation and prevented differentiation in mouse erythroleukemia cells [46]. *c-myc* is abundantly expressed in the heart during the fetal period. However, its expression becomes undetectable soon after birth [47]. This observation suggests a

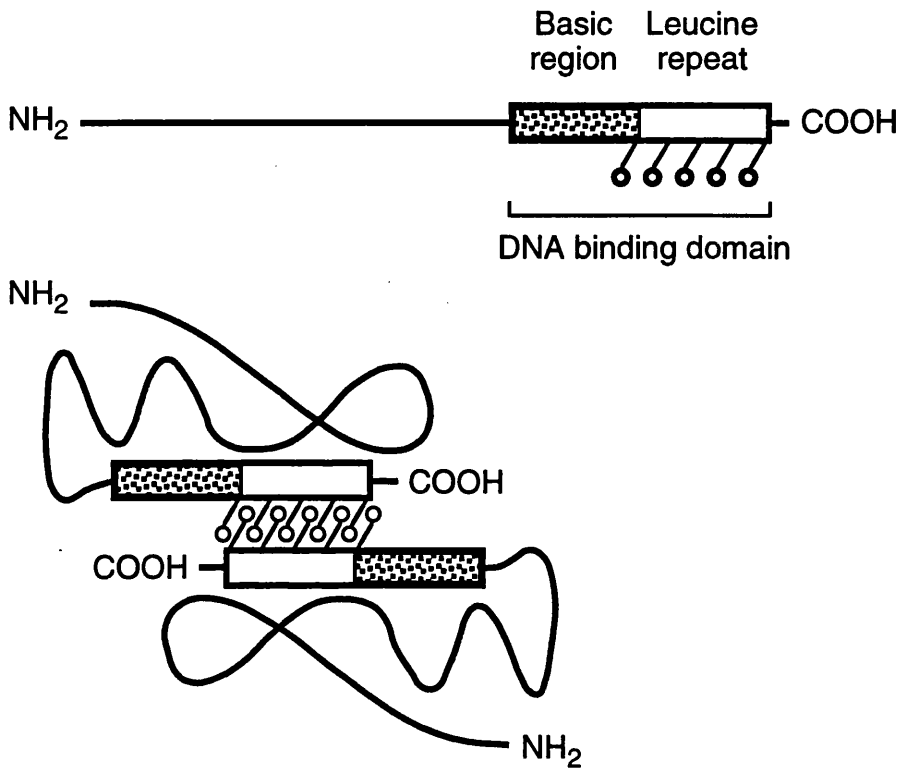

Figure 4 The formation of a leucine zipper.

The Fos and Jun proteins interact via their DNA binding domains. These sequences are located 7 amino acids apart. When multiple interactions of the Fos and Jun binding domains occur, this promotes the formation of an α-helix.

relationship between *c-myc* expression and cardiocyte proliferation, which was supported by findings in transgenic mice [48].

Thus, proto-oncogenes appear to have a key role in cell growth through their involvement in the process of transcription. Various proto-oncogenes have been identified in vascular tissue and their function in vascular tissue may also be of a proliferative nature.

Other functions of proto-oncogenes

The protein products of proto-oncogenes are diverse as are their functions. However there appear to be three main categories under which these functions can be classified:

The *c-mos* proto-oncogene encodes for a protein kinase required for normal progesterone-induced maturation of frog oocytes and plays an important role in the activation of the cell cycle promoter, mitosis phase promoting factor (MPF)[49]. A serine/threonine protein kinase, which is strongly expressed in neonatal and adult rat tissue and cells is encoded by*c-raf* [50].

c-ras proteins were identified as guanine nucleotide-binding proteins (G proteins), in bovine brain, by Yamashita et al. [51]. As G proteins are known to exert strict control of the activity of adenylate cyclase (AC), this suggests a role for Ras proteins as second messengers. There is a delayed increase in *c-ras* mRNA after aortic constriction in adult rat aorta [47]. The fact that proto-oncogenes have second messenger effects and that they occur in vascular tissue where hypertrophy has been induced is strong evidence of a key role for proto-oncogenes in vascular growth.

Many proto-oncogene proteins have been shown to exhibit structural homology with growth factors or their receptors. This function is the most convincing evidence that proto-oncogenes are involved in cell growth. For example, the protein product of *c-sis* has been identified as one chain of the PDGF molecule [52]. The product of *c-erbB* encodes part of the EGF receptor [53]. *C-mas* encodes for a neuronal ANG II receptor [53]. Hunter [54] identified the proto-oncogenes *ros*, *met*, and *trk* as being related to the insulin receptor.

1.3.1.2 Mechanism of action of growth factors (Figure 5)

The plasma membrane contains many lipid precursors which when activated, for example by hormones, can serve as substrates for the generation of second messengers [55]. A growth factor can interact with a receptor on the cell surface to cause activation of the enzyme phospholipase C (PLC) via the action of a G protein. G proteins are composed of three distinct subunits, α, β and γ. The $\beta\gamma$ exist as a tightly associated complex that functions as a unit. The α-subunits have a single site for guanosine diphosphate (GDP) or GTP. The GDP-bound form of α binds tightly to $\beta\gamma$ and is inactive, whereas the GTP-bound form of α dissocates and becomes active. The hydrolysis of phosphatidyl inositol 4, 5 bisphosphate (PIP_2) is markedly stimulated by hydrolysis-resistant analogues of GTP, which will favour the active conformation of the G protein, and by aluminium fluoride (AlF_4^-), which can interact with α-bound GDP to mimic GTP and activate the α-subunit of the G-protein. The inhibition of this cascade by pertussis toxin, which is known to inhibit the G_i-protein, also points to the participation of a G protein in the signalling events associated with cell growth. The activation of PLC then catalyses the breakdown of PIP_2, an inositol glycolipid located in the inner leaflet of the plasma membrane. Many inositol phosphates as well as diacylglycerol (DAG) are the products of this catalytic breakdown. Inositol phosphates can be converted to inositol by the sequential action of phosphatases.

It is now clear that phosphatidylcholine (PC) hydrolysis also contributes to the generation of DAG in the later phases of cellular responses and a possible role of phospholipase D (PLD) in the activation of protein kinase C (PKC) has been proposed [56, 57].

Inositol 1, 4, 5 trisphosphate (IP_3) is a short lived messenger causing the rapid release of calcium ions (Ca^{2+}) from intracellular stores. The elevated Ca^{2+} concentration ($[Ca^{2+}]$) in the cytosol then triggers processes such as smooth muscle contraction, glycogen breakdown and exocytosis. DAG activates PKC which phosphorylates many target proteins at serine and threonine residues, leading to many physiological events. For example, the phosphorylation of glycogen synthase by PKC stops the synthesis of glycogen. PKC is enzymatically active only in the presence of Ca^{2+} and phosphatidylserine (PS). DAG

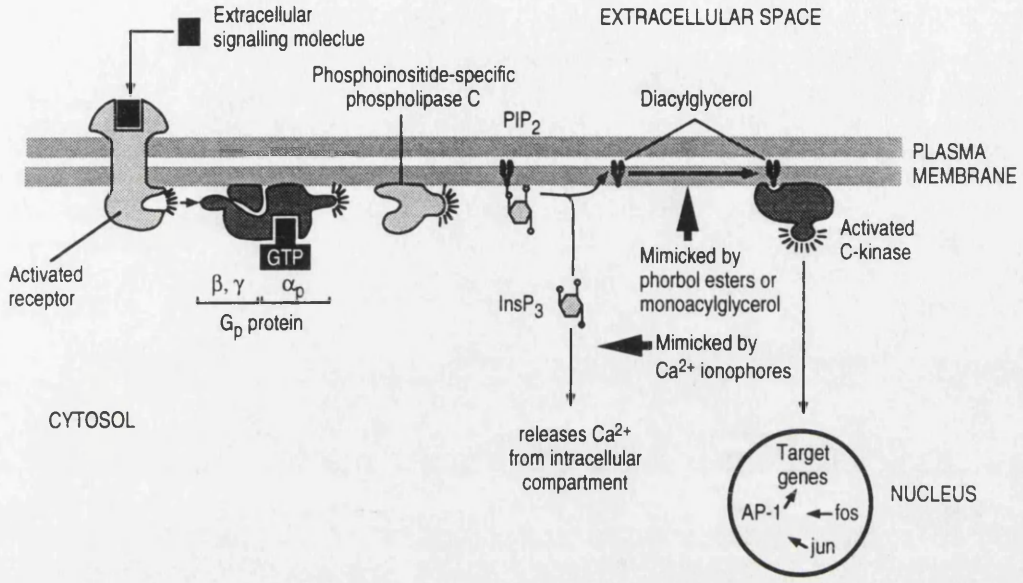

Figure 5 The mechanism of action of growth factors.

The growth factor interacts with its receptor to stimulate PIP_2 hydrolysis via the activation of a G protein. The products of this hydrolysis are IP_3 and DAG. IP_3 facilitates the release of Ca^{2+} from intracellular stores and DAG activates PKC. PKC stimulates the expression of proto-oncogenes which function to regulate the transcription of other genes involved in cell growth.

greatly increases the affinity of PKC for Ca^{2+} and therefore renders it active at physiological levels of this ion [58].

Extracellular signals modulate the activity of many different types of transcription factors. PKC was shown to activate the AP-1 transcription factor [59] (previously discussed in this section) and is responsible for transcriptional induction of many genes.

ANG II (see section 1.3.1.3) when binding to its receptor, activates receptor-operated Ca^{2+} channels and gives rise to Ca^{2+} influx. However, this is of minor importance for ANG II-related trophic effects [60].

1.3.1.3 ANG II

Synthesis

The production of ANG II is summarised in Figure 6. Renin is produced principally in the kidney. This proteolytic enzyme cleaves the amino terminal decapeptide from angiotensinogen, a glycoprotein which is synthesised in the liver, to produce the decapeptide angiotensin I (ANG I). This is further processed by angiotensin converting enzyme (ACE) which removes the two carboxy terminal amino acids to generate the active octapeptide ANG II. ANG II causes vasoconstriction and an increase in blood pressure. This factor also promotes aldosterone biosynthesis and secretion, noradrenaline release, renal sodium reabsorption, glycogenolysis and stimulation of thirst [61, 62].

Local RAS

The RAS is important in maintaining normal cardiovascular homeostasis and its participation in hypertension is well established. The existence of the components of the RAS has been reported in vascular and cardiac myocytes [63], where hypertrophy has been shown to occur. This suggests a possible role for ANG II as a growth factor in this tissue. A local RAS has also been identified in the adrenal cortex [64, 65]. Re et al. [66] observed an ANG I generating activity in canine aortic smc which was inhibited by renin-specific antisera. An immunofluorescent study using renin-specific antiserum, demonstrated the presence of renin in canine aortic smc. Radiolabelling studies using

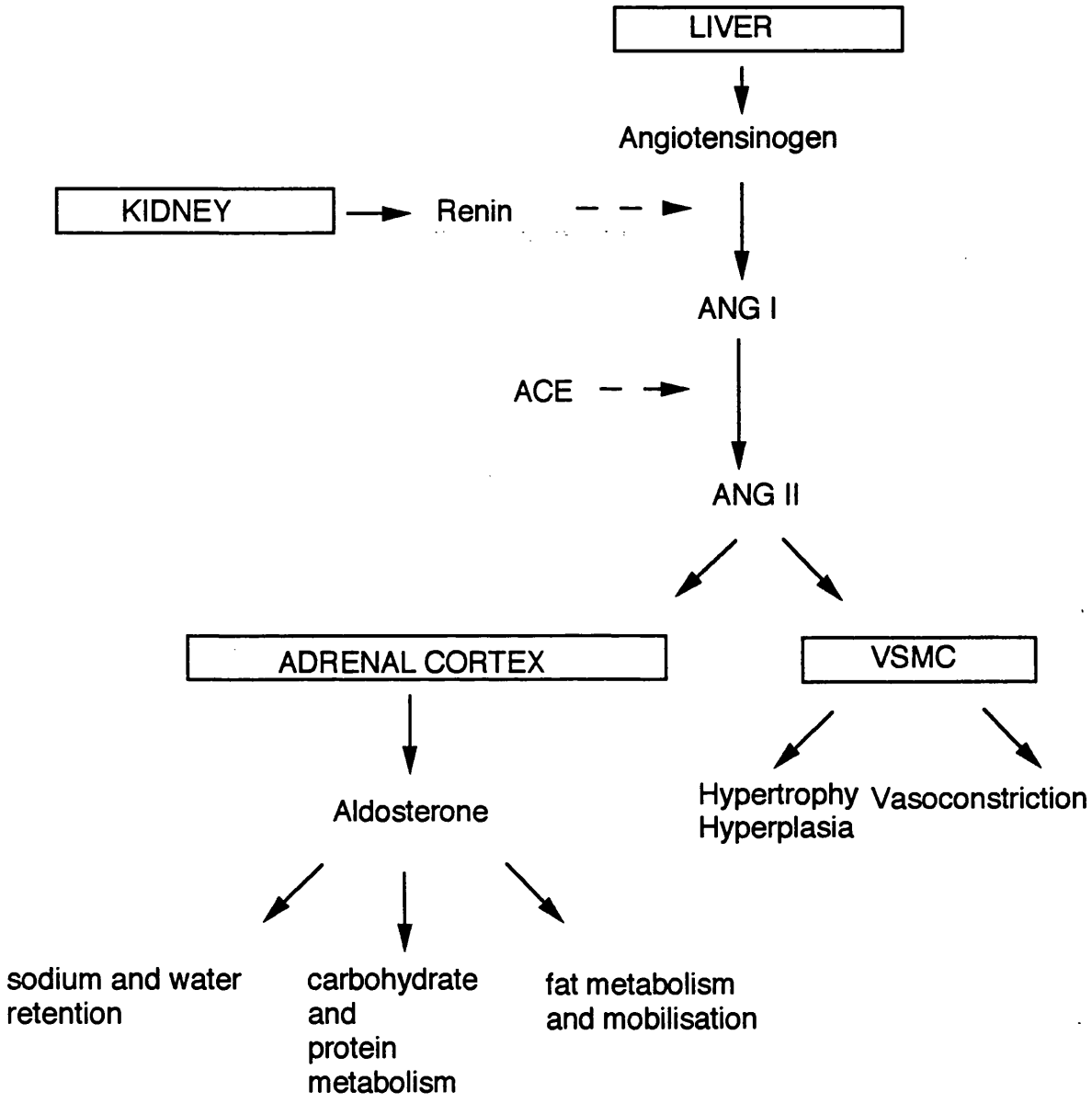

Figure 6 The renin-angiotensin system.
The sequential cleavage of angiotensinogen by renin and ACE respectively, results in the synthesis of ANG II. ANG II functions as a growth factor, vasoconstrictor and stimulator of aldosterone production by the adrenal cortex.

^{35}S-methionine revealed the synthesis of a protein by these cells, with a molecular weight which corresponded to that of renin. When bovine aortic endothelial cells were incubated with angiotensinogen the production of ANG I was observed [67]. The effect of pH on this activity was in agreement with that of bovine renal renin. The presence of renin in bovine aortic endothelial cells was further verified by immunofluorescence microscopy, using antirenin antisera.

ANG II as a growth factor

There are now several papers showing that ANG II has growth promoting effects on vsmc, both *in vivo* and *in vitro*.

Griffin et al. [68] administered sub-pressor concentrations of ANG II by minipump to rats for 10-12 days. Increased media width, increased media cross-sectional area and media/lumen ratio were observed. In the experimental animal model of hypertension, the SHR, ACE inhibitors were effective in preventing aortic hypertrophy [69]. When the endothelium was removed from the carotid arteries of rats, the growth of vascular smooth muscle and extracellular matrix was inhibited by treatment with ACE inhibitors [70]. The ACE inhibitor, perindopril, prevented the development of hypertension in the SHR, suggesting that the growth promoting effect of ANG II may be partly responsible for the elevation in blood pressure observed in this model of hypertension (Harrap et al. [71]).

Hypertrophy and/or hyperplasia?

Whether ANG II-stimulated growth is a result of hypertrophy and/ or hyperplasia is controversial. To answer this question, various techniques have been employed. Cell numbers have been evaluated to determine whether ANG II has produced a hypertrophic response. The rate of ^{3}H thymidine uptake by vsmc has been measured to determine whether ANG II can stimulate DNA synthesis. The effect of ANG II on protein synthesis has been assessed by measuring the rate of ^{3}H leucine uptake by cells.

Lyall et al. [33] observed an increase in the rate of growth when studying the effect of ANG II on rat mesenteric vsmc number. An increase in cell number was also observed when ANG II was added to

human aortic smc [32]. In contrast, Berk et al. [72] discovered that ANG II did not increase the number of aortic smc growing in culture but did increase protein synthesis. Geisterfer et al. [73] demonstrated that ANG II neither stimulated the proliferation of aortic smc made quiescent in a defined serum-free medium nor augmented the cell proliferation induced by serum or PDGF. ANG II increased smc protein content by 20%, as determined by staining with fluorescein isothiocyanate. These findings suggest that ANG II can produce hypertrophy and hyperplasia in smc.

Possible mechanisms

Bobik et al. [74] and Araki et al. [75] have shown that ANG II can stimulate PDGF synthesis in vsmc, which suggests that ANG II may potentiate growth by stimulating the synthesis of other growth factors. In cultured aortic smc, ANG II was shown to activate the phosphoinositide second messenger system (Figure 5) which is involved in cell growth [76]. Naftilan et al. [34, 35, 37] reported that ANG II induced expression of the proto-oncogenes *c-myc*, *c-fos* and *c-jun* in vsmc, which is also indicative of a growth factor role for ANG II in vsmc. Lyall et al. [36] has shown that both increased phosphoinositide turnover and rapid accumulation of *c-fos* mRNA occurred as a result of the incubation of vsmc with ANG II and that these events occurred through the AT_1 receptor. This evidence supports the role of ANG II as a growth factor in vsmc.

1.3.1.4 Other growth factors

The previous sections have described the growth promoting properties of proto-oncogenes and ANG II and demonstrated a role for these factors in the development of vascular hypertrophy, a feature of essential hypertension. A number of other growth factors may also play important roles in the process of vascular hypertrophy.

Endothelin, a potent vasoconstrictive peptide was isolated from cultured porcine endothelial cells [77]. It has been shown to induce hypertrophy [78, 79, 80, 81], stimulate phosphoinositide turnover and

proto-oncogene expression [82, 83], and elevate DNA synthesis [84, 85, 86] in a number of cell types.

AVP, a potent vasoconstrictor and natriuretic factor, when added to cultured smc stimulated protein synthesis [87] and incorporation of [^{3}H] thymidine into DNA [88]. Campbell-Boswell et al. [32] observed that AVP increased the number and size of arterial smc in culture.

PDGF. The 2 forms of PDGF, PDGF-AB and -BB in combination with TGF β (see later) have been shown to stimulate the proliferation of vsmc, isolated from the SHR [89]. PDGF-BB has been shown to increase DNA synthesis and cell growth via Ca^{2+} entry (Ko et al. [90]). In rats with hypoxic pulmonary hypertension, an increased expression of PDGF A- and B-chain genes was observed in the lungs [91].

Insulin and particularly the closely related insulin-like peptides, are mitogenic to vsmc [92]. IGF-1 receptors provide a common pathway for the stimulation of growth and related events (*c-myc* induction) by insulin and IGF-1 in cultured human vsmc [93]. There is evidence to suggest that IGF-1 may play a role in the repair of the endothelium, by regulating smc proliferation [94]. IGF-1 has been detected in conditioned medium from both porcine vsmc and endothelial cells [95]. However, a report published by Murphy et al. [96] localised IGF-1 mRNA to the smooth muscle layer of the adult rat aorta, but not to the endothelium.

Essential hypertension has been postulated as a disorder of growth, which originates in childhood [22, 97]. The growth promoting properties of IGF-1 play an important role in this process.

FGF, a member of the heparin-binding growth-factor family, is present in rat aortic tissue [98] and is produced by vsmc in culture [99, 100]. FGF is characterised by its avidity for heparin and ability to stimulate endothelial cell proliferation *in vivo* and *in vitro* [101]. FGF may also play a role in the repair of the endothelium which may involve the stimulation of vsmc proliferation (Gajdusek et al. [102]).

EGF. This factor was shown to activate S6 kinase in Swiss mouse 3T3 cells and vsmc [103, 104]. Activation of this kinase by phosphorylation induces protein synthesis and initiates DNA synthesis [104, 105]. EGF elicited a greater proliferative response of vsmc derived from SHR than those from WKY [104]. Berk et al. [105] demonstrated that FGF caused contraction of rat aortic strips. FGF has a potential role in the development of vascular hypertrophy through its growth promoting

action. However, the ability of this factor to produce contraction may also be important as a mechanism through which growth factors can contribute to essential hypertension.

TGFβ. The mRNA transcript levels of TGFβ are significantly elevated in parallel with blood pressure [98]. This finding together with the fact that platelets release as much TGFβ upon aggregation as PDGF, suggests that this peptide also has a growth promoting role and may become actively involved in the development of atheroslerotic plaques [106]. Treatment of cultured vsmc with TGFβ lead to downregulation of $PDGF_{AA}$ receptor subunits and concomitant desensitisation to $PDGF_{AA}$ [107]. This may culminate in cellular hypertrophy rather than hyperplasia [69].

HBGF-1. HBGFs are a chemically defined family of polypeptides with mitogenic activity for a variety of cell types. Experimental findings suggest a relationship between HBGF-1, LDL and PDGF in smc proliferation [108].

1.3.1.5 Extracellular matrix (ECM)

Tissues are not composed solely of cells. A substantial part of their volume is extracellular space which is largely filled by an intricate network of macromolecules constituting the extracellular matrix. This matrix comprises a variety of versatile polysaccharides and proteins that are secreted locally and assemble into an organised mesh.

Changes in the component of the ECM, elastin, have been demonstrated which are relevant in the development of hypertension. Elevated elastin synthesis accompanies increased blood pressure, particularly in the large conduit vessels [109] and this trait is maintained in culture with vsmc from the SHR. As discussed earlier, hypertrophic vessels contain an increased amount of collagen [18]. These observations suggest that alterations in the components of the ECM occur in the process of hypertrophy.

1.3.2 Atrial natriuretic peptide (ANP)

ANP is a hormone produced mainly in the atria of the heart. It exhibits diuretic, natriuretic [110] and vasorelaxant activities [111] and inhibits the

secretion of renin, aldosterone and AVP. Atrial distention is the most powerful stimulus to ANP release but other stimuli appear to modulate its rate of synthesis and secretion. In contrast to adult heart ventricles, fetal and neonatal ventricles exhibit high levels of ANP gene expression and ANP synthesis [112, 113], suggesting that ANP may play a greater role in control of the cardiovascular system during early stages of life. A high rate of ANP gene expression is observed in the ventricles in a variety of pathological conditions including human congestive heart failure [114], in rats with myocardial infarction and cardiac failure [115] and in rats subjected to pressure overload [116, 117] and in SHR [118]. Montorsi et al. [119] observed that plasma concentrations of ANP were greater in hypertensive than normotensive patients. These experimental observations suggest that high ANP levels are associated with cardiovascular disease. However, this evidence was contradicted by Franco-Saenz et al. [120]. This group investigated the effects of a 4h infusion of 8-33-Met ANP in patients with hypertension. 8-33-Met ANP infusion caused a prolonged lowering of SBP with no change in DBP or CO. A possible explanation is that lower levels of ANP play a cardioprotective role but that higher levels may potentiate disease.

1.4 Hemodynamic factors in hypertrophy

The role of non-hemodynamic agents, including growth factors in the process of vascular hypertrophy and the development of essential hypertension has been discussed in detail. Hemodynamic factors are the parameters of interest in this project and the following section is a general review of *in vivo* and *in vitro* studies which have demonstrated an effect of hemodynamic load on cellular function. Subsections will deal with the individual forces to which cells within the vessel are exposed, namely shear stress and pressure and the effects that these parameters can induce, with relevance to hypertension.

The *in vivo* studies described are based on the use of the coarctation model of hypertension. This involves constricting the aorta to produce an area of high pressure proximal to the constriction and an area of low pressure distal to this point. Thus tissues can be exposed to a hemodynamic load by positioning the constriction appropriately.

MacIver et al. [121] examined the effects of pressure overload on proto-oncogene expression in cardiovascular tissues. The aorta proximal to the stenosis and mesenteric vessels were exposed to high blood pressure and thus increased load whereas the aorta below the coarctation was exposed to low blood pressure. To examine proto-oncogene signals during the development of pressure-related vascular structural changes, levels of *c-myc*, *c-fos*, and c-*H-ras* mRNA were measured 72h and 9 days after the induction of coarctation. At 72h, there was a significant increase in *c-myc*, *c-fos*, and *H-ras* mRNA. A significant increase in proximal mass was observed at both of these time points but no changes in mesenteric artery morphology was observed in rats with coarctation. This vascular bed was positioned above the coarctation and was presumably exposed to a higher blood pressure and increased load. A structural change and induction of proto-oncogene expression had therefore been anticipated. Previous studies by this group have however shown that morphological changes in this tissue only reach statistical significance 28 days after surgery [122]. This may explain why no changes were observed.

Izumo et al. [117] also observed stimulation of the transcription of the proto-oncogenes *c-fos* and *c-myc* and the heat shock gene, hsp70 in response to pressure overload in the ventricular myocardium, 1h after imposition of a load. Mulvagh et al. [123] observed induction of *c-*

myc mRNA in the isolated rat heart in response to aortic constriction. Komuro et al. [47] studied the expression of several cellular oncogenes during the developmental stage and pressure-overloaded hypertrophy of rat hearts *in vivo*. Pressure overload resulted in increased levels of *c-fos*, *c-myc* and *c-Ha-ras*. An increase in *c-fos* and *c-myc* mRNA was detected at 30 min and 2h respectively, the levels were shown to peak at 8h, and to return to baseline by 48h after the aortic constriction. The levels of *c-Ha-ras* showed a gradual increase. These observations were similar to the time course of expression achieved for these proto-oncogenes through the developmental stages. This suggested that cellular hypertrophy induced by pressure overload may share a similar mechanistic pathway with cell proliferation.

In the same study, MacIver et al. [121] also examined the effect of increased load on phosphoinositide hydrolysis. The products of inositol lipid hydrolysis were measured 72h and 9 days after application of the coarctation. At 72h, coarctation had induced structural changes in the proximal aorta which were associated with increased inositol phosphate production. Increased inositol phosphate production was no longer observed 9 days after surgery, when most of the structural changes were completed. The results suggest that inositol lipid hydrolysis is an important process in the development of vascular hypertrophy in this model of hypertension. The overall conclusions of this study were that stimulation of proto-oncogene expression and phosphoinositide hydrolysis may mediate vascular remodelling and that alternative mechanisms may be involved in mesenteric vessel thickening where slower structural development is involved.

Pressure overload is associated with re-expression of the fetal contractile proteins [124], β-myosin heavy chain isoform [125] and α-skeletal actin [126]. Imamura et al. [127] also demonstrated that myosin heavy chain gene expression was induced by increased pressure load. Many observations have been made describing changes which occur in the process of hypertrophy but the mechanism(s) by which these changes occur are poorly understood.

An advantage of studying the *in vitro* situation is that changes induced by hemodynamic load can be studied independently of humoral factors.

The results of a number of studies have suggested that in blood vessels, the mechanotransduction could be initiated at the level of the

endothelial cells. Lansman et al. [128] proposed that stretch-activated ion channels in endothelial cells mediate the transduction of hemodynamic stresses. Olesen et al. [129] demonstrated that shear stress activated a potassium current in vascular endothelial cells. Signalling from the membrane to underlying vsmcs may take place via gap junctions or by the release of effector molecules (e.g growth factors). Taken together these findings are consistent with the concept that hemodynamic forces can directly initiate intracellular events controlling vascular tone and cell growth. Furthermore, Kent et al. [130] indicated that sodium influx in response to myocyte stretching may be one of the early signals mediating the hypertrophic response to mechanical stimulus in the adult mammalian myocardium. The exact involvement of the different ion channels in mechanical transduction and its relevance to cardiovascular remodelling remain to be determined.

The stimulation of induction of gene transcription in response to load has also been demonstrated from *in vitro* studies. Komuro et al. [131] demonstrated that stretched neonatal rat cardiocytes express *c-fos* mRNA. The expression of *c-fos* mRNA in the myocardium has also been shown to increase by raising coronary blood flow, pressure or contractility in the isolated rat heart [132].

These observations agree with reports by Mann et al. [133] who showed that an increased mechanical load was enough to increase total RNA as well as protein synthesis in adult mammalian cardiocytes. As with *in vivo* observations, the signal transduction pathways mediating these responses are not well understood. However, von Harsdorf [134] demonstrated that phosphatidylinositol turnover was increased by myocardial stretch as indicated by the accumulation of inositol phosphates, suggesting that this intracellular pathway may mediate some of these processes.

1.5 Flow/stretch related forces

In vivo, cells are continuously being exposed to forces existing within the vessel. Such forces can be resolved into two components; pressure acting perpendicular to the surface and shear stress, a tangential dragging component resulting from friction with the endothelial surface [135]. The vsmc constituent of the vessel wall absorbs most of the pressure and the endothelium is subjected to all of the shear stress. To examine the effect of shear stress and pressure on metabolic, physical and morphological properties of various cell types, it is more practical to study the effects of these forces separately.

The parallel flow plate chamber and rotating cone apparatus, which will be described in greater detail in section 1.5.1, have been designed to study the component of shear stress. The pressure component, which is of most interest in this project, has been examined by looking at the effect of stretch on cellular properties. The most popular methods employed to apply stretch to cells will be described in section 1.6.

For practical purposes, many of the initial investigations have looked at the effect of a continuous force on cellular function. However, when the *in vivo* situation is considered it is obvious that the force exerted is not continuous. Blood flows through vessels in a pulsatile manner and therefore the component of shear stress which results from friction between the blood and the endothelial cells is also pulsatile in nature. As the rate of blood flow increases, the radius of the lumen increases to facilitate an efficient transfer of blood and hence the cells in the vessel wall are stretched and/or compressed.

The following section reviews the continuous and pulsatile experiments which have been performed to study the components of shear stress and pressure in various cell types.

1.5.1 Shear stress

Flow is known to influence the constriction and relaxation of small arteries and has been implicated in the appearance of localised atherosclerotic regions in large arteries. Thus, the role of the endothelium as a mechanotransducer of flow-related forces,

particularly shear stress is of great interest. The majority of *in vitro* studies have examined the effect of shear stress on endothelial cell function by using parallel flow plate chambers (Figure 7), designed to provide steady laminar flow. A physiological range of 0-40 dynes/cm^2 was defined by Ohno et al. [136] to mimic the force of shear stress occurring *in vivo*.

The chamber is composed of two stainless steel plates separated by silicone sheeting which serves as a spacer and a gasket. The channel height is defined by this gasket thickness. A single coverslip with confluent endothelial cells is positioned in a circular recess in the bottom plate where a portion of the cell monolayer is exposed to flow. The chamber is maintained at 37°C by a copper heating plate mounted on top of the chamber. The heating plate is equipped with two electrical heat cartridges which receive electric current from a temperature controller. The shear stress is applied to the endothelial monolayer by perfusing medium through the channel using a syringe pump. Because the shear stress is a linear function of the flow rate through the channel, the amount of shear stress exerted can be directly calculated in dynes/cm^2.

1.5.1.1 Biochemical events involved in growth

As discussed earlier, an increased rate of growth is an important event which has been identified in the development of hypertension. Thus, any factor which can stimulate cell growth is of great interest in the study of this disease state. This section reviews the studies which have looked at the effect of shear stress on biochemical events which can lead to cell growth.

IP_3

As previously discussed, activation of the phosphoinositide pathway, is involved in the initiation of cell growth. The effect of shear stress has been tested on this pathway. A shear stress of 24 dynes/cm^2 resulted in a marked increase in levels of IP_3; removal of flow resulted in a gradual return of IP_3 to basal levels [137]. The response of IP_3 levels was partially inhibited by ibuprofen and indomethacin, inhibitors of the enzyme cyclo-oxygenase which is involved in prostaglandin formation, indicating that the IP_3 response was partly dependent on flow-induced

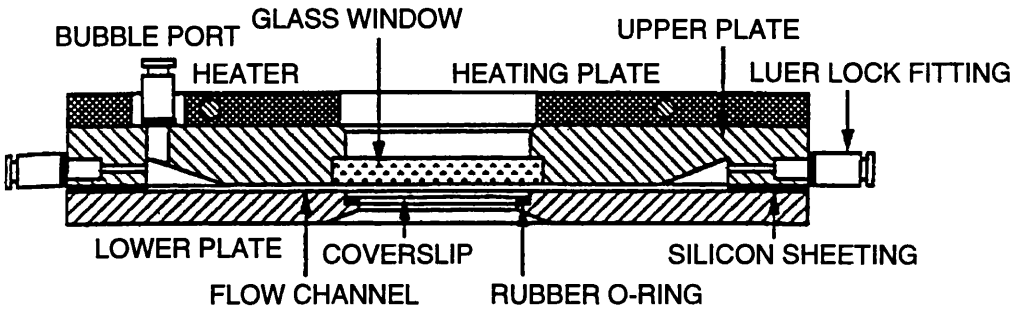

Figure 7 Cross-section of parallel-plate flow chamber, from Ohno et al. (136).

Endothelial cells are placed on a coverslip and subjected to shear stresses as fluid flows across the coverslip.

prostaglandin synthesis. From this evidence, it was suggested that shear stress may be an expernal signal which can be transduced into a biochemical response.

Ca^{2+}

Ca^{2+} is an important second messenger which plays an essential role in processes such as muscle contraction. An elevated intracellular $[Ca^{2+}]$ ($[Ca^{2+}]_i$) can occur by entry through ion channels or as a result of increased release of Ca^{2+} from intracellular stores. Mo et al. [138] and Ando et al. [139] examined the effect of adenosine triphosphate (ATP) on flow-induced changes in cell Ca^{2+} levels, in vascular endothelial cells. ATP is known to influence the tone of smooth muscle by activation of purinoceptors and subsequent activation of the phosphoinositide pathway. An increase in IP_3 levels stimulates Ca^{2+} release which induces release of NO and smooth muscle relaxation. Both groups observed that under flow conditions, ATP increased the $[Ca^{2+}]_i$ of the cells. Shen et al. [140] observed that application of a stepwise increase in shear stress from 0.08-8 dynes/cm^2, to bovine aortic endothelial cells, increased $[Ca^{2+}]_i$, which attained a peak value in 15-40s, followed by a decline to baseline within 40-80s. In the presence of ATP or adenosine diphosphate (ADP), application of shear stress caused repetitive oscillations in $[Ca^{2+}]_i$ in single cells, but an adenosine diphosphatase (ADPase) or adenosine triphosphatase (ATPase) did not inhibit the shear-induced calcium response. This suggests that ATP is not essential for the release of Ca^{2+}. Bodin et al. [141] showed that increased flow induced ATP release from vascular endothelial cells but not smc. Thus, flow alone can stimulate Ca^{2+} release. However, when extracellular ATP is added this causes an amplification of the flow-induced response.

This evidence suggests that shear stress can stimulate Ca^{2+} release from endothelial cells and that this effect can be explained by an increased production of ATP. The further addition of ATP will amplify the Ca^{2+} response leading to a greater production of NO and a greater degree of relaxation.

1.5.1.2 Cell growth

It was of interest to examine whether shear stress could affect the rate of cell growth and therefore be an important contributor to vascular hypertrophy. The factors affecting this growth are discussed below.

Proliferation

A dose-related reduction in proliferation was observed when subconfluent bovine aortic endothelial cells were exposed to shear stress levels of >15 dynes/cm^2 for 48h [142] which would deny a potential growth promoting role for shear stress. Proliferation was totally abolished at 90 dynes/cm^2 for 48h. However, when this time point was exceeded proliferation resumed, which suggests that the length of duration of shear stress is an important factor in the stimulation of cell proliferation. Furthermore, aortic endothelial cells exposed to a shear stress of 30 dynes/cm^2 caused inhibition of proliferation and the shear stress arrested the cells in the G_0/G_1 phase of the cell cycle [143]. These observations are best explained by postulating that cells must adapt to the environment introduced by shear stresses by changes in their shape and cytoskeletal structure. In these circumstances, cell proliferation would be of low priority and mechanisms of cell mitosis would be inhibited at least during the period of adaptation.

Growth factors

The induction of growth factors by shear stress is an important area in the study of hypertension. Such factors might potentiate the growth of vsmc and contribute to vessel hypertrophy.

Hsieh et al. [144] investigated the effect of shear stress on PDGF-A and B chain mRNA levels in cultured human umbilical vein endothelial cells. The levels of both PDGF-A and B mRNA were increased by a physiological shear stress of 16 dynes/cm^2, reaching a maximum approximately 1.5-2h after the application of shear stress and returning almost to control values at 4h. Bovine aortic endothelial cells were exposed to a steady laminar shear stress of 40 dynes/cm^2 using the rotating cone apparatus (Figure 8). A motor induced rotation of a shallow cone which was fitted into a plexiglass holder. This movement caused the displacement of cell culture medium, which resulted in the

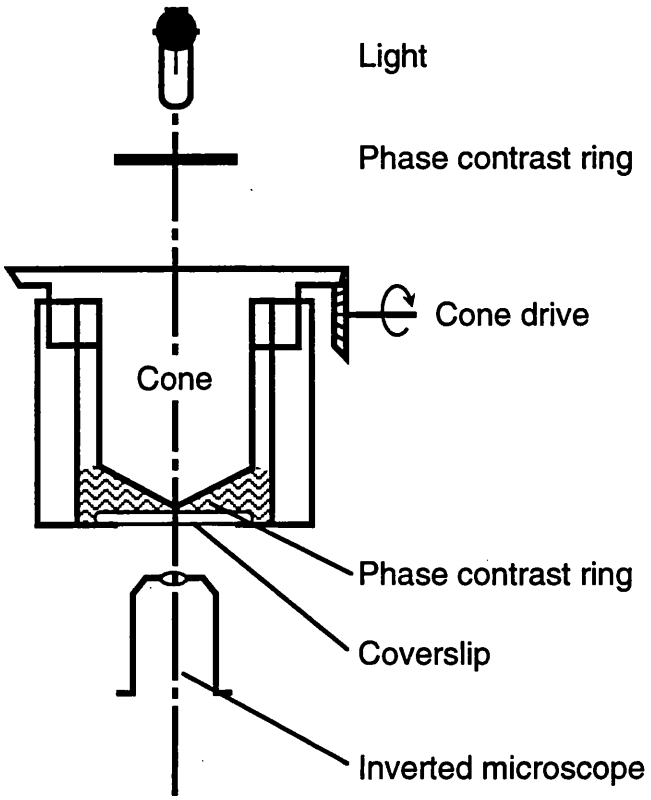

Figure 8 Cross-section of rotating cone apparatus, from Franke et al. (148).

A transparent polycarbonate cone having an angle of 2.5° is fitted into a plexiglass holder and connected to a speed-controlled motor with variable rotational velocities. The cone is placed with its tip on the surface of the coverslip, containing the cells, under microscopic control.

production of a shear stress on the endothelial cell monolayer. $TGF\beta_1$ mRNA levels were increased several-fold compared to static controls within 2h of exposure, and remained elevated for 12h. The increase in mRNA levels was directly proportional to the intensity of the shear stress within the physiological range of 0-40 dynes/cm^2. Shear stress also induced a markedly increased production of $TGF\beta_1$ in cell membranes. Olesen et al. [129] showed that shear stress can activate a potassium ion (K^+) current in vascular endothelial cells. Addition of the K^+ channel blocker tetraethylammonium, attenuated the shear stress-induced increase of $TGF\beta_1$ mRNA and active $TGF\beta_1$ [136]. This illustrated that $TGF\beta_1$ formation in response to shear stress is partially mediated via K^+ channel activation.

1.5.1.3 Cell morphology and structure

Can shear stress provoke a change in cell shape? There is good evidence that this is the case. Cells in a confluent monolayer change from a polygonal to an ellipsoidal shape and align uniformly with the direction of flow during exposure to a unidirectional fluid shear stress of >5 dynes/cm^2 for 24 h [145]. Endothelial cells obtained from the arterial circulation contain bundles of actin filaments known as stress fibres, but few if any are observed in endothelial cells of the venous circulation [146, 147]. To determine whether shear stress is one of the factors which influences the distribution of actin filaments in endothelial cells, Franke et al. [148] exposed confluent monolayer cultures of human vascular endothelium to a fluid shear stress of 2 dynes/cm^2 for 3h, approximately the stress occuring in human arteries *in vivo*. They reported that endothelial stress fibres could be induced in response to critical levels of fluid shear stress. This effect probably protects the endothelium from hemodynamic injury and detachment.

1.5.1.4 Other biochemical events

RAS

A local RAS exists in vascular and cardiac myocytes (1.3.1.3) [63] but its role has not been fully elucidated. The existence of these components has led to the suggestion that the growth factor, ANG II may be

generated locally in these tissues. ANG II production can be studied by measuring ACE activity, the enzyme responsible for the conversion of ANG I to ANG II (see Figure 6). Fischel et al. [149] found that a shear stress of 30 dynes/cm^2 for 24h produced a 70% reduction in cell growth of endothelial cells. This was accompanied by a 2.2 fold increase in ACE activity. The ability of ANG II to stimulate cell growth has been discussed in section (1.3.1.3). The effect of shear stress on ANG II production was examined in the expectation that shear stress would stimulate ANG II production, facilitate cell growth and thus play an important role in the development of vascular hypertrophy. However, shear stress inhibits ACE activity, results in a reduced ANG II production and therefore an inhibition of any growth signal which would be elicited by ANG II. This observation remains unexplained. Further studies verifying this inhibitory effect of shear stress on ACE activity are essential before a final conclusion can be drawn.

Prostaglandins

Prostaglandins are local hormones with short half-lives which exert paracrine and autocrine effects. Although some prostaglandins cause vasoconstriction, most seem to be vasodilator agents. Prostacyclin (PGI_2) can induce relaxation of blood vessels. Since prostaglandins can affect peripheral resistance, they may influence the rate of hypertrophy and possibly even contribute directly to hypertrophy.

The effect of mechanical forces on bone cells such as osteoblasts is of great interest. Previous studies have examined the role of mechanical forces in bone fracture repair [150]. This work is of interest to this project in that their aims were concerned with the ability of mechanical forces to stimulate growth. Reich et al. [137] looked at how osteoblasts in culture respond to mechanical strain. An increase in the rate of prostaglandin E_2 (PGE_2) was observed when they were exposed to shear stresses of between 6 and 24 dynes/cm^2. The effect of pulsatile flow on PGI_2 production by human endothelial cells was investigated by Frangos et al. [151]. The onset of flow led to a sudden increase in PGI_2 production which decreased to steady state within several minutes. The PGI_2 production rate of cells subjected to pulsatile shear stress was more than twice that of cells exposed to steady shear stress and 16 times greater than that of cells in stationary culture. This suggests that the pulsatile nature of blood flow *in vivo* may be an

important physiological mechanism for controlling PGI_2 production (Frangos et al. [152]).

Rubanyi et al. [153] measured the wall tension of intraluminally perfused canine femoral artery segments, and the content of the stable prostaglandin metabolite, 6-keto $PGF_{1\alpha}$. The relaxing activity of the effluent was determined by exposure to coronary artery rings. At steady flow, the effluent contained 6-keto $PGF_{1\alpha}$ and relaxed the bioassay rings. A sudden increase in steady flow from 2-4ml/min or the introduction of pulsatile flow, increased the release of 6-keto $PGF_{1\alpha}$ and induced further relaxations of the bioassay ring. No relaxations were observed with the effluent passing through a femoral artery segment without endothelium. Indomethacin depressed the release of 6-keto $PGF_{1\alpha}$ during increases in flow but the cyclo-oxygenase inhibitor did not affect the relaxation of perfused femoral artery segments containing endothelium. These results suggest that in addition to PGI_2, flow triggers the release of another relaxing substance from vascular endothelial cells. Grabowski et al. [154] also observed that shear stress stimulates prostaglandin production in endothelial cells. Stepwise increases in shear stress from 0-14 dynes/cm^2 caused rapid rises in PGI_2 production to peak values within 2 min, followed by a decline over several minutes. Peak PGI_2 production increased with severity of shear stress.

An increase in prostaglandin production in response to shear stress has been observed in a wide range of cell types. It is therefore likely that in such a situation, prostaglandins may assist in the control of TPR.

Endothelin

As has been previously discussed (section 1.3.1.4), endothelin exhibits growth promoting properties [81, 82, 83] in vascular tissue. Thus, endothelin availability is a factor of great interest. Sharefkin et al. [155] tested the effects of static culture versus high laminar shear stress (25 dynes/cm^2) on endothelin-1 precursor (preproendothelin) gene mRNA transcript levels and endothelin-1 peptide release in cultured human endothelial cells. Application of 25 dynes/cm^2 of shear stress for 24h sharply reduced endothelial cell levels of preproendothelin mRNA and decreased endothelin-1 peptide release into the culture medium.

Yoshizumi et al. [156] produced shear stresses using a rotating cone apparatus. Shear stresses of 8 dynes/cm^2 stimulated the synthesis of endothelin mRNA in polygonal endothelial cells with a peak signal observed within 2 to 4h and also increased the release of immunoreactive endothelin into the culture medium. The levels of endothelin mRNA in the ellipsoidal endothelial cells under high shear stress was not different from that of control level.

These observations suggest that low shear stress conditions favour an increased expression of endothelin gene and an increased release of endothelin into the medium. High shear stress conditions were shown to inhibit both expression and release. This provides evidence of endothelin's possible role in intimal hyperplasia. This condition occurs at sites of low shear stress where higher concentrations of endothelin-1 and increased synthesis of preproendothelin mRNA occurs.

NO

NO has a major role in maintainance of vascular tone.To evaluate the role of NO in flow-mediated control of vascular tone, the effect of shear stress on NO release was studied. The release of NO was greatly increased in porcine aortic endothelial cells on application of a shear stress of 6 dynes/cm^2 [157]. Kelm et al. [158] also looked at the effect of shear stress on NO release. This system involved using microcarrier beads onto which endothelial cells had been grown. Increasing flow from 2 to 20 ml/min enhanced the basal NO release from endothelial cells fivefold. Buga et al. [159] using a similar *in vitro* bioassay system confirmed that increasing the perfusion pressure increased NO release.

Hutcheson et al. [160] perfused rat aortic segments with a buffer solution, using a peristaltic pump at a constant mean flow rate of 9ml/min. Any NO activity induced by shear stress was measured by its ability to relax preconstricted, endothelium-denuded, rat aortic rings. When examining the effect of frequency on shear stress-induced NO release, the amplitude was maintained at 2mmHg while the frequency was varied between 0.1-12Hz. The effect of a varied amplitude was studied by maintaining a frequency of 1Hz and varying amplitude within the range of 2-16Hz. The relaxation of the aortic segments was found to

depend on the applied frequency of shear stress with maximum relaxation obtained between 4.2 and 6Hz. In contrast, increasing the amplitude component facilitated a further constriction of the segments. Incubation of the donor vessel with a NO synthesis inhibitor or removal of the endothelium from the vessel by rubbing, abolished these frequency and amplitude effects.

Shear stress can stimulate NO release from cells. This action may possibly compensate for any change in vessel tone which has been induced by the shear stress. Both the frequency and amplitude components of shear stress control NO release but they produce contrasting effects.

Interleukins (IL)

IL are known to participate in the formation of atherosclerotic plaques. They thus have a role in the development of cardiovascular disease. Cultured bovine aortic endothelial cells secrete IL-1 and IL-6 in small quantities. Cucina et al. [161] subjected endothelial cells to a shear stress of 6 dynes/cm^2 and found an increased production of both IL-1 and IL-6. Thus shear stress increases interleukin production but their precise purpose is not yet clear.

Lipoproteins

Lipoproteins are molecules composed of triglycerides, phospholipids, cholesterol and protein. Their principal function in the plasma is to transport lipids throughout the body. Lipoproteins can be classified by their composition of triglycerides, phospholipids, cholesterol and protein, into three main categories: very low density lipoproteins (VLDL), low density lipoproteins (LDL) or high density lipoproteins (HDL). LDL participates in the formation of atherosclerotic plaques which can lead to ischaemia and disease.

Bovine aortic endothelial cells were incubated with ^{125}I-LDL labelled with a radioactive isotope of iodine, for 2 to 24h, in the presence of shear stress levels of 30 dynes/cm^2 [162]. Increased LDL internalisation was observed after 24h but non-specific LDL endocytosis was not influenced by shear stress levels. This suggests that shear stress (flow) influences LDL internalisation and may provide a potential mechanism by which LDL participates in the formation of atherosclerotic plaques.

1.5.2 Stretch

In vivo, cells are exposed to a pressure component as well as a component of shear stress. To mimic the pressure component *in vitro*, models have been designed which can expose cells to a controlled stretching force, resulting in an increase in the length of the cell. Several groups have examined the phenomenon of stretching on a variety of cell types and a diverse range of responses. The following section summarises the *in vitro* studies which have been performed in this field. The most popular techniques utilised are described in section 1.6.

1.5.2.1 Biochemical events involved in growth

Ion channel activation

This is a possible mechanism by which a growth response can be evoked in a cell. The ability of shear stress to stimulate K^+ channel activation has been mentioned previously (1.5.1.2). The effect of stretch on ion channel activation will now be reviewed in the following section.

The most common technique used in ion channel studies is that of patch clamping. This involves applying suction to the cell membrane using a micropipette. The application of suction causes the membrane to be stretched and can result in the opening of ion channels. Lansman et al. [128] investigated the effect of stretching the cell membrane of aortic endothelial cells. A channel permeable to Ca^{2+} was activated and its opening frequency shown to increase with increasing stretch. Davis et al. [163] discovered that patch pipette suction activated a non-selective cation channel that was permeable to K^+, sodium ions (Na^+) and Ca^{2+}, in vsmc. Taniguchi et al. [164] examined the effects of membrane stretch on Ca^{2+}-activated K^+ channels in rabbit thick ascending limb cells, also by using a cell patch clamp technique. Pressure applied to the patch membrane increased fractional open probability in the presence of Ca^{2+} in the pipette. The activity returned to control on releasing the negative pressure. Large conductance, Ca^{2+}-activated K^+ channels in rabbit pulmonary artery smc were activated by membrane stretch [165]. Activation by stretch appeared to occur by a direct effect of stretch on the channel itself or a closely associated component. In patches of cell

membrane, stretch activation was seen under conditions which avoided involving cytosolic factors, release of Ca^{2+} from intracellular stores, stretch-induced transmembrane flux of Ca^{2+} or other ions potentially capable of activating the channel. Membrane stretch by patch clamping activated single-channel ionic currents in cultured mesangial cells which were permeable to Na^+, K^+ and chloride ions (Cl^-)[166]. Channel opening probabilities were directly related to the degree of suction, with threshold activation achieved for 5-10 mm Hg. These channels may represent a cellular mechano-reflex in mesangial cells. Ypey et al. [167] discovered that stretching the membrane of chick osteoclast cells activates channels permeable to K^+, Cl^- and phosphate ions. Using patch-clamp electrophysiology, Bear [168] discovered a non-selective cation channel permeable to Na^+, K^+ and Ca^{2+} in rat liver cells.

The above studies show that ion channel activation is a stretch-mediated response induced in a range of cell types. The presence of mechanotransducing ion channels in such cells suggest that this is a common mechanism by which cells respond to an altered mechanical load.

Inositol phosphates

The effect of mechanical strain on phosphoinositide turnover has been studied as a potential second messenger involved in stretch-mediated effects. 20% stretch of pulmonary vsmc for 45s resulted in increased intracellular masses of IP_3 and inositol tetraphosphate (IP_4); 34±7 % and 58 ±12 % respectively [169]. Repetitive stretch of these cells did not further alter the masses of either of the compounds. Stretching also increased inositol phosphate levels in cardiocytes [170]. Rosales et al. [171] deformed endothelial cells using a cyclic, vacuum system (see section 1.6) and looked at the effect of strain on inositol phosphate production. Two procedures were adopted. The first set of experiments involved deforming endothelial cells at a frequency of 60 cycles/min for either 0, 1, 5, 10, 25, 50 or 100 cycles of stretch. The second involved deforming cells at a frequency of 60 cycles/min for 24h and then increasing the the frequency to 100 cycles/min for 0, 1, 5, 10, 25, 50 or 100 cycles. In each set of experiments lithium chloride was included, to minimise inositol phosphate degradation. The results demonstrated that either the initiation of pulsatile stretch or an acute change in the

cyclic stretch frequency stimulated the generation of IP_3, its metabolites inositol diphosphate (IP_2) and inositol monophosphate (IP) and diacylglycerol. Brophy et al. [172] looked at the effect of decreasing cyclic strain on IP_3 generation in endothelial cells. No differences were found in IP_3 mass between endothelial cells that were stationary for 24h and cells exposed to cyclic strain for 24h. An immediate, significant increase in IP_3 was observed after a decrease in strain frequency. These results suggest that it is a change in the stretch frequency which elicits phosphoinositide hydrolysis in endothelial cells and that steady state cyclic strain conditions have no effect on hydrolysis.

The effect of stretch on phosphoinositide hydrolysis has also been examined in the intact rat heart. Increased release of inositol phosphates was detected when the right atria of rats were stretched [173]. The procedure involved inserting a balloon into the right atrium of the heart via the vena cava. Using a syringe the balloon was inflated and the atrium stretched. Stimulation was detectable after 1 min with significant increases observed after 10 or 20 min.

Isolated cells and intact tissues have shown a stimulated rate of phosphatidylinositol hydrolysis, in response to stretch. From the results it appears that a change in the strain experienced by the cells is the major factor which affects the rate of hydrolysis. An increased phosphatidylinositol hydrolysis is an event observed prior to cell growth. This therefore favours a role for stretch in the stimulation of growth.

PKC

The above results suggest that PIP_2 hydrolysis occurs in response to stretch. Thus it is interesting to see whether stretch stimulates PKC activity. Rosales et al. [174] subjected endothelial cells to a 24% strain at 60 cycles/min and observed a biphasic translocation of PKC from the cystolic to the membrane fraction. There was an early rise in PKC activity in the membrane at 10s which paralleled those of IP_3 and DAG concentrations, and a second rise which occurred after 100s of cyclic strain and was sustained up to nearly 8 min. These results support the ability of stretch to stimulate PKC activity via an increased DAG production. Such events are important in the stimulation of cell growth.

Ca^{2+}

The effect of stretch on $[Ca^{2+}]_i$ has also been studied.

Katusic et al. [175] suspended rings of canine basilar arteries in organ chambers and measured isometric tension using a force transducer. Stretch applied to the arteries caused the development of active tension in rings with endothelium but not in those in which the endothelium had been removed. Blockade of Ca^{2+} entry with diltiazem, or inhibition of cyclo-oxygenase with indomethacin, abolished the endothelium-dependent response to stretch. These results suggest that Ca^{2+} channel activation stimulates the release of a factor from the endothelium which may be identified as a prostaglandin.

Wirtz et al. [176] applied hydrostatic pressure to rat alveolar type II cells and measuredthe $[Ca^{2+}]_i$ in single cells, before and after stretching. A single stretch of 16% caused a transient increase in cytostolic $[Ca^{2+}]$. Both Ca^{2+} mobilisation and exocytosis exhibited dose-dependence to the magnitude of the stretch stimulus.

The purpose of the study conducted by Armstrong et al. [177] was to determine if passive stretch of rat soleus muscles would increase total muscle $[Ca^{2+}]$ and mitochondrial $[Ca^{2+}]$. Soleus muscles from female rats were isolated and incubated *in vitro* for 2h at resting length, or at the maximal *in situ* length. Total muscle $[Ca^{2+}]$ and mitochondrial $[Ca^{2+}]$ were elevated in both groups.

Each of these studies uses different techniques but all illustrate the fact that Ca^{2+} plays an essential role in stretch-mediated responses. The results support the assumption that stretch increases phosphoinositide hydrolysis, the formation of the products IP_3 and DAG and that IP_3 formation facilitates Ca^{2+} release from intracellular bound stores.

Proto-oncogenes

In section (1.3.1.1) the importance of proto-oncogenes in the control of growth has been reviewed. Komuro et al. [131] stretched rat neonatal cardiocytes by 9.3 ± 0.9 % and demonstrated that stretch stimulated *c-fos* expression in a stretch length-dependent manner. This was followed by an increase in amino acid incorporation into proteins. *c-fos* mRNA rose within 15 min of cardiocyte stretching, peaked at 30 min and declined to undetectable levels by 240 min. In the presence of cycloheximide, a protein synthesis inhibitor, a greater increase in *c-fos*

mRNA was observed on stretching, suggesting that this gene expression was not stimulated by newly synthesised proteins. A transfected chloramphenicol acetyltransferase (CAT) gene, used as a reporter gene, was linked to upstream sequences of the *c-fos* gene including its promoter and transfected into myocytes. On stretching these myocytes, the *c-fos* and CAT genes were expressed, suggesting that mechanical loading regulates *c-fos* mRNA transcription.

Sadoshima et al. [178] also examined the effect of stretch on *c-fos* induction in neonatal cardiocytes. However, this study also looked at the expression of *c-myc*,*c-jun* , the zinc finger class gene, Egr-1 and the cytokine-like gene, JE, in response to a 20% stretch. Peak expression was observed at 30 min for *c-fos* , *c-jun* , JE and Egr-1. Peak *c-myc* expression was attained at 1h. 12-48h of 20% stretch caused a progressive accumulation of ANP (1.3.2) and skeletal α-actin mRNAs (1.5.2.3). In this study, stretching for 48h induced the expression of β–myosin heavy chain mRNA. Shorter periods of stretch stimulated the expression of proto-oncogenes which as has been previously discussed are involved in the process of cell growth. Longer periods of stretch stimulated the expression of fetal genes; these genes have been shown to cause phenotypic changes that are characteristic in *in vivo* models of hypertrophy [117]. The fact that this *in vitro* study has initiated changes which occur in the *in vivo* situation is an encouraging indicator that stretching systems closely mimic the pressure force which is experienced in the vessel wall.

Stretching of cardiac myocytes also increased *c-fos* mRNA levels [179]. The accumulation of *c-fos* mRNA by stretching was suppressed by PKC inhibitors but not by stretch channel blockers. Activation of PKC by phorbol esters stimulated the synthesis of *c-fos* mRNA. Another factor which stimulated *c-fos* expression was sodium influx. However, the addition of stretch channel blockers did not affect *c-fos* mRNA production. Why sodium influx stimulated *c-fos* mRNA expression remains unexplained.

Proto-oncogene and fetal gene expression have been induced in response to stretch. The above experimental findings suggest that PKC activation is the mechanism by which proto-oncogene expression is induced in myocytes and cardiocytes. It is reasonable to assume that PKC activation is also responsible for the expression of the fetal genes in response to cardiocyte stretching. This evidence further supports the

the ability of stretch to stimulate second messenger systems which are involved in cell growth.

Protein synthesis

After gene expression has been induced the next step in the sequence of events is protein synthesis. Mann et al. [180] examined the growth-regulating effects of load changes in the isolated, quiescent, adult cardiocyte. An approximate increase in length of 10% resulted in mean increases of 186% in nuclear RNA synthesis and 89% in cytoplasmic protein synthesis.

Banes et al. [181] using a vacuum system (see section 1.6) exposed a fibroblast layer to a pressure of 0.13%, for periods of 25s stress and 5 min relaxation. This activity had no effect on a protein that co-migrates with actin, whereas a protein that co-migrates with tubulin decreased from 12.7 ± 0.451% in control cells to 8.53 ± 0.182 % in stretched cells. Mechanical load has inhibited the synthesis of a protein in this case.

The effect of mechanical activity in the tibialis anterior muscles of rabbits, was studied by Goldspink et al. [182]. Electrical stimulation in this muscle produced an increase in protein synthesis.

Both increased and decreased protein synthesis has been induced by exposing cells to a mechanical force. It is important to recognise that different techniques were used and that different cell types were studied. Thus further work is required to explain these contrasting observations.

1.5.2.2 Cell growth

DNA synthesis

The effect of stretch on the rate of DNA synthesis in a cell, is a very attractive area of study because increased DNA synthesis is observed prior to cell division. Thus measuring DNA synthesis gives a good indication of tissue growth. Hasegawa et al. [183] stretched bone cells by 4% and observed a 64% increase in the number of cells synthesising DNA. Brunette [184] discovered a similar increase in DNA synthesis on stretching epithelial cells by 4.2%. The ratio of cells with increased DNA synthesis in cultures stretched for 2h, to those in unstretched controls was 1.92±0.34.

Sumpio et al. [185] exerted a 24% strain on porcine smc for 10s, followed by a 10s relaxation, for 7 days. This cyclic tension decreased cell number and DNA synthesis in comparison with control smc. This is in contrast to the results of previous studies for endothelial cells. Sumpio et al. [186] had previously showed increased proliferation in endothelial cells when exposed to cyclic stretch. The cells maintained a random orientation whereas smc exhibited a decreased proliferation and were shown to adopt a uniform pattern. Fetal rat lung cells were exposed to 48h of an intermittent stretch pattern of 5% elongation at 60 stretches/min for 15 min, of each hour. Cell numbers were increased by 10%, cell doubling time was reduced from 71 to 55 hours, ^{3}H thymidine incorporation into DNA increased by 61% and the thymidine labelling index increased 2.8 fold, compared to non-stretched controls [187]. This effect did not appear to be mediated by prostaglandins or leukotrienes because ibuprofen or BW 755C, prostaglandin synthase inhibitors, leukotriene biosynthesis inhibitors BW 755C or MK-866 and leukotriene D_4 receptor antagonist MK-571 did not abolish stretch mediated effects. Nishioka et al. [188] applied cyclic stretch to osteoblast-like (HT-3) cells and measured [^{3}H] thymidine incorporation. Within 5 days of cyclic stretch, DNA synthesis was increased approximately 3-fold.

It is apparent that whether stretch induces an increase or decrease in DNA synthesis is dependent on which cell type is being studied. It is therefore necessary to be cautious when extrapolating results from one tissue to another.

Proliferation

The most accurate index of growth is to look at the rate of growth itself. Vandenburgh et al. [189] developed a computerised system which applied forces similar to those experienced by differentiating skeletal muscle myoblasts. This system generated three dimensional artificial muscles. These muscles contained parallel networks of long unbranched myofibres organised into fascicle-like structures. Tendon development was initiated and the muscles were capable of performing directed functional work.

The study of Antonio et al. [190] investigated the effect of stretch on avian muscle fibres. A weight equal to 10% of the bird's mass was

attached to the right wing while the left wing served as the intra-animal control. The weight was attached to the wing for 24h periods interspersed with 48 to 72h rest intervals. The actual stretch time was 5 days while the length of treatment was 15 days. Muscle mass and length was shown to increase significantly 53.1+/- 9.0 and 26.1+/-7.3% in the stretched anterior latissimus dorsi. Fibre number remained unchanged. Mean fibre area increased significantly by 27.8+/-6.0% in the stretched latissimus dorsi. These results indicate that stretching muscle fibres can stimulate their growth. In this study, intermittent stretch produced muscle fibre hypertrophy without fibre hyperplasia.

Until now, the effect of a physical force on processes which are involved in cell growth have been examined but now these studies have gone one step further to look at the growth process itself. The above experimental evidence confirms that a stretching force can stimulate cell growth via the second messenger events which have been previously discussed.

1.5.2.3 Cell morphology and structure

Shear stress can alter cell shape (1.5.1.3). Does stretch have an effect on this parameter? The majority of smc of muscular and elastic arteries are orientated at an angle of 20-40° to the longitudinal axis of the artery. Betz et al. [191] reported that repeated local transmural electrical stimulation of the carotid artery wall of rabbits caused a proliferation of smc into the subendothelial space. The smc of the proliferate lie with their longitudinal axis parallel to the direction of flow, i.e. at right angles to the resultant vector of the distending forces. Within 6 months after a 4 week stimulation period, the subendothelial cells of the proliferate change their orientation and are finally arranged as in the normal media, whereas the cells at the base of the proliferate remain in an orientation parallel to the longitudinal axis of the artery.

Dartsch et al. [192] found that mechanical stimulation of aortic smc to produce an increase in cell length within the range of 2-20%, altered the orientation of the vsmc. The cells which were stretched with an amplitude of 2% remained in random orientation after 14 days of continuously performed cyclic stretching. The cells which were stretched 5% for 12 days orientated at an angle of 61± 9 degrees to the direction of stretching, while the cells which were stretched with an

amplitude of 10% for 6 days orientated at an angle of 76±5 degrees. The cells on stationary and unstretched membranes remained in random orientation.

Terracio et al. [193] subjected cardiac myocytes, endothelial cells and fibroblasts to a 10% cyclical distention 10 times/min for 72h. Within 24h of being exposed to the mechanical stretch, the cells became elongated and orientated perpendicular to the direction of the stretch. This indicates that cyclical mechanical stimulation directly influences the cellular organisation of the heart cells *in vivo*. Samuel [194] stretched adult rat cardiac myocytes in a unidirectional manner, using a computerised mechanical cell stimulator. A continuous unidirectional stretch of the substratum during the cell attachment period induced a 3-fold increase in the number of rod-shaped myocytes orientated parallel to the direction of movement.

Stretch can therefore affect the orientation of cells. To determine whether physical forces can alter cell shape by reorganising the cytoskeleton, the effect of stretch on actin gene expression was determined [195]. Fibroblasts were stretched within the range of 0-9.2%. 9.2% stretch produced the greatest increase in F-actin gene expression and 3.3% the least. These observations provide evidence that the microfilament system of fibroblasts exhibits rapid dynamic responses to mechanical deformation which may result in an altered cell shape. Mesangial cells were exposed to continuous stretch-relaxation for 72 to 96h at a rate of 100 cycles/min at an applied pressure of 7 to 8kPa [196]. Fluorescein-isothiocyanate-labelled phalloidin staining indicated an increase in the density of actin filaments in these cells.

The fact that stretch can alter cell orientation may be of importance in the process of remodelling which is observed in hypertension. The fact that actin gene expression is affected by stretch may explain why this change in cell behaviour has occurred. Any effects load may have on actin could result in vasoconstriction, increased resistance and elevated blood pressure.

1.5.2.4 Other biochemical events

Adenosine 3' 5'-cyclic monophosphate (cAMP)

The enzyme AC is present in the plasma membrane of most cells. In the presence of magnesium ions, this enzyme catalyses the conversion of

ATP to cAMP. cAMP functions to promote protein kinase activation, a second messenger effect which may be important in cell growth. It is broken down by phosphodiesterases. Does stretch affect this system?

Mills et al. [197] examined the effect of a strain of 24% on AC activity (ACA), in porcine, coronary artery smc. ACA decreased significantly after 5 min. However, the extent of reduction did not become more significant after 30 min of strain. Adopting a similar procedure, this group have also shown that basal and forskolin stimulated ACA were stimulated by acute cyclic strain, in bovine aortic endothelial cells [198]. ACA increased progressively from 1 to 5 min and returned to basal by 7 min. Because ACA is increased in response to strain in endothelial cells the effect of strain on cAMP levels was determined. Iba et al. [199] were unable to detect an increase in cAMP levels in human saphenous vein endothelial cells. These experiments were performed in the presence of the the phosphodiesterase inhibitor, 3-isobutyl-1-methylxanthine (IBMX), to prevent the degradation of cAMP.

At present, it is unclear why contrasting results were obtained for ACA activity, in smc and endothelial cells. Why an increased ACA activity did not elicit an increase in cAMP levels in the presence of IBMX is also unclear and requires further validation.

Prostaglandins

As previously mentioned, prostaglandins such as PGI_2 which exerts a vasodilator action, are involved in the control of vessel calibre. Therefore, any effect mechanical load may have on the production/release of this factor is of vital importance. Differences in secretion of PGI_2 by venous and arterial endothelial cells, grown in a static or mechanically active environment, was investigated by Upchurch et al. [200]. Endothelial cells from bovine aortas and venae cavae were subjected to cyclic deformation, up to 17% elongation and 60 cycles/min. After 3 to 5 days the supernatant fluids were assayed for PGI_2 activity. Under static or control conditions, venous endothelial cells secreted significantly more PGI_2 than did arterial cells from the same animal. Sumpio et al. [201] subjected aortic endothelial cells to 10s cycles of 24% elongation and 10s of relaxation for 1, 3 or 5 days. The medium was collected to assess for PGI_2 activity. Cyclic stretching

increased PGI_2 activity in a time-dependent manner. Carosi et al. [202] cyclically strained bovine aortic endothelial cells by 5% or 10%, for 24h at 1Hz. At a physiological level of 10% cyclic strain, PGI_2 secretion rates were increased by 2.5- fold above stationary controls. Because no effect was observed at 5%, it is evident that a threshold level of activation was required before an increase in PGI_2 secretion could occur. A stretch frame was utilised by Vandenburgh et al. [203] to stretch skeletal muscle by 20%. This resulted in increased prostaglandin synthesis.

Each of these studies agrees that stretching can induce PGI_2 production. This may be a general effect for different cell types as enhanced PGI_2 production was observed in both endothelial cells and skeletal muscle. Under conditions of stress, PGI_2 production may be stimulated by cells to compensate for any changes in vessel calibre which this state may have induced.

Endothelin

The activity of the potent vasoconstrictor endothelin in a cell is one of the factors which determines vessel diameter and hence resistance. The way in which the cell responds to mechanical stretch with respect to endothelin, has not been fully elucidated.

Bovine aortic endothelial cells increase production of endothelin into culture medium up to 6-fold in response to cyclic stretch [202, 204].

Harder et al. [205] looked at the effect of increased pressure on cerebral artery function. When the cerebral arteries were pressurised to between 40 and 160 mmHg, there was a 13.2% reduction in diameter. The reduction in diameter was lost and vessels dilated to pressure when the endothelium was removed. When the denuded vessel was exposed to an intact donor vessel, the denuded vessel recovered its ability to contract, suggesting that increased pressure may cause the release of a contractile substance from the vascular endothelium. Oxyhemaglobin, a NO antagonist, did not alter the response to pressure in these isolated cerebral arteries further suggesting that the reduction in diameter results from the release of a contractile substance from the vascular endothelium, and not inhibition of NO.

NO

If stretch altered release of NO, this may have an adverse effect on vessel diameter. The enhanced release of NO resulting from increasing the tension of aortic rings of rabbit aorta was described by Ohno et al. [206]. The levels of the second messenger guanosine 3', 5'-cyclic monophosphate (cGMP), which is stimulated by NO, was monitored on stretching the aortic rings. Tissue cGMP levels significantly increased with the increase in resting tension in endothelium-intact rings, but not in denuded rings. These stretch-induced endothelium-dependent tissue cGMP increases were unaffected by the calcium channel blockers, nicardipine and diltiazem.

Hishikawa et al. [207] exposed human endothelial cells to increased pressure by pumping compressed helium into the flask in which they had been grown. Increasing the transmural pressure was shown to decrease NO release from endothelial cells .

In aortic rings, pressure was shown to increase NO release, but in endothelial cells a decrease was observed. In these studies, different cell types and different animal models were used. This is the best explanation for these contrasting results. Further work is required to verify the effect of pressure on NO production.

Tissue plasminogen activator (t-PA)

The fibrin component of clots are broken down by the serum protease, plasmin. Plasmin is formed by the activation of plasminogen, an inactive precursor. This conversion is carried out by t-PA. The activity of t-PA can be controlled by the action of plasminogen activator inhibitor (PAI-1).

Due to vessel wall damage, vascular cells may be exposed to a high pressure environment. After completion of the clotting process, the magnitude of forces may decrease and conditions return to normal. It is obvious that such cells experience a range of different pressures throughout this process. Do changes in pressure influence the production of factors involved in vessel repair?

Increased levels of t-PA were found in the culture medium of endothelial cells subjected to cyclic stretch [208].

ECM

The ECM represents a major component of the cell which actively participates in signal transduction (see section 1.3.1.5). It is therefore important to determine whether mechanical stress causes a modification of cell structure and/or matrix elaboration which may then affect the function of specific second messenger systems. Sumpio et al. [209] subjected smc to a regimen of 10s elongation (25%), followed by 10s relaxation, continuously for 5 days. This three-cycle-per-min stretching stimulated smc production of collagen. Bovine aortic endothelial cells were subjected to 24% cyclic deformation, 3 cycles/min, 10s of elongation alternating with 10s of relaxation, for 5 days [210]. Endothelial cell production of collagen was inhibited with repetitive deformation. The reasons why smc increased collagen production but endothelial cells reduced production in response to stretch, using a similar procedure, are presently unclear.

Harris et al. [196] examined the effect of continuous stretch-relaxation upon mesangial cell growth and function. Mesangial cells were exposed to a continuous stretch-relaxation regimen for 72 to 96h at a rate of 100 cycles/min at an applied pressure of 7 to 8kPa. The peak and minimal deformation values were chosen to represent glomerular capillary pressures *in vivo*. The mesangial cells adopted a stellate or straplike morphology. The mechanical stretch/relaxation treatment increased the % of protein representing collagenous proteins in these cells with an increase in the relative amounts of types I and III collagens. There was a selective increase in the relative amount of type I homotrimer, a molecular form of type I collagen. Furthermore, Riser et al. [211] found that exposing mesangial cells to repeated mechanical strain increased collagen type IV and collagen type I production. This evidence suggests that high pressures like those which exist in the condition of nephrosclerosis, induce the production of proteins in mesangial cells which may have a potential role in the development of this state.

Leung et al. [212] used a motor system to stretch arterial smc cyclically and found that this treatment resulted in up to fourfold increase in the rates of type I and III collagen, hyaluronate and chrondroitin 6-sulphate synthesis. Synthesis of types I and III collagen was increased to the same degree. Nishioka et al. [188] applied cyclic stretch on HT-3 cells using a computerised, pressure-operated

instrument that physically deformed cells. The synthesis of collagenous protein in the cell extracts, after cyclic stretching, was examined on day 7 and findings compared with those of static controls. HT-3 cells cultured under conditions of cyclic stretch produced significant amounts of collagenous protein. Stretching appears to be a powerful stimulus for collagen production in different cell types.

Sottiurai et al. [213] showed that subjecting arterial smc to 110% stretching of their original length, 52 times/min for 8, 48 and 56h caused myofilaments to be largely replaced by rough endoplasmic reticulum. Cyclically stretched cells were also shown to form numerous intercellular contacts and showed little evidence of cytoplasmic degradation while stationary cells showed few contacts and contained numerous cytosomes and lamellar bodies. Stretch had induced significant changes in the components of the ECM which may have pronounced effects on the signalling mechanisms of these cells.

Studies on endothelial cells suggest that one class of cell adhesion molecules, integrins, act as mechanoreceptors and transmit mechanical signals to the cytoskeleton [214].

Two components of the ECM, namely collagen and integrins are affected by cell stretching. These results suggest that stretching may have pronounced effects on the transduction of signals throughout the matrix.

ANP

ANP is released by atrial distension *in vivo*. Application of tension to atrial cardiocytes *in vitro* causes a dose-dependent increase in immunoreactive ANP release into the culture medium [215].24h after the stretch stimulus, an increase in ANP mRNA levels could be detected. The calcium channel blocker, verapamil, had no effect on stretch-dependent immunoreactive ANP release, whereas the calmodulin inhibitor, calmidzolium, suppressed basal as well as stretch dependent secretion. This implies that an important relationship exists between intracellular calcium metabolism and immunoreactive ANP release.

ANP secretion was measured in non-contracting preparations of combined right and left rat atria by Page et al. [216] who found that by increasing distending pressure, ANP secretion was increased. Schiebinger et al. [217] stimulated ANP production in isolated rat left atria using norepinephrine and endothelin. By altering the tension of the

atria in the range of 0, 0.5, 1.5 g, an increased ANP production in response to these stimuli was attained. The maximum ANP concentration was achieved at a tension of 1.5 g. The possible role of pressure as a stimulus for increased ANP production in ventricular hypertrophy was investigated by Kinnunen et al. [218]. ANP gene expression was increased in the hypertrophic ventricular cells of SHR. Stretching of the ventricles produced a rapid but transient increase in ANP secretion and ANP release with rising pressure. Newman et al. [219] quantified the secretion of ANP-containing granules in myocytes in response to different degrees of atrial distension. Stretch was produced by altering the perfusion pressure and hence altering the degree of distension of rat atria. By increasing the degree of distension of the right atrium a proportional rise in the release of secretory granules from individual myocytes was produced. This supports the ability of stretch to stimulate ANP secretion from secretory granules.

Enzyme activity

To study the effect of stretch from a more general viewpoint, it is ideal to study the activity of enzymes which are always present in the cell. Creatine kinase which is associated with energy production in heart and skeletal muscle and alkaline phosphatase which is involved in bone growth, are examples of such enzymes. Vandenburgh et al. [220] used a mechanical cell stimulator to stretch and relax muscle cells. In this study, the skeletal muscle was exposed to a stretching force which ranged from 3.5-46%. Initiation of mechanical stimulation increased the efflux of creatine kinase during the first 8-10h of activity but the efflux rates returned to control levels after this time period. Decreased total cell protein content accompanied the elevation of creatine kinase efflux. Creatine kinase release from a cell is normally indicative of cell death. Thus, it is not surprising that a decrease in protein content was also observed which suggested cell damage/death had been induced by the stretch regimen. These observations can be explained by the fact that large values of stretch were used which obviously damaged the cells and resulted in release of creatine kinase and possibly other proteins from the cells.

Nishioka et al. [188] applied cyclical stretch to osteoblast-like cells using a computerised, pressure-operated instrument. Cyclical stretch enhanced alkaline phosphatase activity. The effect was considered to

be regulated through PGE_2 production because stretch reduced levels of PGE_2 in the medium. When PGE_2 was added there was a significant decrease in alkaline phosphatase activity. The reason why stretch stimulates alkaline phosphatase activity and the mechanism by which PGE_2 affects this activity are not clear and require further study.

Metabolic rate

Metabolic rate can be studied by measuring glucose uptake by the cell since glucose is the energy source required for glycolysis. It is also reasonable to measure lactate release because this is a byproduct of glycolysis during increased skeletal muscle function. Hatfauldy et al. [221] mechanically stimulated avian pectoralis muscle cells by repetitive stretch-relaxations of the cells substratum and studied the effect on the rates of deoxy-D-glucose uptake and lactate efflux. During the first 4-6h of mechanical stretching, the deoxy-D-glucose uptake and lactate efflux increased 34 and 26% respectively. At 8 and 24h of activity, neither parameter was elevated relative to control values. Rates significantly elevated with continued activity beyond 24h and reached maximum levels by 48h.

No significant increase in the rates of deoxy-D-glucose uptake and lactate efflux at 8 and 24h activity can be explained by the fact that the increased glycolysis observed during the first 4-6h produced a dramatic increase in lactate levels which led to inhibition of glycolysis. An increased lactate concentration decreases the $[pH]_i$ and inhibits glycolytic enzymes present in the cell. In muscle and blood, lactate levels are quickly removed and metabolised, a circulatory system does not exist in tissue culture and lactate levels can therefore accumulate to inhibit glycolysis. In the experiment the tissue-cultured muscle cells were fed fresh medium at 24h, this would result in a change in the intracellular pH of the cells. This is why glycolysis was seen to resume after 24h.

Parathyroid hormone-related protein (PTHrP)

PTHrP exhibits similar biological effects to parathyroid hormone. The expression of the parathyroid hormone gene is confined to the parathyroid gland but PTHrP expression is found in mammalian and

avain tissues. The function of PTHrP in these tissues is unknown but such a widespread distribution suggests a paracrine or autocrine role.

PTHrP in the pregnant rat uterus is dependent on the occupancy of the uterus by the fetus. PTHrP gene expression is dependent on the degree of stretch of the uterus. To determine whether stretch of smooth muscle is a stimulus for PTHrP gene expression, its activity was measured in uterine tissue and in the rat bladder. An intrauterine balloon system was developed that allowed experimental reproduction of the mechanical effects of the fetal pup *in utero* [222]. Increased PTHrP mRNA in the unoccupied horn of unilaterally pregnant or virgin rats could be elicited as early as 1h after balloon inflation and was maintained for up to 72h. This suggests that mechanotransduction is responsible for a preterm peak in PTHrP mRNA expression. The effect of stretch on PTHrP in the rat urinary bladder was measured by Yamomoto et al. [223]. It was observed that under normal conditions, the PTHrP mRNA levels in the bladder correlated with the urine volume, i.e. the extent of bladder distension. When bladders were distended by the accumulation of urine, levels of PTHrP mRNA increased dramatically with time. On limiting the distension to one half of the bladder, the increase in mRNA was observed only in the distended portion.

These observations verify a physiological role for PTHrP in uterine and bladder smooth muscle function.

Arrythmias

Previous observations have shown that stretch can cause the release of a factor(s) which can have a slowly developing effect on the cardiovascular system. Studies on isolated hearts have shown that stretch can also have an instant action on the heart by triggering arrythmias [224, 225]. This can lead to ventricular fibrillation which is frequently fatal. It is therefore necessary to study this action of stretch in greater detail.

1.6 Methods used to exert pressure on cells

When designing a system to exert physical forces on cells, many factors have to be considered. The first is whether a compressive force which will produce a decrease in cell length or a stretching force which will increase cell length is required. The range over which the force will function is a very important initial factor because if this has to be altered expensive changes in the design of the system may be required. The ability of the system to provide a reproducible force is also necessary. The size of the system has to be considered and will depend upon which factor is being measured e.g a large number of cells are required for RNA extraction when measuring changes in mRNA levels induced by a particular stimulus. Thus, the system has to be large enough to facilitate a reasonable cell growth. The system must be sterile so as to minimise any contamination problems.

The following section describes the more popular used techniques which have been developed to look at the effect of pressure on cellular function.

1.6.1 Petriperm dishes

Petriperm dishes are cell culture dishes which are manufactured by Bachofer Ltd, Germany. These dishes have flexible membrane bases which can be deformed. Important features are that they facilitate the growth of a number of different cell types and their tightly fitting lids minimise contamination.

Using the principle of Petriperm dishes, Hasegawa et al. [183] devised a simple method for applying mechanical stretching to bone cells, as shown in Figure 9. Bone cells were cultured in the flexible membrane of Petriperm dishes. The dishes were placed over a template with a convex surface and then a lead weight was placed on top of the dish. This caused the membrane to adopt the shape of the template and thus stretched the membrane and the tightly attached cells. A template producing a 4% increase in surface area was used. The deformation of the dish was reversible, making it possible to alternate periods of mechanical stretching with periods when no stress was applied; i.e a cyclic regimen. As already mentioned, the degree of stretch was dependent on the curvature of the template and could be

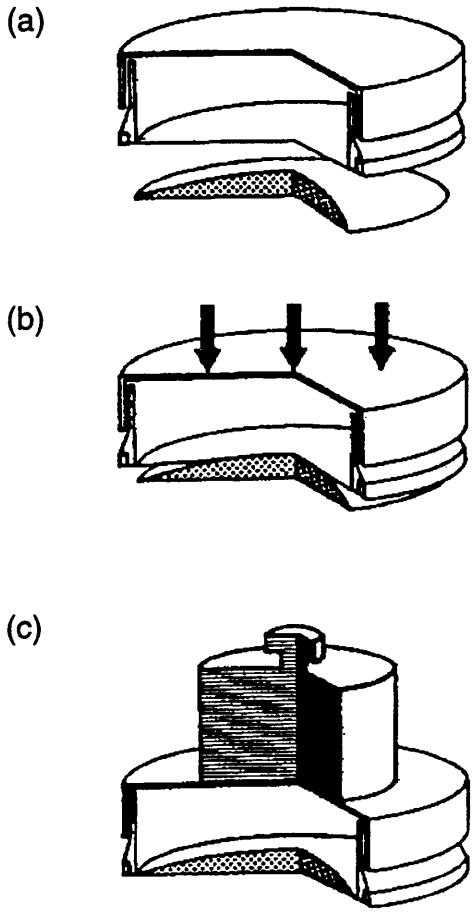

Figure 9 A schematic representation of the apparatus used to stretch cells, from Hasegawa at al. (183).

(a) The system is composed of a petriperm dish and a covex template.

(b) The petriperm dish is placed on top of the convex template.

(c) A weight is then placed on top of the dish, causing the flexible base of the dish to be upwardly displaced, to adopt the shape of the convex template. Cells grown in the dishes are therefore stretched.

varied by either changing the curvature of the template or by altering the weight applied.

More recently, Gardner et al. [215] also used Petriperm dishes to stretch atrial cardiocytes. The cells were grown in the dishes and placed over a reservoir containing saline solution. By infusing a known volume of saline into the resevoir, the flexible membrane of the petriperm dish was upwardly displaced and thus the attached cells stretched.

There are several problems with these methods. It is inconvenient to be continually applying and removing a weight or infusing and removing saline when conducting experiments. It would also be difficult to modify the systems to study a cyclic force instead of a continuous one. This method does not produce a uniform displacement of the base of the dish. The central area is displaced to a greater extent than the periphery of the base. This means that the cells grown in the dishes will be stretched by different amounts. An additional drawback of the method used by Hasegawa et al. [183] is that only a 4% increase in surface area was achieved, which is small.

The previous two methods have involved upward displacement of the petriperm bases. It is also possible to achieve a downward displacement. A new vaccum-operated instrument was constructed by Banes et al. [181]. This was able to apply static or variable duration, cyclic tension to cells *in vitro*. The unit used a vaccum to deform a petriperm dish which could yield a 0.13% compression to cells situated on the inner surface, measured by strain gauge recordings. The stress unit consisted of a plexiglass manifold bearing six gasketed vaccum ports (Figure 10). Rubber gaskets were recessed 1.5mm in the plexiglass and the gasket remained 1.5mm above the plane of the vacuum port. The gaskets received a coat of vacuum grease and the plates were centred over the ports. One side of the unit contained a metered fitting to which a vacuum could be applied and measured, while the other side had a bleed valve used to adjust the vacuum level. The stress unit fitted onto a tray inside a CO_2 incubator. Vacuum and bleed hoses were led through a vent at the top of the incubator to avoid disturbing the internal atmosphere. On application of the vacuum, the culture plates were drawn flush with the vaccum port opening, achieving a maximum deflection of 1.5mm at the plate centre. When the

Vacuum system

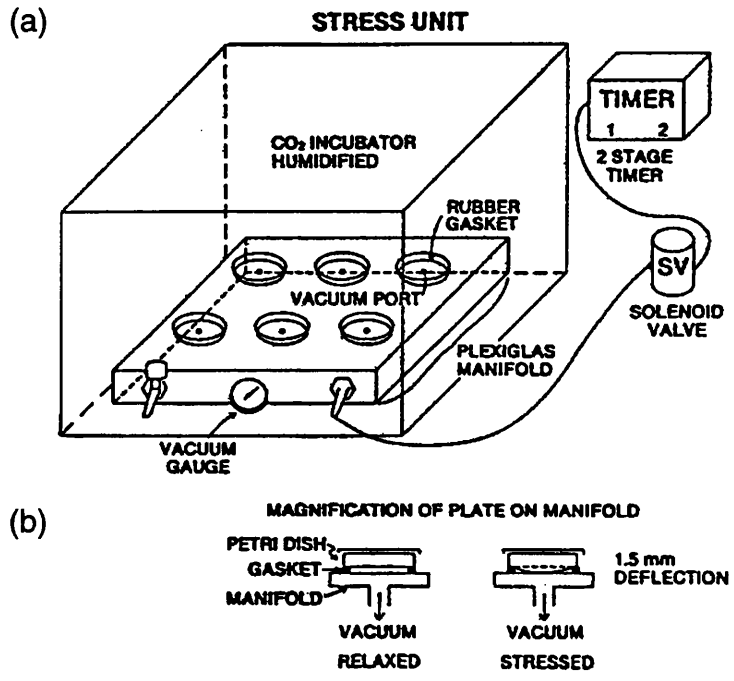

Figure 10 Schematic of vacuum-operated system, from Banes et al. (181).

(a) The three components that constitute the tension unit are a solenoid valve, timer and a vacuum unit.

(b) The flexible base of a petriperm dish is vertically displaced by a vacuum and cells grown in the dish are stretched.

vacuum was released, the plates returned to their original conformation for a chosen period of relaxation.

The vacuum system has proved to be a popular technique but its main disadvantages are that the stretch produced is uneven and only a small stretching force can be generated using this system. Again, the central area of the base of the dish is displaced greater than the periphery. Therefore, the cells grown in the dish are stretched by varied amounts. A greater range of stretch is required to conduct a thorough study of the effect of stretch on various aspects of cell function.

A different method which also used Petriperm dishes was designed by Brunette [184] to stretch epithelial cells. The apparatus was composed of an orthodontic screw embedded in an acrylic resin to fit a petriperm culture dish. The petriperm dish was utilised because the flexible plastic membrane of the dish could be stretched by turning the screw. The amount of stretching was not uniform throughout the dish. In the central area where the observations were made there was a 4.2% increase in length in the axis along which the force was applied.

1.6.2 Stretch frame

The system devised by Vandenburgh et al. [203] involved the use of stretch frame, which were horizontally adjustable by means of a thumb screw. Figure 11 illustrates the system used to stretch skeletal muscle myotubes. Clear silicone membranes, on which the cells were grown, were attached to the base of the apparatus. By turning the screw, an increase in the length of the silicone was achieved and hence the attached cells stretched. This system could achieve a stretch of 10.8% in magnitude.

The major disadvantage of the stretch frame system was that it appeared that the amount of stretching would be non-uniform throughout the silicone sheet and therefore the cell layer, and would be most pronounced in the central area. Vandenburgh et al. [203] had not shown any silicone measurements at different positions on the silicone to prove otherwise. A uniform distribution of stretch is an important requirement for the study of this factor on cellular function.

Stretch frame

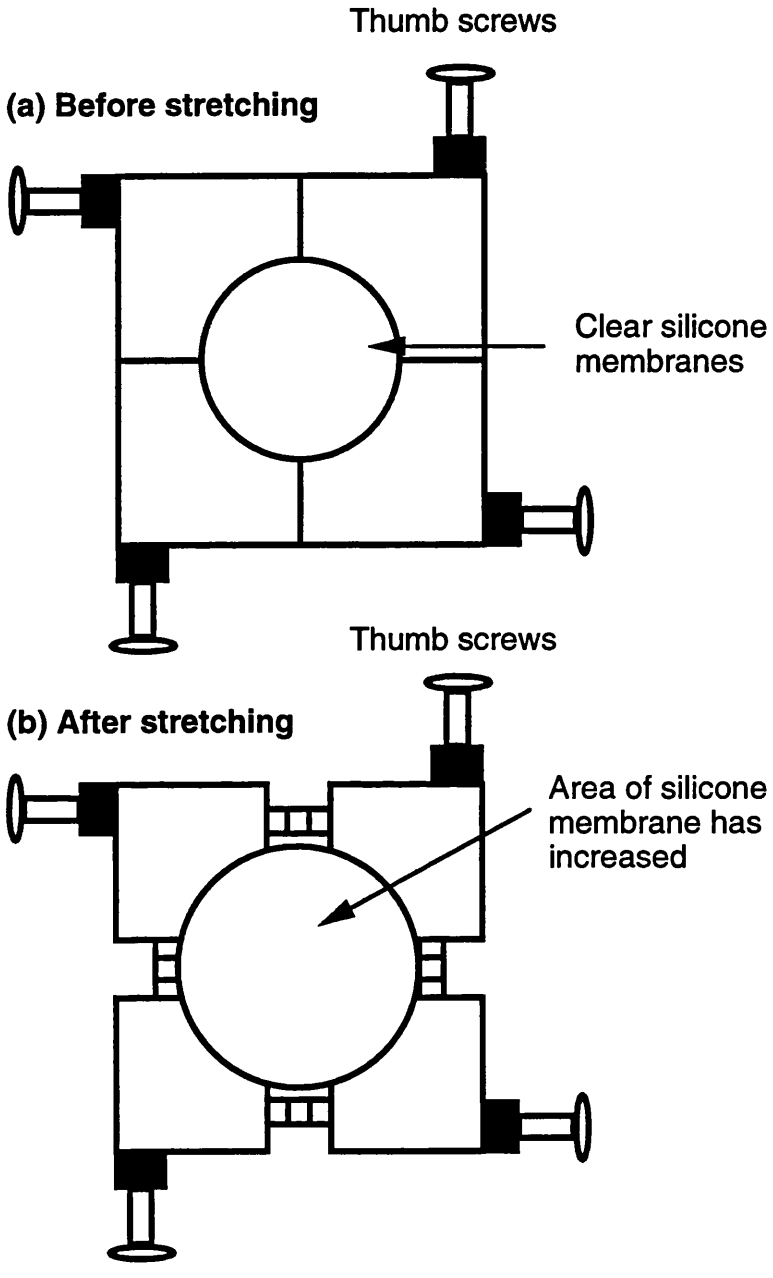

Figure 11 Schematic of a stretch frame, from Vandenburgh et al. (203)

(a) Cells are grown on a silicone membrane which is attached to the frame.

(b) By turning the thumb screws the area of the silicone membrane is increased and the attached cells stretched.

1.6.3 Compressive forces

Richardson [150] developed a system which could apply compressive forces to bone cells in culture in the study of bone fracture repair. An electric motor and gearing system were used to provide a controlled source of cyclic loading (Figure 12). A cam translated the circular motion produced by a motor, into an axial motion of a pumping rod. Bone cells were grown on silicone discs containing a notch which exactly fitted the end of the pumping rod. As the rod came into contact with the disc, the silicone and the attached cells were compressed.

A major problem encountered by Richardson [150] was that the bone cells adhered poorly to the silicone. To improve this, the effect the following cell adhesion-promoting agents was analysed; 10 and 100μgml^{-1} l poly-lysine, 25μgml^{-1} fibronectin, 2 and 20% gelatin. However, neither of these agents were suitable. Another approach used stainless steel pins to anchor chick tibial explants against the silicone. A further method used to hold explants in position involved raising small flaps of the silicone surface to act as sprung clips. This was successful but the resulting silicone surface was uneven so this prevented microscopic examination of the growing cells. The final method used involved holding bone fragments in place using cyanoacrylatate ("superglue"). This was effective and did not prevent cell growth but disrupted the migration of cells onto the silicone surface. At the end of this project no suitable adhesive had been found. An additional disadvantage of this system is that it was difficult to maintain sterilility. Because of all these problems the proposed experiments were not completed.

1.6.4 Conclusions

The latter system which subjected cells to a compressive force was the only system which experienced contamination problems. Sterility is one of the most important features of a cell culture system. To use this system, the design would have to be altered to overcome this problem. Poor cell adhesion was also experienced which, as mentioned earlier, is also an important feature required of such a system. If cells are not suitably attached to their substrate, they will detach when a force is

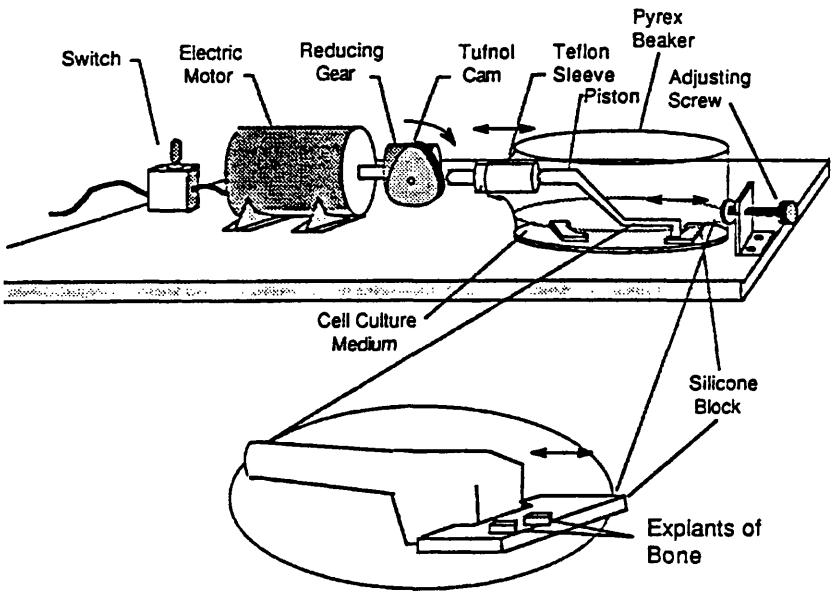

Figure 12 Schematic of system used to compress cells, from Richardson (150)

Cells grown on silicone blocks are subjected to a compressive force when rotation of a tufnol cam displaces a piston and causes the piston to make contact with the blocks.

applied. For these reasons, this method is not convenient to use in the study of pressure on cells.

Each of the techniques which used Petriperm dishes were successful because cells grow well in these dishes and were free from any sterility problems. Their only drawback is that due to the size of the dishes, the extent to which the membrane can be displaced is very small. The maximum stretching force that was generated using Petriperm dishes was 4.2%. To mimic the forces to which cells are subjected *in vivo*, a greater range of stretch is required. Another drawback of using Petriperm dishes is that when the flexible base is stretched the central area is stretched to a greater extent than the periphery. Each cell requires to be stretched by the same amount.

It was speculated that the stretch frame would also produce a non-uniform force. This appears to be an important problem which is associated with the design of each of these systems. In other aspects, the use of a frame appeared to be a suitable method which could be employed in such investigations.

The primary objective of my project was to develop a system capable of mechanically stretching vsmc and endothelial cells, in culture. The system had to feature each of the essential characteristics previously discussed and also solve the problems of non-uniform stretch and restricted range of stretch which had been experienced using other systems. On achieving a suitable system preliminary experiments were proposed, to study the role of mechanical forces in the development of vascular hypertrophy.

CHAPTER TWO

MATERIALS AND METHODS

2.1 Materials

2.1.1 Biochemicals

Agarose, ANG II, antibodies, bovine serum albumin, bromphenol blue, cesium chloride, coomassie brilliant blue G, dextran sulphate, Dowex mixed resin, Dowex-1 chloride, emetine, ethidium bromide, formamide, 2-[N-Morpholino] ethanesulfonic acid (MOPS), phosphate buffered saline (PBS) tablets, polyvinylpyrrolidine, rabbit anti-human von Williebrand factor, sephadex, and sodium acetate were purchased from Sigma (Dorset, England).
Agar, bacto agar, casamino acids and yeast extract were purchased from Difco (Surrey, England).
Buffer tablets (pH7), sodium dodecyl sulphate, trichloroacetic acid and hydrochloric acid were bought from BDH (Poole, England).
Diaminoethanetetra-acetic acid (EDTA), formaldehyde (38% w/v) glycerol, sodium hydroxide, sodium chloride, sodium citrate, sodium dodecyl sulphate and formaldehyde were bought from FSA laboratories (Loughborough, England).
HB101 and DH5α competent cells were purchased from Gibco BRL (Paisley, Scotland).
Ficoll 400 was bought from Pharmacia LKB (Buckinghamshire, England).
RNAzol B was purchased from Biogenesis Ltd. (Bournemouth, England).
Analar ethanol was purchased from Hayman Ltd. (Essex, England).
Isopropanol and chloroform were purchased from Rhone Poulenc Chemicals Ltd. (Manchester, England).
Decon 75 solution was purchased from Scotlab (Coatbridge, U.K).
Fluorescein was purchased from Amersham International PLC (Buckinghamshire, England).
Vectashield mounting medium was purchased from Vector laboratories (Burlingame, California).

2.1.2 Radiochemicals

18.5 μCi of deoxy (5-^{3}H) cytidine 5'-triphosphate ammonium salt (CTP), (3000 Ci/ml) and 1 mCi of myo-[2-^{3}H] inositol (10-20 Ci/mmol) were purchased from Amersham International PLC (Buckinghamshire, England).

2.1.3 General solutions/buffers

Concentrated (20x) sodium saline citrate (SSC)

175.3g of sodium chloride and 88.2g of sodium citrate were dissolved in 800ml of glass distilled water (dH_2O). The solution was brought to pH 7.0 using 5M hydrochloric acid, the final volume adjusted to 1 litre with dH_2O, and the pH rechecked. The solution was autoclaved and stored at 4°C. The final concentrations of sodium chloride and sodium citrate were 3 M and 0.3M respectively.

1xSSC, 0.5xSSC and 0.1xSSC were obtained by dilution of 20xSSC in dH_2O.

Deionised distilled water (ddH_2O).

Approximately 50g of Dowex mixed resin was added to 3 litres of dH_2O and stirred for 2h using a magnetic stirrer. The water was then filtered, autoclaved, cooled and stored at 4° C.

L-broth/agar plates

5g of β-lab yeast extract, 5g of sodium chloride, 10g of casamino acids and 2ml of 1M sodium hydroxide solution were dissolved in 1 litre of dH_2O and autoclaved. The solution was cooled and stored at 4°C.

0.5M EDTA , pH 8

18.6g of EDTA were dissolved in 80ml of dH_2O. The solution was brought to pH 8 with 5M sodium hydroxide solution and the volume made up to 100ml with dH_2O.

Tris EDTA (TE) electrophoresis buffer

0.2ml of 0.5M EDTA (pH 8) and 0.121g of Tris chloride [final concentration 100mM] was dissolved in 80ml of dH_2O and the volume made up to 100ml using dH_2O. The resulting solution had a pH of 8.0.

Concentrated (50x) Denhardt's reagent

1g of polyvinylpyrrolidine, 1g ficoll and 1g bovine serum albumin were dissolved in 80ml of dH_2O. The volume was made up to 100ml with dH_2O. The solution was aliquoted and stored at -20°C.

Concentrated (10x) MOPS

41.2g MOPS was dissolved in 1600ml of 0.1M sodium acetate and the pH of the solution adjusted to 7.0 with 10M sodium hydroxide solution. 20ml of 0.5M EDTA was then added, the pH adjusted to 8.0 and the volume made up to 2 litres with dH_2O. This solution was stored at 4°C.

1xMOPS was obtained by dilution of 10xMOPS in dH_2O.

RNA loading dye solution

500µl of bromphenol blue (0.1mg/ml), 500µl of glycerol and 500µl of deionised formamide were combined and mixed thoroughly. One part ethidium bromide 1mg/ml was then added to 2 parts of this solution. The dye solution was stored at -20° C.

DNA loading dye solution

500µl of bromphenol blue (0.1mg/ml) was combined with 500µl of glycerol. The solution was mixed thoroughly and stored at -20°C.

Dowex-1-formate

Dowex-1 chloride (100g) was washed with 1litre of dH_2O to remove broken beads, transferred to a scintered glass funnel and washed with 2 litres of 2M sodium hydroxide. It was then further washed with 1 litre of dH_2O, 500ml of 1M formic acid, 5 litres of dH_2O and finally with dH_2O until a constant pH of 5.5 was achieved. The Dowex was then poured from the funnel and stored in dH_2O.

Versene solution

Versene was purchased from the University of Glasgow, Department of Virology. The recipe for the versene was: 80g of sodium chloride, 2g of potassium chloride, 11.5g of sodium hydrogen phosphate, 3.3g potassium hydrogen phosphate, 2g of EDTA and 15ml of phenol red (1%) were dissolved in 10 litres of dH_2O. The pH of the solution was 7.12 -7.3. The solution was autoclaved and stored at 4°C.

Trypsin solution

Trypsin solution was also purchased from the University of Glasgow, Department of Virology. The recipe for the solution was : 8g of sodium chloride, 2ml of potassium chloride (19%), 0.1g of sodium hydrogen phosphate, 1g of dextrose and 3g of tris amino methane, were dissolved in 700ml of dH_2O. 1.5ml of phenol red (1%), penicillin (100,000U) and 0.1g of streptomycin were added to this solution. The volume was made up to 1 litre with dH_2O and 2.5g of trypsin added. The solution was then autoclaved and stored at -20°C.

Trypsin/versene

This solution contained 20ml of versene and 5ml of trypsin.

2.1.4 Cell culture reagents and disposable apparatus

Collagen (type I), collagenase (type II), elastase (type IV), fibronectin, gelatin, Hanks' balanced salt solution (HBSS), poly-l-lysine and soya bean trypsin inhibitor were purchased from Sigma (Dorset, England). Penicillin (100U/ml), streptomycin (100mg/ml) and fungizone (250μg/ml) were purchased from Gibco BRL (Paisley, Scotland).
Dulbecco's modified Eagle medium (DMEM) containing 4.5g/litre dextrose, DMEM without glutamine or inositol, heat inactivated foetal calf serum (FCS), L-glutamine, heat inactivated horse serum (HS) and tissue culture flasks were bought from ICN Flow (Irvine, Scotland).
Cell scrapers were purchased from Northumbria Biologicals Ltd. (Northumberland, England).
Silicone sheeting was bought from Altec (Hampshire, England). Sterile, disposable 10ml pipettes and sterile bijoux containers were purchased

from Sterilin Ltd. (Hounslow, England).
Sterile 0.22μm filter units were bought from Millipore S.A. (Molsheim, France).
Glisseal sealant was purchased from BDH (Poole, England). Plastic, sterile forceps were purchased from Steriseal (Worcestershire, England).

2.1.5 Molecular biology reagents and disposable apparatus

Geneclean II kits were obtained from Stratech Scientific (Luton, England). Qiagen plasmid kits were purchased from Hybaid (Middlesex, England). Oligolabelling kits were purchased from Pharmacia (Buckinghamshire, England). Blot transfer systems 11.14, restriction enzymes and reaction buffers were obtained from Gibco BRL (Paisley, Scotland). Micro-centrifuge tubes were purchased from Scotlab (Coatbridge, Scotland). Sterile pastettes, universal containers and pipette tips were bought from Alpha Laboratories (Hampshire, England). Hybond-N transfer membranes were purchased from Amersham (Buckinghamshire, England). RNA zol^{TM} was bought from Biogenesis Ltd. (Bournemouth, U.K).

2.2 General methods

2.2.1 Glassware

All items of glassware were washed in solutions of the detergent Decon 75, rinsed with dH_2O and dried in an oven at 60°C.

2.2.2 Micropipetting

Solution volumes in the range of 1-25μl were transferred accurately using digital pipettes obtained from Scotlab (Coatbridge, Glasgow). 10-1000μl were transferred reproducibly using Finn-pipettes purchased from Lab systems (Hampshire, England).

2.2.3 pH measurement

Measurements of pH were carried out using a digital, pH/temperature meter obtained from FSA (Loughborough, England). This apparatus was regularly standardised using a solution of pH7, prepared using buffer

tablets.

2.3. Cell culture

2.3.1 General equipment

The following is a list of the general items of equipment used in cell culture ;
Heraeus laminar flow hood : FSA laboratories (Loughborough, England).
Heraeus CO_2 incubator : MDH (Hampshire, England).
Diavert inverted microscope : Leica UK Ltd. (Milton Keynes, England).
Electronic Coulter counter (ZM) : Coulter Electronics Ltd. (Luton, England).
Fume hood : Fumair Ltd. (Hertford, England).

2.3.2 Vsmc preparation

Vsmc were grown from mesenteric arteries of male (150-200g) Sprague-Dawley rats (Plate 1). Mesenteric arteries (6 arteries per preparation) were removed under sterile conditions, cleaned of residual fat by blunt dissection and incubated for 5 min in DMEM containing 1.25mg/ml type II collagenase, 0.25mg/ml type IV elastase and 0.05mg/ml soya bean trypsin inhibitor. The adventitia was then removed by dissection. The cleaned arteries were then cut into small pieces and incubated in fresh enzyme solution, with periodic trituration, until a single cell suspension was obtained. Cells were then collected by centrifugation (200g/5min), resuspended in 5ml growth medium ; DMEM containing 10% FCS, 10% HS, 100U/ml penicillin, 100mg/ml streptomycin and 2mmol/l L-glutamine, and grown in 25cm^2 tissue culture flasks. This growth medium was used for all cell culture work, unless otherwise stated. Cells were maintained at 37°C in a 5% carbon dioxide (CO_2)/95% air humidified atmosphere. Plate 2 shows vsmc 2 days in culture and Plate 3 confluent vsmc. For the first few days in culture the cells were spindle shaped, contained substantial bundles of myofilaments (assessed by electron microscopy) and contracted in response to addition of ANG II. Figures 13a and 13b show the contraction of vsmc on addition of ANG II, as assessed by time-lapse video recordings. The smooth muscle nature of the cells was also consistent with the lack of staining for von Williebrand factor (see section 2.3.2.1). At confluence the cells displayed the hill and valley

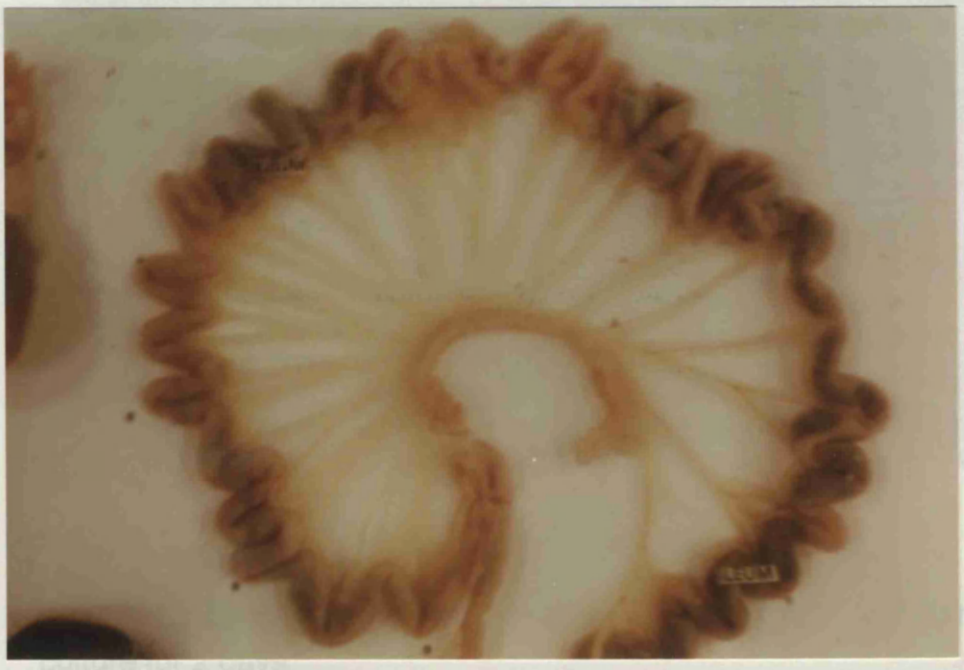

Plate 1. Rat mesenteric bed.

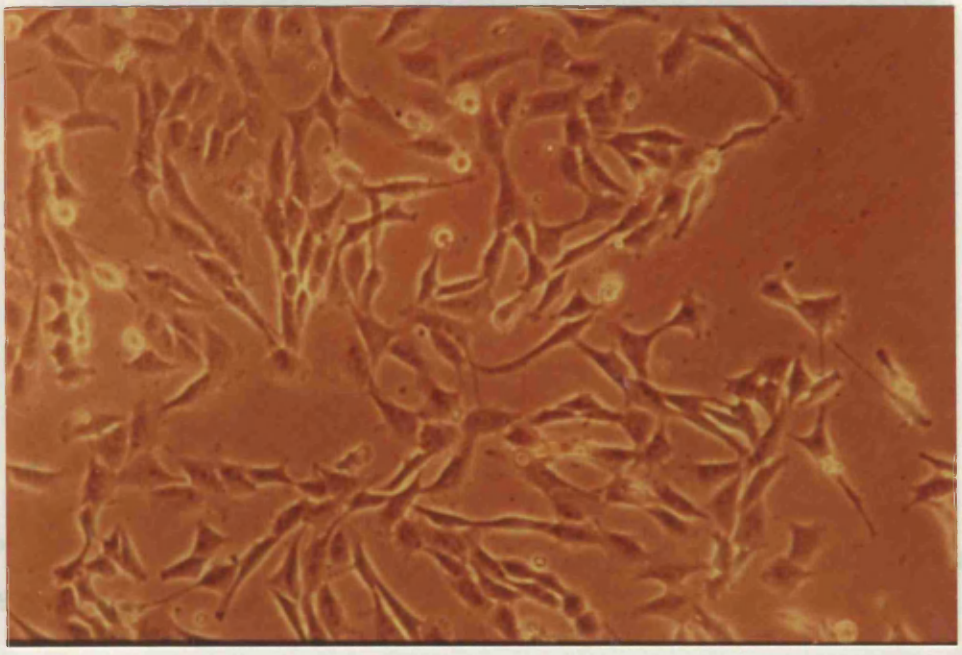

Plate 2. Vsmc prepared as described in section 2.3.2 and grown in culture for 2 days.

Plate 3. Vsmc grown in culture for 5 days. By this time they have reached confluence.

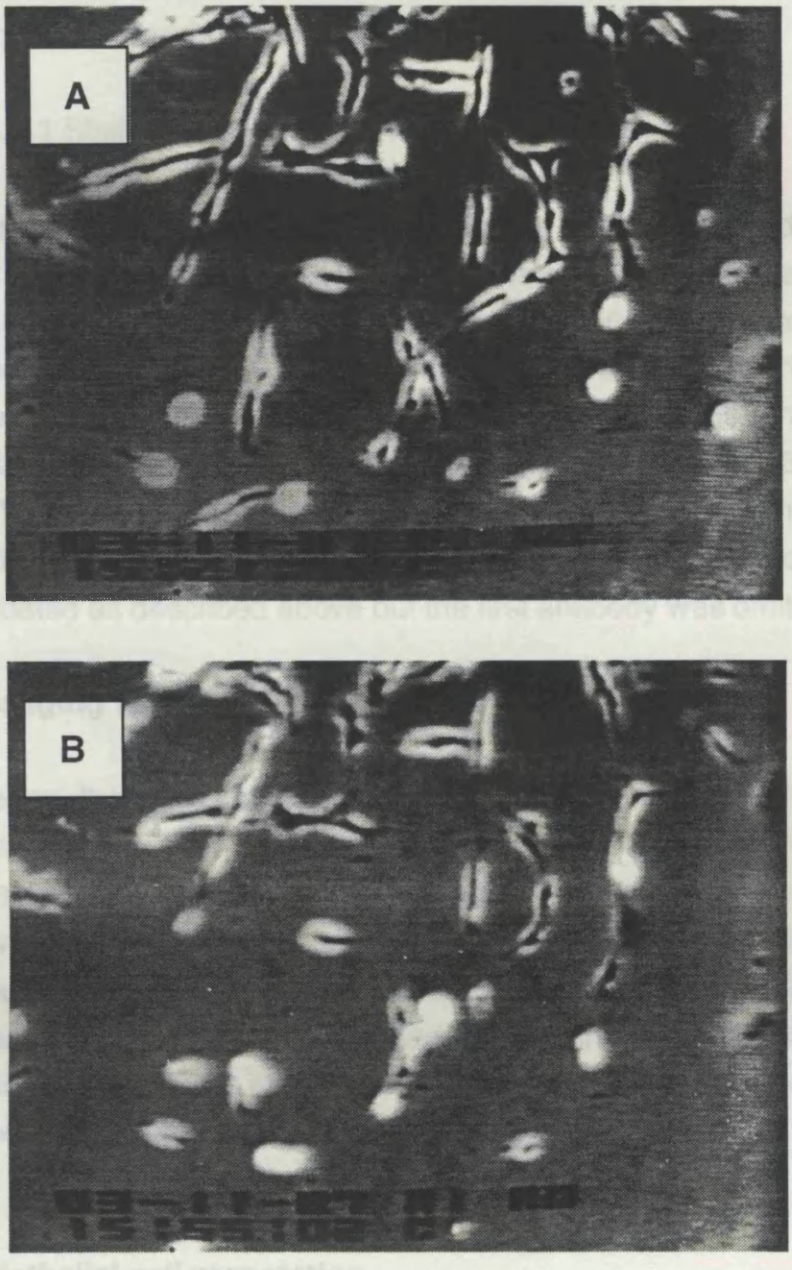

Figure 13.
Vascular smooth muscle cells before (A) and after (B) addition of ANG II, 10^{-5}M. (B) shows the contractile response of the cells to ANG II.

characteristics of smooth muscle cell cultures when examined with phase-contrast microscopy and would grow to form multi-layers.

2.3.2.1 Staining cells with von Williebrand factor

Cells were plated down in plastic tissue culture flasks and fixed in ice cold 50% acetone/methanol (1:1), at 4°C. The cells were washed with PBS (x1) for 5 min and then incubated with rabbit, anti-human, von Williebrand factor (Diluted 1 in 200 in 1xPBS) for 30 min, at 37°C. The cells were then washed with 1xPBS for 3, 15 min incubations. The cells were next incubated with donkey, anti-rabbit Ig, fluorescein, for 30 min, at 37°C. This was followed by 2, 15 min washes in x1 PBS. The cells were finally mounted in Vectashield mounting medium. Control cells were incubated as described above but the first antibody was omitted.

2.3.3 Passaging vsmc

At confluence, the medium was decanted and an appropriate volume of versene added, to cover the bottom of the flask, for 10s. The versene was decanted and an appropriate volume of a versene/trypsin (4:1) solution was added to the flask for 10s. The versene/trypsin solution was also decanted and the flask of cells incubated at 37 °C until all of the cells detached. The cells were triturated using a fine tipped pipette and transferred into new flasks at a 1 : 3 split ratio. Vsmc were used between the second and seventh passage for experiments.

2.3.4 Endothelial cell preparation

Bovine aortae were obtained from the local abbatoir and flushed through with a saline solution composed of 0.9% sodium chloride, 250μg/ml fungazone, 100U/ml penicillin and 100μg/ml streptomycin, to remove excess blood. The ends of the aortae were tied off with string and brought back to the laboratory (Figure 14). The fat was removed from the outer vessel wall using scissors and forceps and the intercostal arteries tied off with thread. Approximately 20ml of a collagenase mixture containing 1.25mg/ml collagenase, 250μg/ml fungazone, 100U/ml penicillin and 100μg/ml streptomycin was introduced to the vessel via a syringe and incubated at 37°C for 15 min. The vessels were massaged

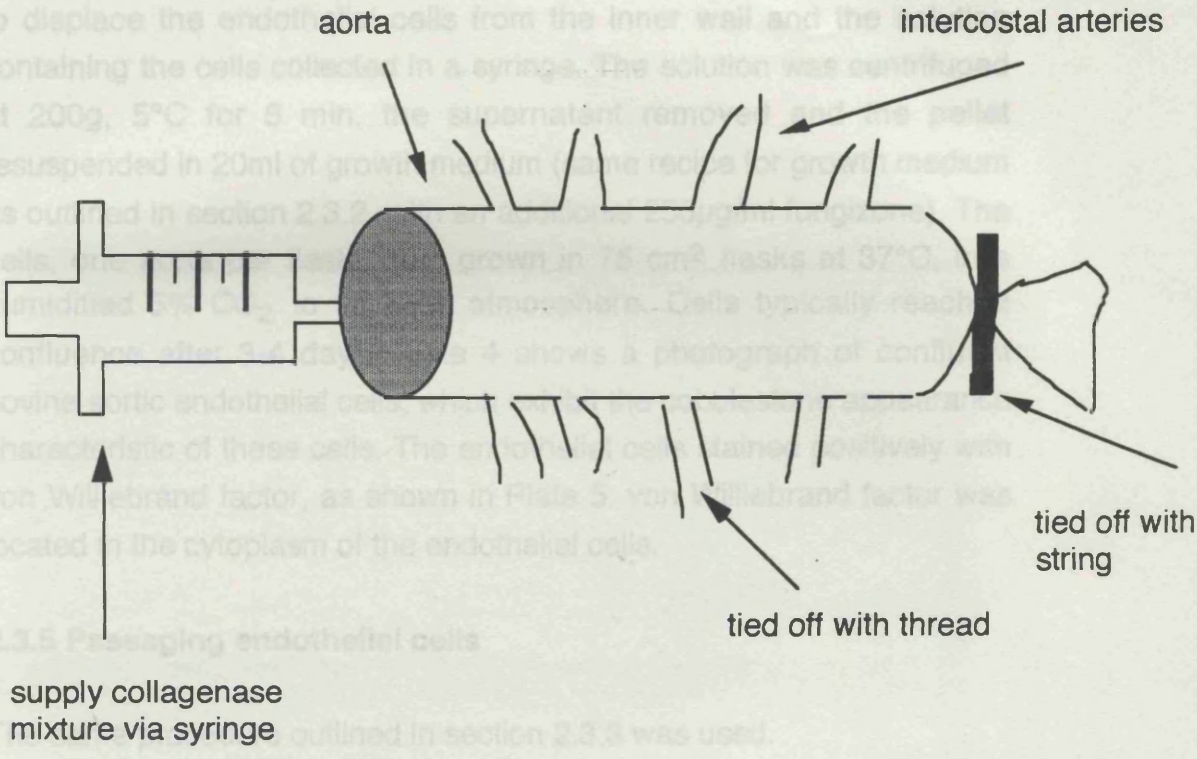

Figure 14 Preparation of endothelial cells from bovine aortae.
Aortae were flushed through with saline and brought back to the laboratory. The ends were tied off with string and the intercostal arteries tied off with thread. Endothelial cells were displaced from the inner wall of the vessel by enzymatic digestion followed by gentle rubbing of the vessel.

to displace the endothelial cells from the inner wall and the solution containing the cells collected in a syringe. The solution was centrifuged at 200g, 5°C for 6 min, the supernatant removed and the pellet resuspended in 20ml of growth medium (same recipe for growth medium as outlined in section 2.3.2, with an additional 250μg/ml fungizone). The cells, one aorta per flask, were grown in 75 cm^2 flasks at 37°C, in a humidified 5% CO_2 to 95% air atmosphere. Cells typically reached confluence after 3-4 days. Plate 4 shows a photograph of confluent bovine aortic endothelial cells, which exhibit the cobblestone appearance characteristic of these cells. The endothelial cells stained positively with von Williebrand factor, as shown in Plate 5. von Williebrand factor was located in the cytoplasm of the endothelial cells.

2.3.5 Passaging endothelial cells

The same procedure outlined in section 2.3.3 was used.

2.4 Pre-treatment of silicone sheeting

Silicone sheets were cut into rectangles 8x5cm in area, cleaned by washing in 0.1% Decon 75 solution and then rinsed thoroughly in dH_2O. The silicone was transferred to aluminium foil, autoclaved at 121°C and dried at 60°C overnight.

2.5 Growth of vsmc on Petriperm dishes and silicone sheets

2.5.1 Treatment of Petriperm dishes with cell adhesion-promoting agents

Petriperm dishes were coated with either collagen, fibronectin, gelatin or poly-l-lysine, as described below.

Collagen: A 0.01% collagen solution in 0.1M acetic acid was filter sterilised and 10ml of the solution applied to the silicone. The silicone was incubated at 37°C for 3h, rinsed with serum-free medium and allowed to dry at 37°C for 3h.

Fibronectin: 10ml of a 25μg/ml fibronectin solution dissolved in serum-free medium was applied to the silicone, incubated at room temperature for 20 min, rinsed with serum-free medium and allowed to dry at room

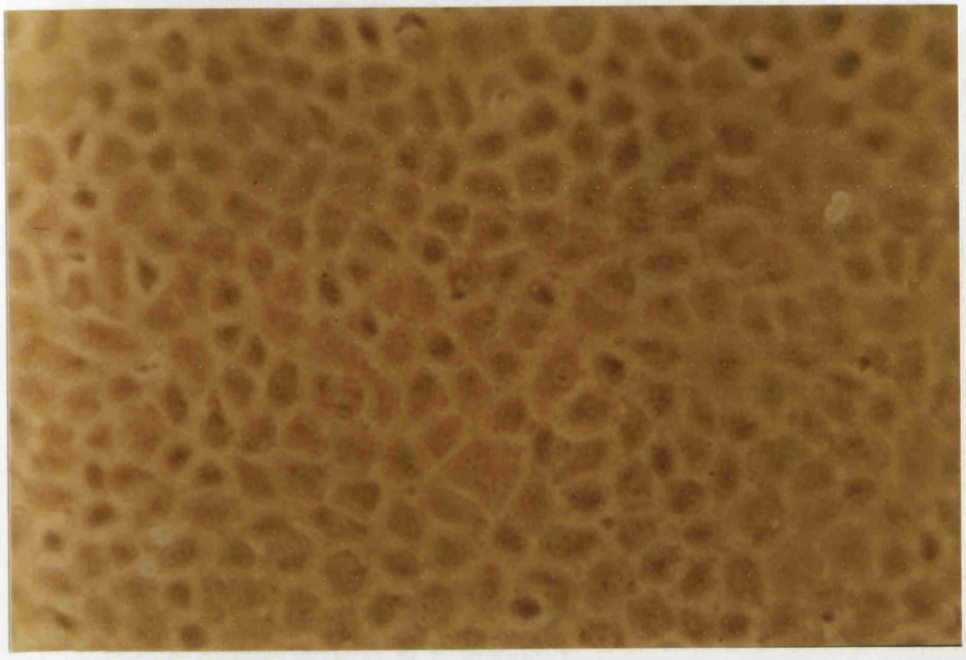

Plate 4. Endothelial cells prepared as described in section 2.3.4 and grown in a tissue culture flask, for 4 days. The confluent endothelial cells adopt a cobblestone appearance.

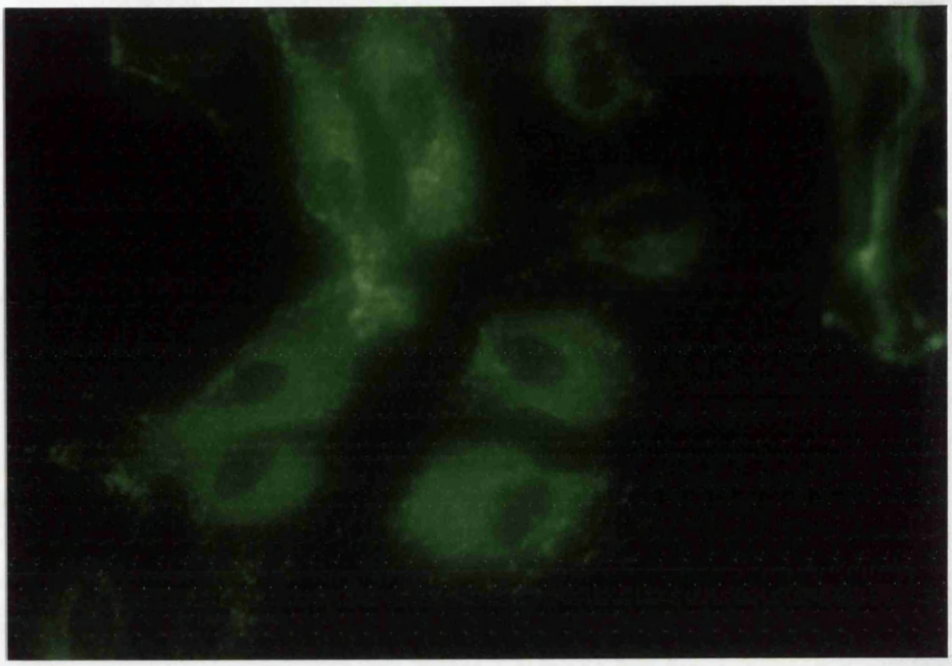

Plate 5. Photograph of endothelial cells which have been stained with von Williebrand factor, as described in section 2.3.2.1.

temperature in a laminar flow hood.

Gelatin: 10ml of a 2% gelatin solution was applied to the silicone and incubated at 37°C for 2h. The silicone was rinsed with serum-free medium and allowed to dry at 37°C for 3h.

Poly-l-lysine: 10μg/ml of poly-l-lysine dissolved in serum-free medium was added to the silicone and incubated at 37°C for 3h. The silicone was rinsed with serum-free medium and allowed to dry at room temperature in a laminar flow hood.

In all experiments, cells were plated at a cell density of 0.05 x 10^6 cells per Petriperm dish. After 3 days in culture the cells were detached from the dishes using the standard methods outlined in section 2.3.3, and cell numbers determined using an electronic Coulter counter.

2.5.2 Treatment of silicone sheets with cell adhesion-promoting agents

The protocol used was the same as that described for Petriperm dishes in 2.5.1. However, 0.8 x 10^6 cells in 10ml of growth medium, were plated onto the stretching apparatus.

2.5.3 Plating vsmc on the stretching apparatus

The perspex components of the apparatus were sterilised overnight in 70% ethanol and air dried in a flow hood. Autoclaved silicone sheets were mounted onto the vertically aligned screws at a resting tension and each piece of apparatus fully constructed. 0.8 x 10^6 cells in 10ml of growth medium were placed onto the fibronectin-treated silicone sheets.

2.5.4 Distribution of vsmc on silicone sheet

To demonstrate that vsmc were growing uniformly across the silicone membrane, the following experiment was performed. Cells were grown to confluence on fibronectin-coated silicone and stained for protein as follows. The growth medium was removed from the wells and 10ml of formaldehyde (2%) placed onto the silicone for 10 min. The solution was then removed and replaced with 10ml of 1% coomassie brilliant blue G stain for 20 min. The silicone was rinsed thoroughly with 1xPBS to remove any excess stain and each piece of silicone photographed. As a control, silicone sheets which did not have vsmc attached were also

stained in a similar manner.

2.6 Endothelial cells

2.6.1 Endothelial cell adhesive experiment

The same procedure as that outlined for vsmc (section 2.5.1).

2.7 Stretching and ANG II experiments

2.7.1. Varied time intervals

2.7.1.1 Stretching vsmc and endothelial cells by 20% over various time intervals

When confluent, vsmc or endothelial cells on fibronectin-coated silicone were deprived of serum for 24h. After this period the medium was removed and replaced with 12ml of serum-free medium. The length of silicone was increased from a resting tension of 80mm to 96mm, by turning the handle, to produce a 20% stretch. Cells were exposed to 20% stretch for the following time points; 0, 15, 30, 60, 180 or 360 min.

2.7.1.2 Treating vsmc with ANG II over various time intervals

When confluent, vsmc in 180 cm^2 tissue culture flasks were deprived of serum for 24h. After this period, the medium was removed and replaced with 50ml of serum-free medium containing 1μM ANG II. Vsmc were treated with ANG II for 0, 15, 30, 60, 180 or 360 min.

2.7.3 Effect of increasing stretch length

When confluent, vsmc on fibronectin-coated silicone, were deprived of serum for 24h. After this period the medium was removed and replaced with 12ml of serum-free medium. In this experiment, the vsmc were exposed to a varied stretch of either 0, 5, 10, 15 or 20%, over a fixed time interval of 15 min. These degrees of stretch were achieved by increasing the length of the silicone to 84, 88, 92 or 96mm respectively.

2.7.4 Effect of 20% stretch on vsmc numbers

Vsmc were plated at a cell density of $0.4x10^6$ cells/per piece of apparatus in standard growth medium. This was designated as day 0 of the study. On day 1, the number of cells present on 3 pieces of apparatus was evaluated using a Coulter counter, the medium removed from each of the remaining pieces of apparatus and replaced with DMEM containing 10% FCS, 100U/ml penicillin, 100mg/ml streptomycin and 2mmol/l L-glutamine. 10 pieces of apparatus were stretched by 20% and the remaining 10 unstretched pieces were used as controls. On day 2, the medium was removed from 3 stretched and 3 control pieces of apparatus and the number of vsmc present in the medium determined. The number of cells growing on the silicone for the 3 stretched and 3 control pieces of apparatus was then determined. This procedure was also repeated on days 3 and 4.

2.7.5 Effect of 20% stretch on phosphoinositide metabolism

Phosphoinositide metabolism was measured by a modification of the procedure of Berridge et al. [226]. Vsmc were plated at a density of 0.8 $x10^6$ cells onto fibronectin-coated silicone sheets. Cells were grown until they reached confluence. They were then washed twice with serum-free medium and incubated for a further 48h in 10ml of inositol free DMEM containing 4×10^{-6} Ci/ml myo-[2-^{3}H] inositol. At the end of the incubation, the medium was removed and the cells washed with 10ml of HBSS followed by a 5 min wash with HBSS containing 10mmol/l glucose and 1% bovine serum albumin (HBG). The cells were then incubated for 10 min with 10ml HBG containing 10mmol/l lithium chloride to inhibit inositol-1 phosphatase. The vsmc were then stretched by 20% at 37°C for 20 min. Incubation of unstretched vsmc with either 10% FCS or 10^{-7}M ANG II for 20 min were used as positive controls. Incubations were terminated by removal of the medium followed by addition of 6.2ml of ice cold methanol. The cells were then scraped from the silicone and transferred into polypropylene tubes. After addition of chloroform (3.1ml) and ddH_2O (3.1ml), the contents were mixed, allowed to stand for 30 min and centrifuged at 250g for 15 min. An aliquot of the upper phase (400μl) was transferred to a glass tube containing 2.2ml H_20 and 250μl of a 50% slurry of Dowex-1-formate. After addition of the aqueous

solution to the Dowex, the tubes were mixed and left until the Dowex had settled. The aqueous solution was then removed by aspiration. The resin was washed twice with 4ml ddH_2O, twice with 4ml 60 mmol/l ammonium formate, followed by 5 mmol/l sodium tetraborate and then twice again with ddH_2O. The inositol phosphates were eluted from the resin with 3 washes of 0.6ml 1 mol/l ammonium formate, followed by 3 washes of 0.1 mol/l formic acid. The eluates from the ammonium formate and formic acid washes were combined to give a final volume of 3.6ml and added to 10ml Ecoscint A. The samples were counted for 10 min in a scintillation counter.

2.8 Molecular biology

2.8.1 General equipment

Whirlimixer, magnetic stirrer and silica cuvettes : FSA laboratories (Loughborough, England).
Power supply, spectrophotometer, gel electrophoresis apparatus (G-100 tank) : Pharmacia LKB (Buckinghamsire, England).
Grant water bath, microcentrifuge, autoclave, electronic balance, magnetic stirrer, pH meter : Scotlab (Bellshill, Scotland).
Techne hybridiser and transilluminator : GRI (Essex, England).
UV stratalinker : Stratagene (Cambridge, England).
Microwave : Comet (Glasgow, Scotland).
Series 900 mini monitor : Mini instruments (Essex, England).
Hypercassettes and Fuji x-ray film : Amersham (Buckinghamshire, UK).

2.8.2 Transforming bacterial cells

HB101 and DH5α-competent cells, which had been stored at -70°C, were thawed on ice. A 1μl aliquot of the appropriate plasmid, at a concentration of 500 μg/ml, was added to a 100μl aliquot of HB101 or DH5α cells and left on ice for 30 min. The cells were heat shocked by incubation at 42°C for 90s and then placed on ice for 2 min. 0.5ml of L-broth was then added and the cells incubated at 37°C in an orbital incubator for 60 min. 100ml of agar was autoclaved, allowed to cool and separated into 2, 50ml portions. To one portion the appropriate antibiotic was added e.g. tetracycline at a final concentration of 30μg/ml, or ampicillin at a concentration of 50μg/ml. Four plates, each containing

25ml agar were poured and allowed to set. After the 60 min incubation the transformed cells were spread onto one agar plate containing the antibiotic and one agar plate without antibiotic. Untransformed cells were used as a control and spread onto the remaining two plates, with and without antibiotic. The plates were then incubated at 37°C overnight.

The results obtained for a successful transformation were as follows;

untransformed / without antibiotic	growth
untransformed / antibiotic	no growth
transformed / without antibiotic	growth
transformed / antibiotic	growth

2.8.3 Plasmids

The details of the plasmids used in this study are described below:

The 1.3Kb *v-fos* complementary deoxyribonucleic acid (DNA) [cDNA] in the plasmid pAT153 was a gift from Dr. Ann Wyke, Beatson Institute for Cancer Research, Glasgow. The plasmid was initially obtained from Curran et al. [227] The plasmid was amplified in DH5α cells and then excised using the restriction enzymes Bgl II and PVU II and reaction buffers, according to the manufacturer's instructions.

The plasmid pSP65 containing a 0.8kb insert of *c-myc* was also a gift from Dr. Ann Wyke, Beatson Institute for Cancer Research, Glasgow. The plasmid was initially obtained from Hayashi et al. [228] The plasmid was amplified in DH5α cells and excised using the restriction enzymes ECoRI and Hind III.

The pBS5K plasmid containing nucleotides 53-1444 of *c-jun* was a gift from Dr. R. Breathnach, Universite de Nantes, Nantes, Cedex, France. The plasmid was initially obtained from Angel et al. [229] The plasmid was amplified in DH5α cells and excised using ECoRI.

2.8.4 Small scale preparation of plasmid DNA

10ml of L-broth containing the appropriate antibiotic, was added to 4 universal containers. Three single colonies were taken from the plate containing transformed cells with antibiotic (section 2.8.2) and one colony transferred into each of three universal containers. One colony from the untransformed cells without antibiotic plate was transferred into

the fourth universal to act as a control. The cells were incubated overnight at 37°C in an orbital incubator. The following day, three universals contained turbid solutions i.e those which contained transformed cells. The remaining universal contained a solution of untransformed cells. (The following protocol was performed in accordance with the manufacturers instructions and utilised solutions provided in a midi Qiagen kit). The most turbid solution (1ml) was placed into an Eppendorf tube, spun for 15s at 15,000g in a microcentrifuge and the supernatant removed. Another 1ml of the solution was added to the Eppendorf tube, spun for 15s at 15,000g, the supernatant poured off and drained. A further 1ml of the solution was added, spun for 15s, the supernatant removed and drained. The pellet was resuspended in 4ml of buffer P1 consisting of 100μg/ml RNase, 50mM Tris/hydrochloric acid, 10mM EDTA, pH8. 4ml of buffer P2 containing 200mM sodium hydroxide and 1% sodium dodecyl sulphate was then added and the tubes mixed and left at room temperature for 5 min. 4ml of buffer P3 consisting of 3M potassium acetate at pH 5 was then added and mixed. The solution was spun at 4°C, 15,000g, for 30 min. The supernatant was removed using a fine tipped pipette and further spun at 4°C, 15,000g, for 10 min, to obtain a particle-free lysate. A Qiagen tip 100 was equilibrated with 3ml of buffer QBT containing 750mM sodium chloride, 50mM MOPS, 15% ethanol at pH 7, 0.15% Triton-X-100 and emptied by gravity flow. The supernatant was applied to the tip and washed with 10ml of buffer QC consisting of 1M sodium chloride, 50mM MOPS and 15% ethanol at pH 7. The DNA was eluted with 5ml of buffer QF. Buffer QF is composed of 1.25M sodium chloride, 50mM Tris/hydrochloric acid and 15% ethanol, at pH 8.5. The DNA was precipitated with 0.7 x the volume of isopropanol and spun at 4°C, 15,000g, for 30 min. The DNA was washed with 10ml of 70% ethanol, spun for 15 min at 15,000g, 4°C, drained and 200μl of TE buffer added. The DNA sample was stored at -70°C.

2.8.5 Large scale preparation of plasmid DNA

(The following protocol was performed according to the manufacturers instructions. Solutions were provided in the Qiagen kit. All buffers used are the same as in 2.8.4).

A 2ml aliquot of the solution of overnight culture, produced in the small scale preparation was removed, added to 500ml of broth containing the appropriate antibiotic (tetracycline at a concentration of

30μg/ml, or ampicillin at a concentration of 50μg/ml), the contents poured into a large glass dimple flask and placed in the orbital incubator at 50g, 37°C, overnight. The following day 8.5ml of the culture was removed, added to 1.5ml of autoclaved glycerol, mixed and aliquoted into 1ml batches. The samples were frozen in an ethanol/dry ice bath and stored at -70°C. Of the remaining solution approximately 250ml was placed into plastic centifuge tubes, balanced and spun at 15,000g, 4°C for 5 min. The supernatant was removed, tubes drained and the pellets resuspended in 10ml of buffer P1. 10ml of buffer P2, prewarmed at room temperature, was then added, mixed gently and incubated at room temperature for 5 min. Next 10ml of buffer P3 was added and immediately mixed gently. The solution was spun at 15,000g, 4°C for 30 min and the supernatant removed using a fine tipped pipette. The supernatant was further spun at 4°C, 15,000g for 10 min, to obtain a particle-free lysate. A Qiagen tip 500 was equilibrated with 10ml of buffer QBT and emptied by gravity flow. The supernatant was applied to the tip, washed with 30ml of buffer QC and the DNA eluted with 15ml of buffer QF. The DNA was precipitated with 0.7 x volume of isopropanol and spun at 4°C, 15,000g for 30 min. The DNA was washed with 20ml of 70% ethanol, spun for 15 min at 15,000g, 4°C, drained and 500μl of TE buffer added. The DNA sample was stored at -70°C.

2.8.6 Quantification of DNA and ribonucleic acid (RNA)

5μl of the DNA/RNA sample was added to 995μl of ddH_2O in an Eppendorf tube. The solution was mixed and transferred into a silica cuvette. The absorbance of the solution at 260nm and 280nm was measured using a spectrophotometer. The absorbance of the solution at 260nm and 280nm is directly proportional to the concentrations of RNA or DNA respectively present in the sample. The ratio of the absorbance values obtained at 260nm and 280nm (i.e A_{260}/A_{280}) is an index of the purity of the RNA sample. This ratio varied from 1.8-2.0, where 2.0 represented a pure RNA sample with minimal protein contamination. The amount of DNA present in 1ml of a sample was calculated by multiplying the A_{280} value x50 because an optical density of 1 represents 50μg of DNA. The amount of RNA present in 1ml of a sample was calculated by multiplying the A_{260} value x40 because an optical density of 1 represents 40μg of RNA. The total amount of DNA/RNA present in the sample was then calculated by multiplying the above value by the dilution factor. For

example 5μl of sample was diluted in a total volume of 1ml. Thus the sample was diluted 1 : 200. To obtain a value for the total amount of DNA/RNA in the sample the calculated value had to be multiplied by 200.

2.8.7 Digestion of plasmid with restriction enzymes

cDNA	Reaction buffers
v-fos	React II and sodium chloride
c-myc	React III & React II
c-jun	React III

5μl *v-fos*, 2μl React II (x10), 2μl PVU II and 11μl ddH_2O were placed in an Eppendorf tube and incubated at 37°C for 3h. To this reaction mixture 2μl Bgl II, 3μl sodium chloride (1M) and 8μl ddH_2O were then added and incubated at 37°C for a further 3h.

5μl *c-myc*, 1μl EcoRI, 1μl React III and 3μl ddH_2O were placed in an Eppendorf tube and incubated at 37°C for 3h. To this reaction mixture 1μl Hind III, 1μl React II and 8μl ddH_2O were then added and incubated at 37°C for a further 3h.

5μl *c-jun*, 2μl EcoR1, 1μl React III and 2μl ddH_2O were placed in an Eppendorf tube and incubated at 37°C overnight.

For each cDNA, after the appropriate incubation period, a 15μl sample of the cut plasmid was run on a DNA gel, to ensure that the reaction was complete.

2.8.8 DNA gels

The gel was prepared by dissolving 0.8g agarose in 100ml of TE buffer and the solution microwaved to melt the agarose. 1μl of ethidium bromide (10mg/ml) was added to the solution and allowed to cool to room temperature. The solution was then poured into a perspex plate (78mm x 105mm) containing a plastic comb. The plate was placed into a G-100 tank and submerged in TE buffer. 2ml of DNA loading dye was added to the samples which were loaded into the wells of the gel. The samples were run at 60V for 3h.

The insert was cut from the DNA gel using a scalpel blade and

separated from agarose using the components supplied in a gene cleaning kit.

2.8.9 Gene cleaning

The components required for this procedure were supplied in a Geneclean II kit.

The gel slice was weighed into an Eppendorf tube and a volume of saturated 6M sodium iodide added, corresponding to 2.5x weight of the gel slice. The tube was placed in a water bath at 50°C. If after 5 min at 50°C the slice had not dissolved, it was returned to the water bath for a further 1 min. Next "glass milk" (silica matrix) was resuspended by thoroughly mixing and the appropriate volume added to the sample (5μl of glass milk for each 5μg of DNA present, then another 5μl for each 1μg). The sample was spun at 15,000rpm in a microcentrifuge for 10s and the supernatant removed. To the pellet 200μl of NEW solution (containing NaCl, Tris, EDTA, H_2O and ethanol), which was supplied in the kit, was added and the pellet resuspended using a fine tip. The samples were then spun for 10s at 15,000rpm, the supernatant removed and the process repeated twice more. Any remaining solution was removed using a fine tip and 50μl of TE buffer added. The pellet was resuspended in TE buffer and incubated at 50°C for 3 min, then spun at 15,000rpm for 30s. The supernatant which contained the eluted DNA was removed. A further 50μl of TE buffer added to the original tube and the pellet resuspended. The solution was spun at 15,000rpm for 30s and the DNA removed. This latter step was repeated a third time. The 3x50μl DNA samples were then combined together in an Eppendorf tube. 5μl of the gene cleaned DNA and 5μl of a DNA ladder were run on a DNA gel, to ensure that the isolation of the insert had been successful. The DNA was then aliquoted into 50ng batches. Scans of DNA gels containing samples of (1)*v-fos*, (2)*c-myc* and (3)*c-jun* after gene cleaning, are shown in Figure 15. The length of these fragments was checked by comparing the positions of the inserts to that of the DNA ladder.

2.8.10. Northern analysis

When preparing RNA from vsmc and endothelial cells grown on silicone, the cells were removed from the silicone in 10ml of serum-free medium,

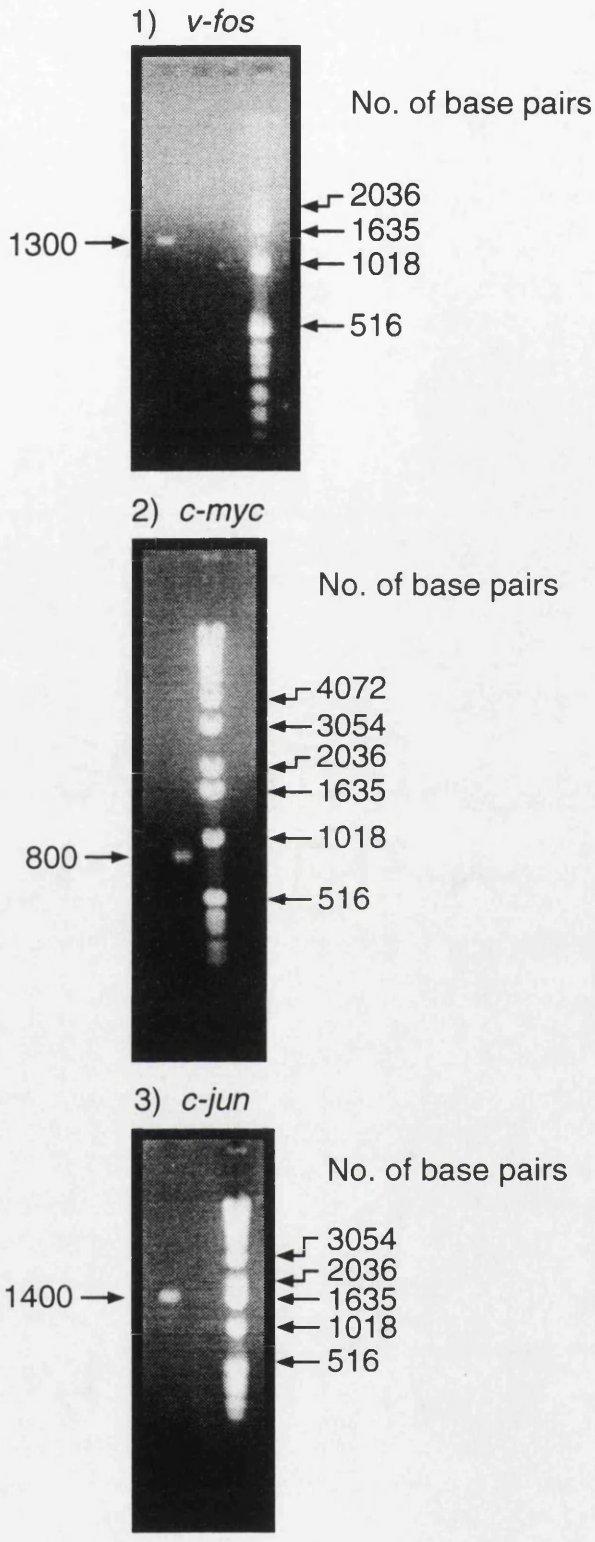

Figure 15.

DNA gels containing gene cleaned samples of 1) *v-fos*, 2) *c-myc* and 3) *c-jun*. The samples were run against a DNA ladder and their length calculated by comparing their positions on the gel to the bands of the DNA ladder.

using a cell scraper, transferred into a universal container and the silicone rinsed with a further 5ml of medium. When preparing RNA fromcells grown in tissue culture flasks, the cells were removed from the flasks in 15ml of serum-free medium, using a cell scraper, transferred into a universal container and the flask rinsed with a further 8ml of medium. The sample was spun at 200g, 5°C for 5 min and the supernatant removed. 1ml of RNAzol B was added to the sample and vortexed. The contents were then transferred into an Eppendorf tube containing 100μl chloroform, vortexed and placed on ice for 5 min. The Eppendorf tube was spun at 15,000rpm in a microcentrifuge for 15 min. The upper layer was transferred into a clean Eppendorf tube and an equal volume of isopropanol (approximately 600μl) added. The sample was placed on ice for 45 min, spun at 15,000rpm for 15 min, the supernatant removed and the pellet drained. 500μl of 70% ethanol was added to the pellet and the RNA stored at -70°C. When required, the RNA samples were spun at 15,000rpm for 15 min and drained until almost dry. 100μl of ddH_2O was then added to each sample, vortexed to dissolve the RNA and placed at 65°C for 10 min. The amount and purity of RNA was determined as described in section 2.8.6. 10μg aliquots of RNA were transferred to Eppendorf tubes containing 250μl of ddH_2O, 500μl of ethanol (AR grade) and 25μl of 3M sodium acetate, pH 5.2 and stored at -70°C.

In preparation for electrophoresis RNA (10μg) was dissolved in 10μl of ddH_2O and 5μl of the following solution was then added: deionized formamide, 1250 μl; 37% formaldehyde, 400μl; 10x MOPS (0.2mol/l), 0.05mol/l sodium acetate pH7.0; 0.01mol/l Na_2EDTA, 250μl, and heated at 65°C, for 10 min. Samples were chilled on ice, 2μl of RNA loading dye added and run on agarose gels.

2.8.10.1 RNA gels

1.2g of agarose was dissolved in a solution containing 10ml of x1 MOPS (20mmol/l) and 73ml of ddH_2O, by heating in a microwave until dissolved. 17ml of formaldehyde (6%) was then added to this solution and left to cool to room temperature. The solution was then poured into a perspex plate (78mm x 105m) containing a plastic comb. The plate was then placed into a G-100 tank and submerged in TE buffer. The samples were run at 60V for 3h.

2.8.10.2 RNA transfer

RNA was transferred from the gels to nylon membranes in 20xSSC by a blotting process. After blotting overnight the RNA was crosslinked onto the nylon membrane using ultra violet radiation and rinsed with 5xSSC solution. The membrane was placed in plastic sheeting and stored at -20°C.

2.8.10.3 Prehybridisation

250μl of salmon testes DNA (100μg/ml) was boiled for 5 min and then placed on ice for 5 min. The DNA was added to a prehybridisation solution containing 500μl of 10% sodium dodecyl sulphate (0.1%), 5ml of 50x Denhardt's solution (5x), 12.5ml of 20xSSC solution (5x), 27ml of ddH_2O and 5g of dextran sulphate (1%). 15ml of the solution was poured into a hybridisation tube. The membrane containing RNA was placed inside the tube with the RNA side facing uppermost and any air bubbles removed by pressing on the membrane with a plastic pipette. The tube was placed inside the hybridisation incubator at 65°C and the filters prehybridised for at least 4h.

2.8.10.4 Random priming cDNA probes

Reagent mix and Klenow fragment used in this procedure were supplied in an oligolabelling kit (Pharmacia, Buckinghamshire, England).

The reagent mix was composed of a buffered aqueous solution containing deoxy adenosine triphosphate (dATP), deoxy guanosine triphosphate (dGTP), deoxy thymidine triphosphate (dTTP) and random hexadeoxtyribonucleotides.

24μl of ddH_2O was added to 10μl of a cDNA probe (50ng) and boiled for 5 min. 10μl of reagent mix and 5μl of CTP were added and all the components gently mixed together. 1μl of klenow fragment was then added to the tube and placed in a water bath at 37°C for a 1h incubation. The radiolabelled probe was separated from unincorporated ^{32}P CTP on a sephadex G-50 column.

2.8.10.5 Hybridisation

The radioactive cDNA was boiled for 5 min, placed on ice for 5 min and injected into the hybridisation tube containing the filter. The tube was then replaced into the hybridisation incubator and left for approximately 18h, at 65°C.

2.8.10.6 Washing filters

Filters were washed with 10ml of 1xSSC containing sodium dodecyl sulphate at a final concentration of 0.5%, at 65°C, for 20 min. The filter was monitored using a mini monitor and if the counts were >10 counts/min a further wash was performed with 0.5xSSC (0.5% sodium dodecyl sulphate) solution at 65°C, for 20 min. The radioactivity of the filter was again determined and if the reading was still >10 counts/min a third wash was performed at 0.1xSSC (0.5% sodium dodecyl sulphate) solution. Autoradiography was performed with Kodak X-omat film at -70°C for 1-2 days.

CHAPTER THREE

RESULTS (A)

DEVELOPMENT OF CELL STRETCHING SYSTEM

3.1 Background

The initial aim of the project was to design a system capable of mimicking the forces to which vascular cells are subjected *in vivo*. In the vessel wall, the principal flow-related forces to which cells are exposed are shear stress and pressure (see section 1.5). This project focussed on the effect of pressure. *In vivo*, with increased and decreased blood flow, changes in blood vessel calibre occur. Consequently, the cells of the vessel wall are compressed and stretched. To simplify this situation of interest, this project examined the effect of a stretching force on cellular function in an environment free of humoral influences.

When choosing which method to stretch cells, it was important to examine the techniques which had already been used to apply mechanical forces to cells in culture. As discussed in section 1.6, two principal techniques have been used to produce a stretching force. The first system involves displacing the flexible bases of Petriperm dishes and the second the use of stretch frames. Both systems are suitable for stretching cells and exhibit the essential features required of a cell culture system. An important feature is that sterility can be maintained throughout the studies. The major disadvantages associated with these methods is that stretch is non-uniform and the range to which cells can be stretched is restricted. The greatest degree of stretch was achieved in the centre of Petriperm dishes and in the case of the stretch frames one would expect to achieve the greatest stretch in the centre of the silicone sheet. This means that cells grown on the dishes and the silicone are stretched by different amounts, relative to their position on the substrate. It is easier to interpret results obtained from cells which have been stretched by a fixed length, regardless of their position on the apparatus.

3.2 First prototype

On reviewing the literature and assessing the requirements of the stretching apparatus, it seemed most practical to include Petriperm dishes in the design of the system. Advantages of using Petriperm dishes in addition to their suitability as a substrate for cell growth, was that they were suitable for the sectioning of cells and for processing procedures required for histological analysis. Another advantage was that the Petriperm dishes were not bulky and could be easily housed in an incubator. Furthermore, the dishes were available commercially. It was proposed that cells would be grown on the dishes and when confluent they would be vertically displaced by means of a vacuum. Displacement of the bases using suction was chosen because the introduction of a vacuum pump inlet into the incubator was feasible by boring a hole at the rear of the incubator.

3.2.1 Growth of vsmc and endothelial cells in Petriperm dishes

In previous published experiments (section 1.6), several cell types grew well on the Petriperm dishes. Therefore the ability of Petriperm dishes to facilitate the growth of vsmc and endothelial cells was tested.

Figure 16 shows the effect of various cell adhesion-promoting agents on vsmc growth in Petriperm dishes. Petriperm dishes were coated with either 0.01% collagen (type I), 25 μg/ml fibronectin, 2% gelatin solution, or 10 μg/ml poly-l-lysine, as described in section 2.5.1. Control dishes remained untreated. Vsmc were seeded in the dishes at a density of 0.05×10^6 cells per dish, allowed to grow for 3 days and cell numbers determined. There was no significant difference in the number of cells present in the dishes which had been coated with either collagen or poly-lysine, compared to control values. Coating the dishes with gelatin and fibronectin resulted in a 2- and 2.4-fold increase respectively. Thus fibronectin was chosen as the most suitable cell adhesion-promoting agent. To ensure that endothelial cells also grew

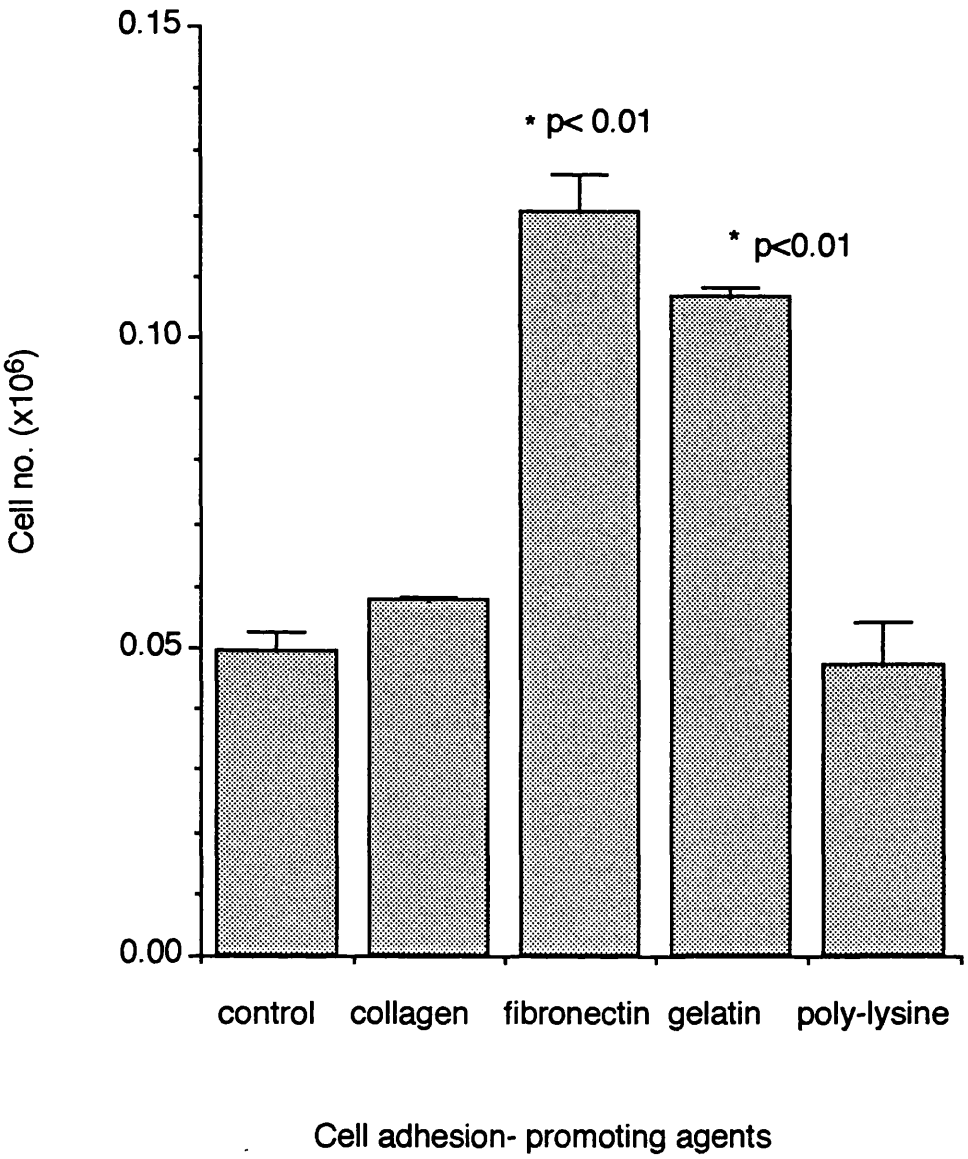

Figure 16. Effect of coating Petriperm dishes with collagen (0.01%), fibronectin (25μg/ml), gelatin (2%), or poly-lysine (10μg/ml) on vsmc growth. Vsmc were plated at a density of $0.05x10^6$ cells and grown in Petriperm dishes, as described in the methods (section 2.5.1). After 4 days in culture, cell numbers were determined using an electronic Coulter counter. Values are expressed as mean ± S.E.M.

well in fibronectin-coated Petriperm dishes, a similar experiment was performed. Petriperm dishes were coated with 25 μg/ml fibronectin and vsmc seeded at a density of $0.1x10^6$ cells per dish. Control dishes did not receive fibronectin treatment. The cells were left to grow for 4 days and cell numbers determined. A 1.5-fold increase in the number of cells in dishes which had been coated with fibronectin was observed, compared to the number of cells grown in untreated dishes (Figure 17). Thus coating of Petriperm dishes with fibronectin was a suitable treatment to potentiate vsmc and endothelial cell growth.

3.2.2 Design

Figure 18 illustrates the first prototype apparatus developed. It consisted of a perspex block onto which an "o" ring was raised 1.3mm above the base. A Petriperm dish was placed on top of the "o" ring after greasing and on application of a vaccum the membrane was vertically displaced. This apparatus could be placed inside an incubator, maintained at a humidified 37°C atmosphere, with 95% air / 5% CO_2.

3.2.3 The effect of stretch on *c-fos* messenger RNA (mRNA) expression

The aim of the first experiment was to determine whether a "stretching" force could induce proto-oncogene expression. Proto-oncogenes are known to be expressed prior to cell proliferation.

Vsmc were seeded at a density of $0.2x10^6$ cells per dish and left to grow for 3 days, until confluent. The cells were made quiescent by serum deprivation for 24h and then stretched for either 0, 15, 30, 60, 180, or 360 min. Control vsmc remained unstretched. RNA was prepared from the vsmc and the effect of stretch on the expression of the proto-oncogene *c-fos* mRNA determined. The results obtained are illustrated in Plate 6. A maximum *c-fos* mRNA expression was achieved after 30 min of stretching and was abolished by 180 min. The time course of induction for *c-fos* mRNA on stretching was similar to that previously described by Lyall et al. [36] for ANG II in vsmc. This was

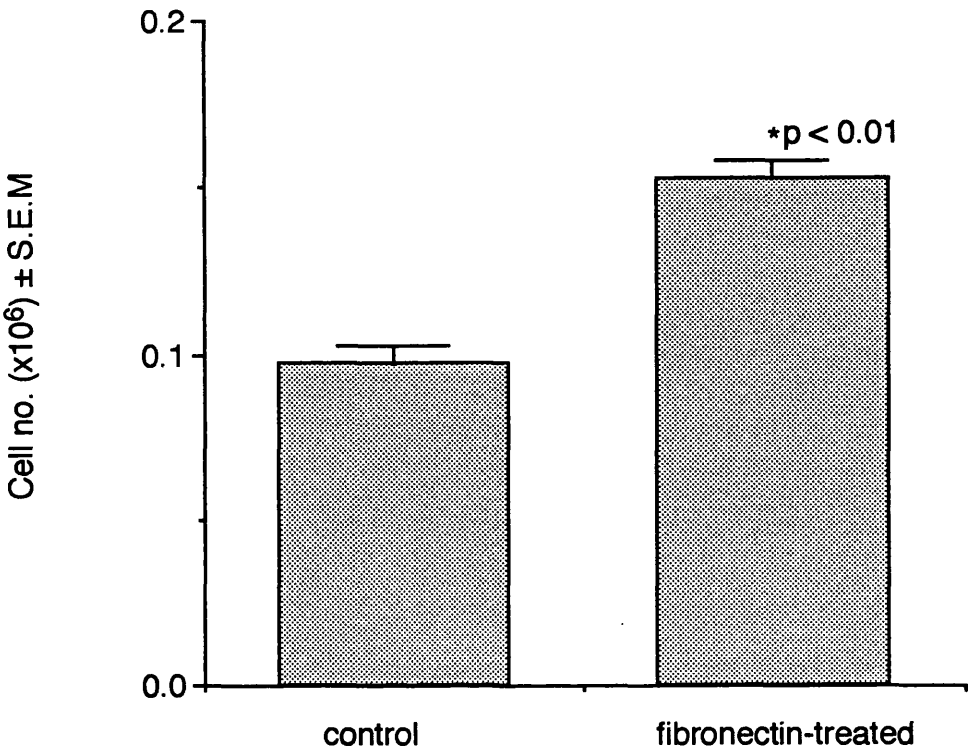

Figure 17. Effect of coating Petriperm dishes with fibronectin (25μg/ml), on endothelial cell growth. Endothelial cells were plated at a density of $0.05x10^6$ cells and grown in the Petriperm dishes, as described in the methods (section 2.5.1). After 4 days in culture, cell numbers were determined using an electronic Coulter counter. Values are expressed as mean ± S.E.M; n=5.

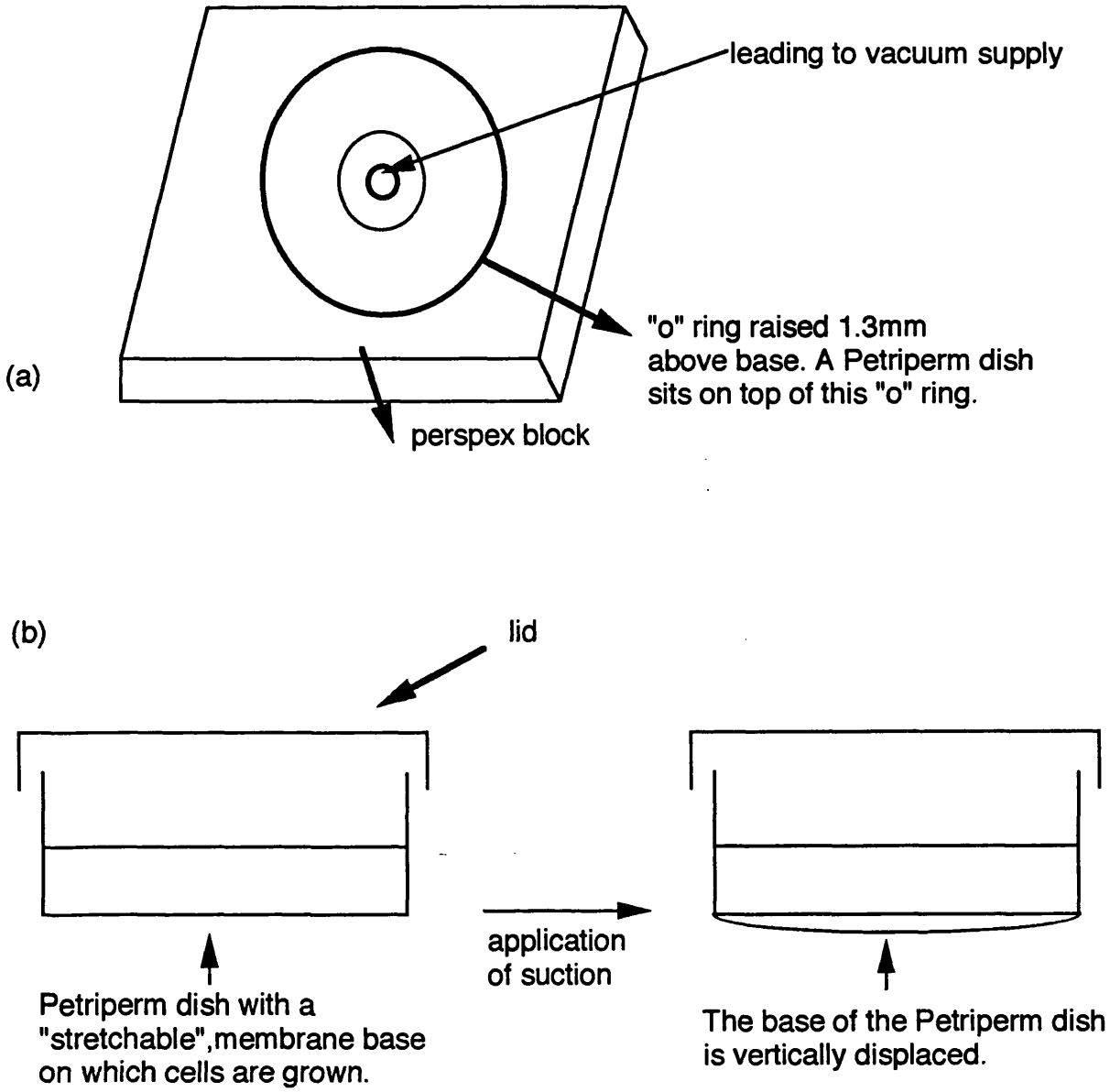

Figure 18. First prototype of stretching system.
(a) This is a schematic representation of the prototype. The system is composed of a perspex base of which a circular area has been cut out to allow the introduction of a vacuum and a rubber "o" ring. A Petriperm dish is positioned over the "o" ring.
(b) A cross sectionional area of a Petriperm dish is shown in Figure 18b. Application of a vacuum results in the vertical displacement of the base of the dish.

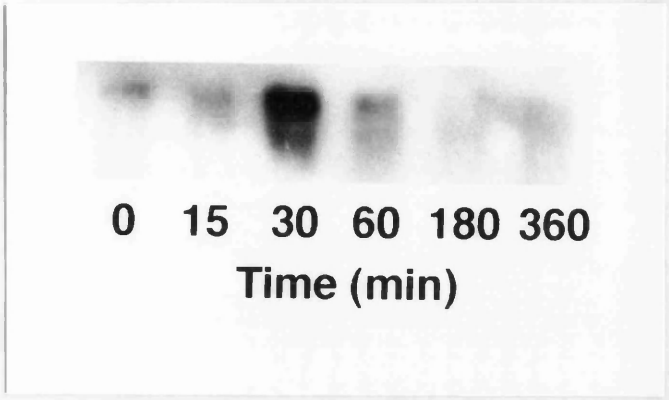

Plate 6. A representative autoradiograph showing the effects of stretch on *c-fos* mRNA induction, in vsmc. Vsmc were plated at a density of $0.2x10^6$ in Petriperm dishes and grown to confluence. Cells were deprived of serum for 24 hours and then stretched for 0, 15, 30, 60, 180 or 360 min. RNA was extracted from the cells, run on agarose gels and blotted onto nylon membranes, as described in the methods (section 2.8.10). The membranes were hybridised with a *v-fos* cDNA probe and exposed to x-ray film for 48h, at -70°C.

very exciting because it showed that stretch produced similar effects to a growth factor (ANG II), and that the experimental system was functional.

3.2.4 Displacement of Petriperm dish base

It was possible to observe the vertical displacement of the membrane by the naked eye. This was further verified by applying suction to a Petriperm dish and then pouring in 5ml of a plaster of Paris/water mixture (50:50). After 15 min the plaster had set and the vacuum was switched off. When the mould was removed from the dish it was evident that under suction the flexible membrane had adopted a dome shape, as shown in Figure 18b. These findings illustrated that the membrane was stretched. Clearly from the shape that the base of the Petriperm dish adopted, the stretch was not uniform over the base of the dish.

When the base of the dish is relaxed it is flat and when displaced it adopts a convex shape. To calculate the area of of the convex surface the formula used is: Area=3.14(r^2 + h^2), where r= the radius of the Petriperm dish, which was measured as 2.5cm, and h=the vertical displacement of the membrane, which for this system is 1.3mm (see Figure 19). From these figures the area of the convex surface was calculated to be 19.69cm^2. It was necessary to calculate the area of the membrane in the unstretched state. This was calculated using the equation for the area of a circle; Area=3.14(r^2), where r=2.5cm. Thus the area of the flat surface was 19.63cm^2. Application of the vacuum thus produced a 0.06cm^2 increase in area, which was an overall increase of 0.3%.

3.2.5 Problems with first prototype

From these observations two major problems became apparent. The first was that base of the dish was stretched in a non-uniform manner and thus the cells grown in the Petriperm dishes were stretched by different amounts. The second problem was that a maximum stretch of 0.3% was too small to reproduce physiological conditions. *In vivo*

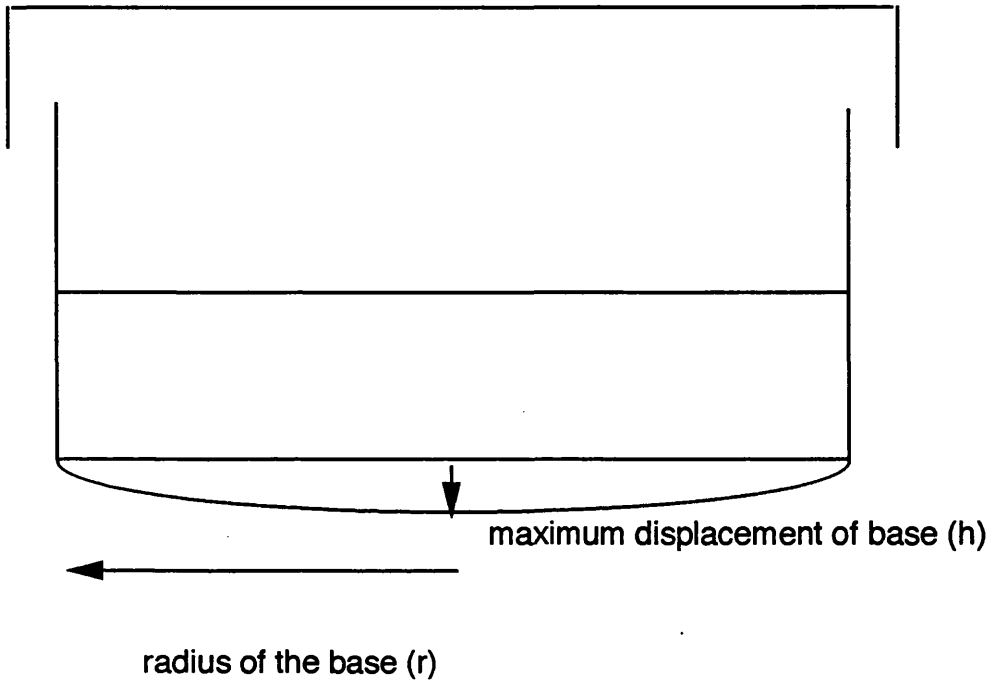

Figure 19. A cross-sectional area of a Petriperm dish under suction. Measurements of the radius of the base and the maximum height by which the base could be displaced are shown in this figure.

studies suggest that vessels experience greater forces than could be achieved using this initial prototype. For example, Hebert et al.[227] measured changes in rat resistance vessels, in response to baroreceptor stimulation, and found a 12.03 ± 2.7% increase in diameter length. Although the degree of stretch could be increased by increasing the height of the "o" ring, the consequence of this would be for the base to adopt a more elongated shape giving a stretch of even more non-uniform nature. An additional disadvantage of this system was that a Petriperm dish has a relatively small base area. A confluent cell layer yielded approximately 20μg of total RNA, which was only enough RNA to perform Northern analysis a restricted number of times. Larger dishes were not commercially available. Although the vacuum system was not suitable for further investigations, it had illustrated that fairly minimal stretch could induce expression of *c-fos* mRNA by vsmc.

3.3 Second prototype

An apparatus capable of achieving a stretch from 0-20%, to cover the range used by other groups and to enable work to be performed outwith these values was planned. This could be achieved most practically by a stretch frame system. The problem of non-uniform stretch which had been previously experienced using this method was to be resolved in the design of the new system. The advice and skills of engineers from Glasgow University, Department of Physics and Astronomy were employed. Careful design and precision engineering were adopted in the development of the system.

3.3.1 Design (Plate 7)

The apparatus was made of a perspex base onto which 4 screws were vertically aligned. The base had a rectangular area in the centre cut out for examination of the cells by inverted microscopy. Rectangular pieces of silicone sheeting containing holes at each corner were mounted onto the base by placing them over the 4 screws. The sheet was secured by

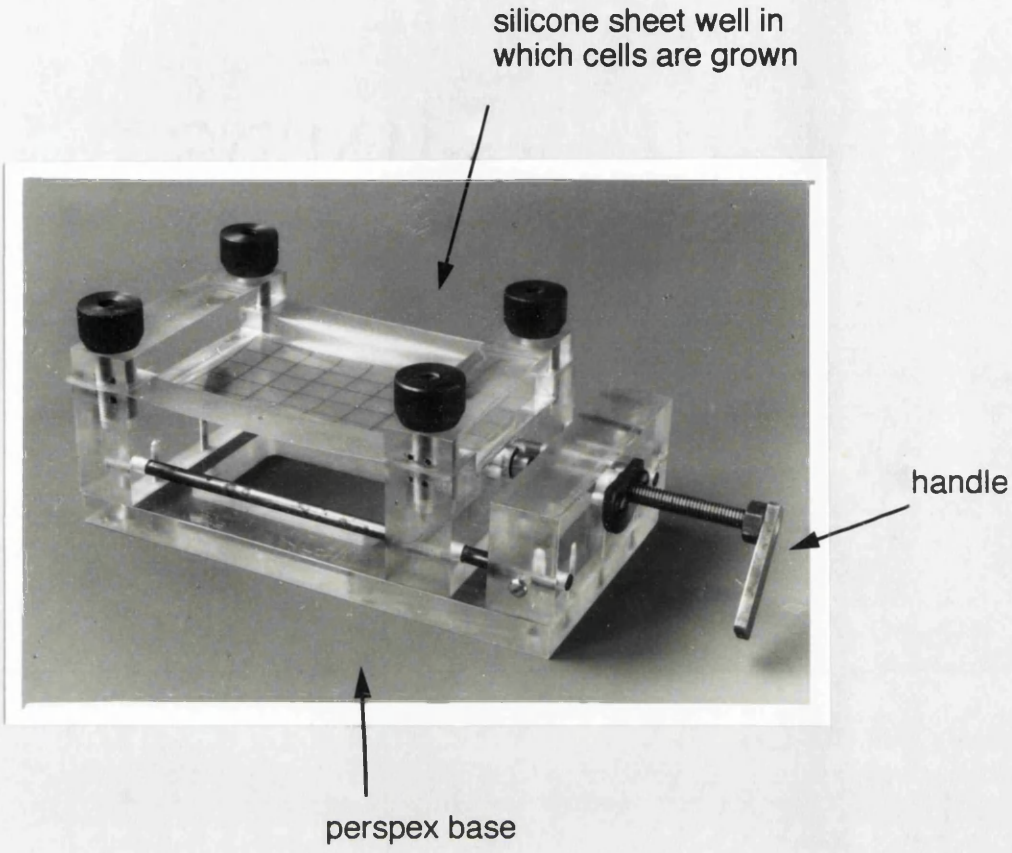

Plate 7. Initial design of cell stretching apparatus.

two pieces of perspex which were placed on top of the silicone in a parallel configuration. When secured, the silicone sheet adopted a rectangular well shape in which cells could be grown. A perspex lid was placed on top of the silicone to minimise contamination. To increase the length of silicone sheet, the handle at the side was turned in a clockwise direction. In the unstretched position the distance between perspex blocks was 80mm. To stretch the silicone and hence the tightly attached cells by 5%, the distance between the perspex blocks was increased to 84mm. 10%, 15% and 20% were achieved by increasing the distance between the blocks to 88, 92 and 96mm, respectively.

To check that the apparatus did not leak, 10ml of serum-free medium was poured into the silicone well of one piece of apparatus and placed overnight in an incubator. No leaking occurred. This prototype could produce a stretch of up to 15%. Subsequent systems which could produce a maximum stretch of 20% were achieved by increasing the length of the perspex base. In the initial design, the screws of the apparatus were made of brass. In subsequent systems, these were changed to plastic to minimise corrosion. Plate 8 illustrates the modified version of the stretching apparatus. The plans of the apparatus are shown in Figure 20. 24 identical pieces of apparatus were constructed and checked for leaking as before.

3.3.2 Properties of the silicone sheet in response to stretch

The uniformity of stretching throughout the whole area of the sheet was tested. This had been a limitation in other stretching systems. A grid of 40, 1cm^2 squares was drawn on a piece of silicone sheeting 8x5cm in area and the change in length of the squares as the silicone was stretched by 0, 5, 10, 15 and 20% was measured. The measurements were performed at 37°C, the temperature maintained in an incubator, to ensure that the elasticity properties of the silicone were not affected by temperature. Five pieces of silicone sheeting, each from a different batch, were examined.

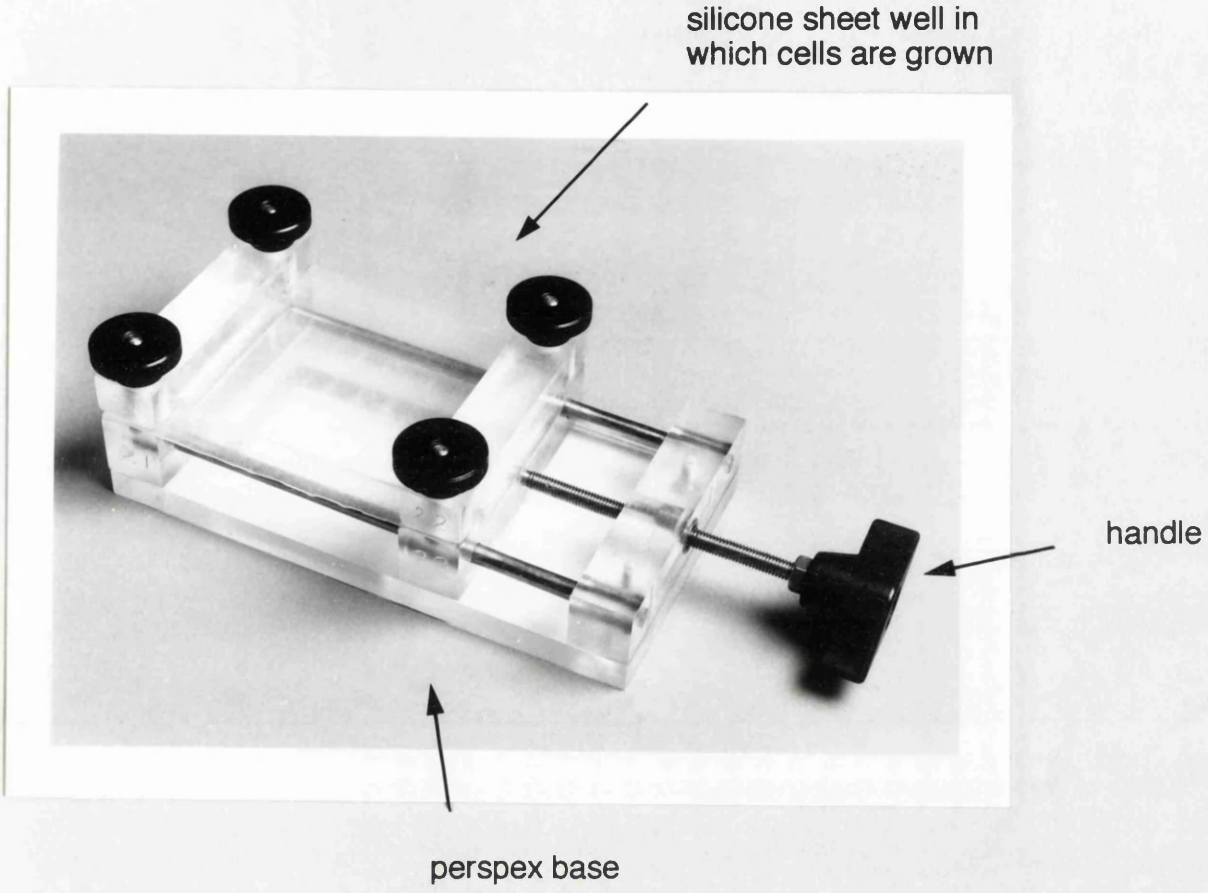

Plate 8. Modified design of cell stretching apparatus.

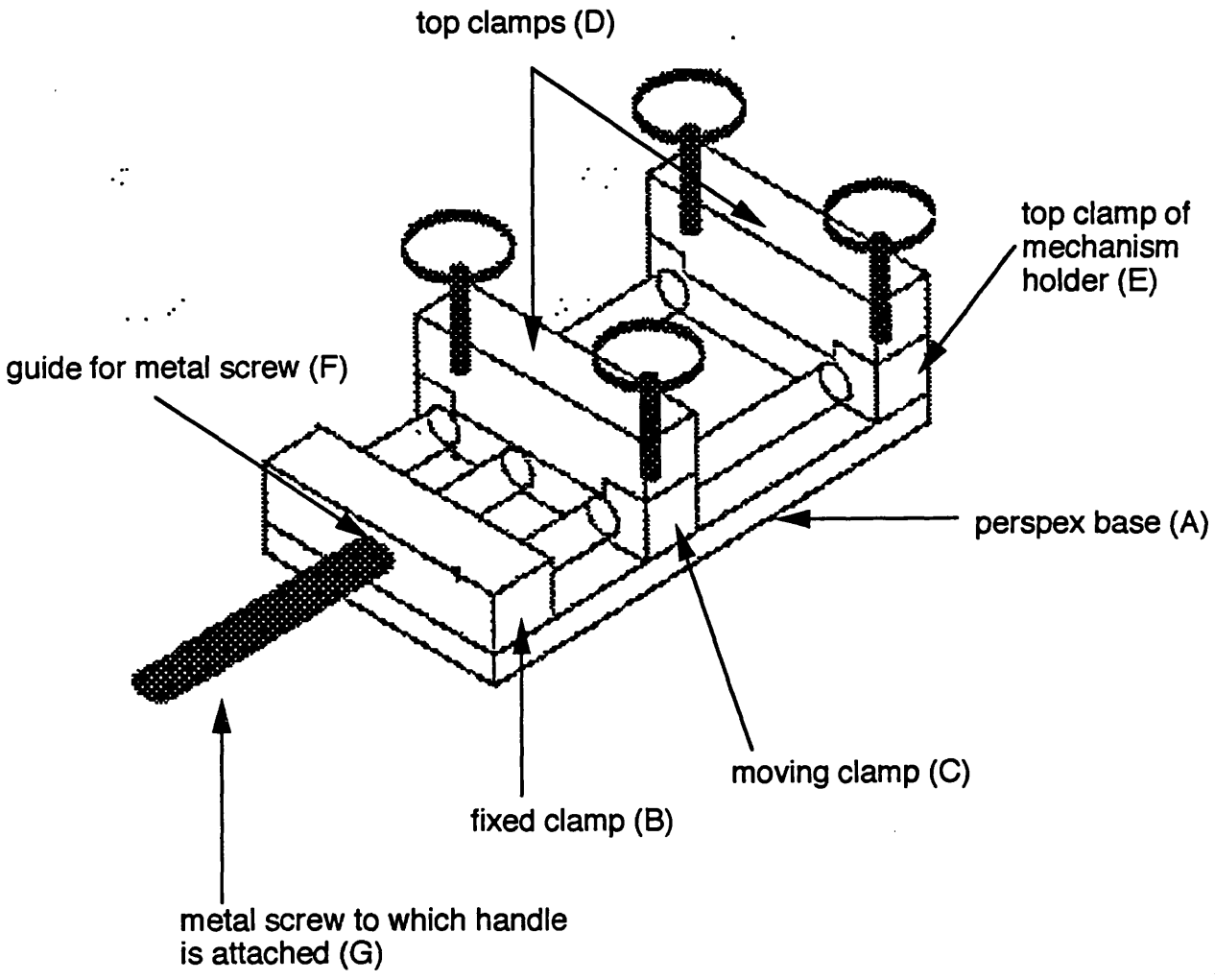

Figure 20. Three dimensional drawing of the stretching apparatus showing the positions of the various components. Figures 20 A, B, C, D, E, F, G show the plans for each of the components of the apparatus labelled A-G, in the above diagram.

GLASGOW UNIVERSITY — PHYSICS & ASTRONOMY

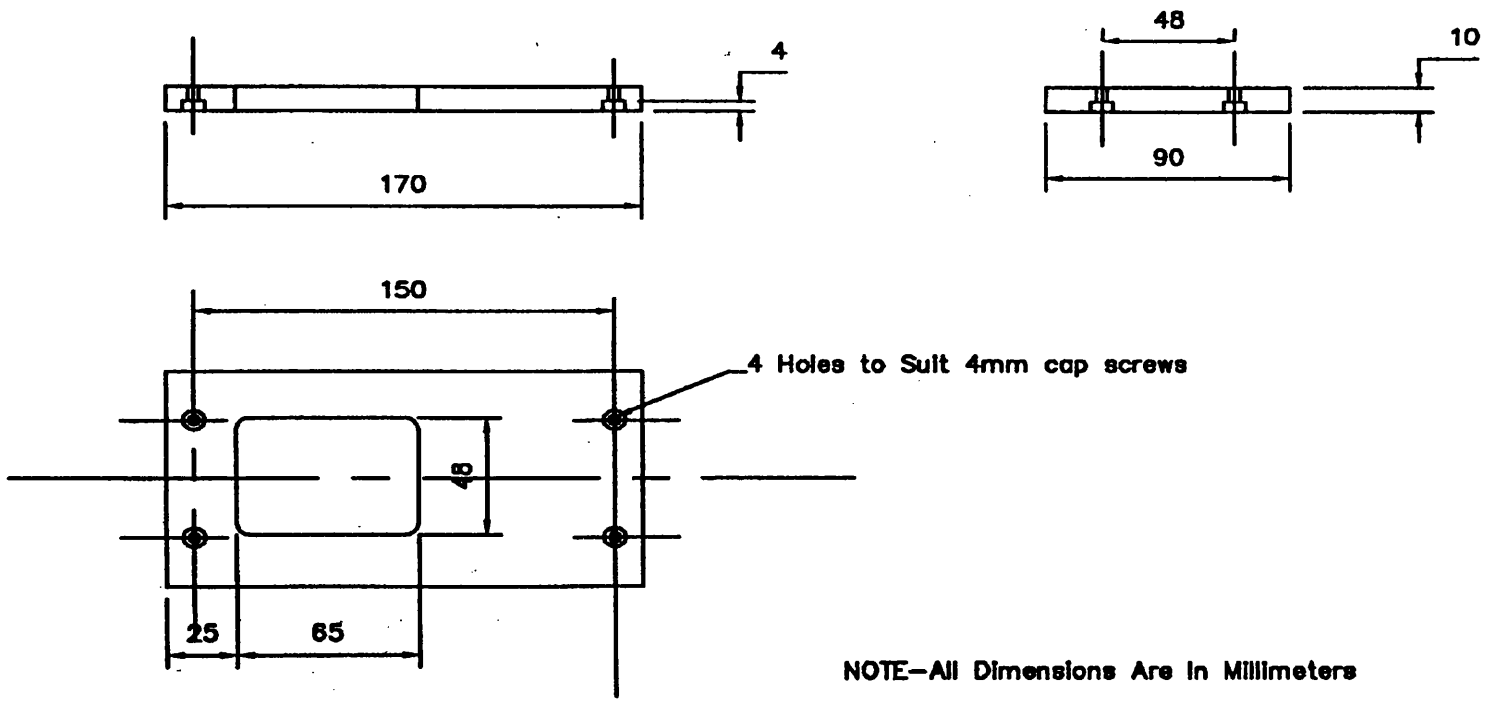

NOTE–All Dimensions Are In Millimeters

A PERSPEX BASE

unless otherwise specified TOLERANCES are					
one place (0) ±0.76 (±0.030)				DESCRIPTION BASE	
two place (00) ±0.38 (±0.015)					
three place (000) ±0.13 (±0.005)	DRAWN	DATE	SCALE	ISSUE	MATERIAL PERSPEX	DRAWING No WI 0174–1
	T.L.N	11–11–91	N.T.S.	1	

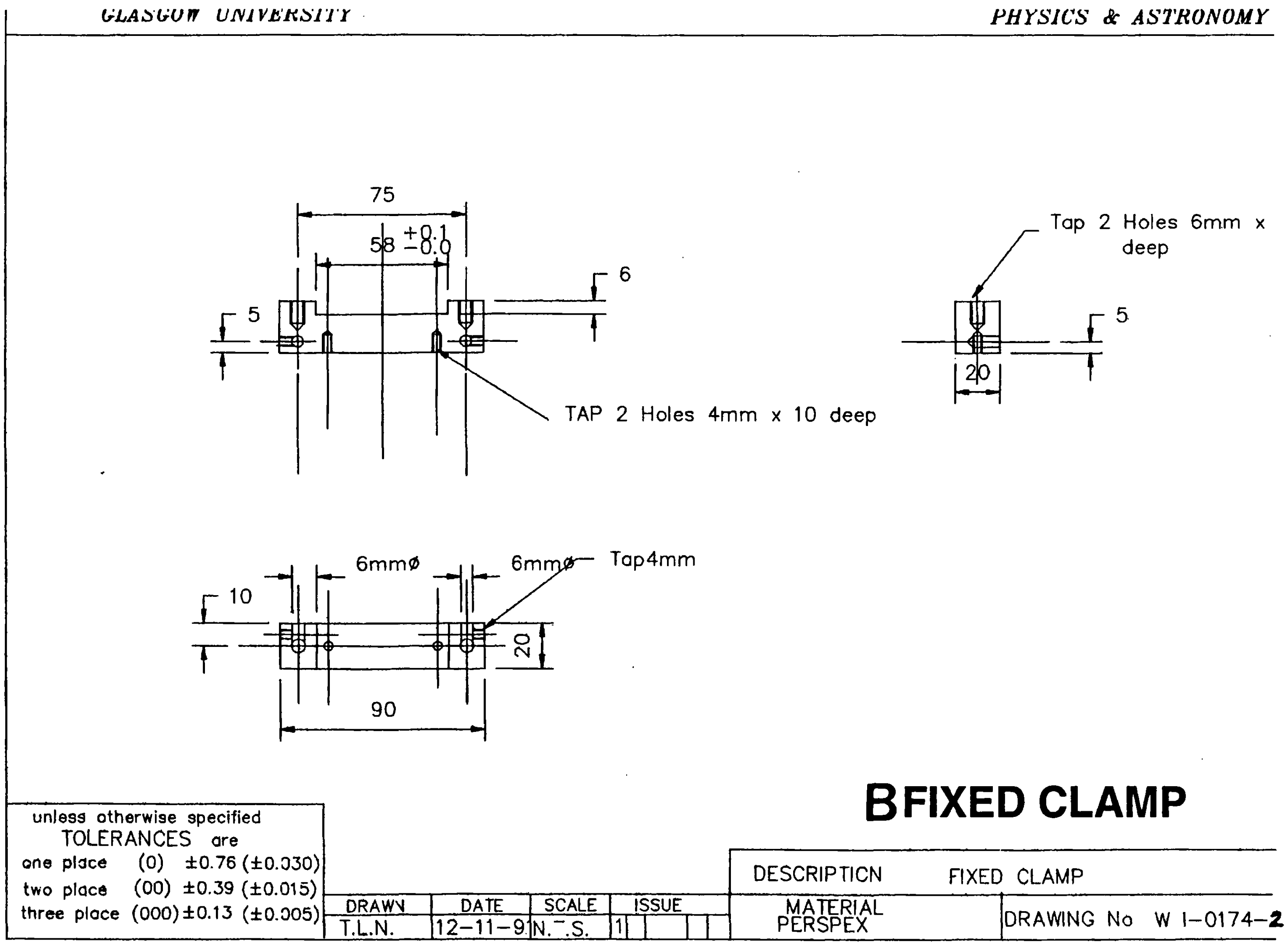
GLASGOW UNIVERSITY
PHYSICS & ASTRONOMY
75
58 +0.1 −0.0
6
5
TAP 2 Holes 4mm x 10 deep
Tap 2 Holes 6mm x deep
5
20
6mmø
6mmø
Tap4mm
10
20
90
BFIXED CLAMP
unless otherwise specified
TOLERANCES are
one place (0) ±0.76 (±0.030)
two place (00) ±0.39 (±0.015)
three place (000) ±0.13 (±0.005)
DRAWN T.L.N.
DATE 12-11-9
SCALE N.T.S.
ISSUE 1
DESCRIPTION FIXED CLAMP
MATERIAL PERSPEX
DRAWING No W I-0174-2

GLASGOW UNIVERSITY *PHYSICS & ASTRONOMY*

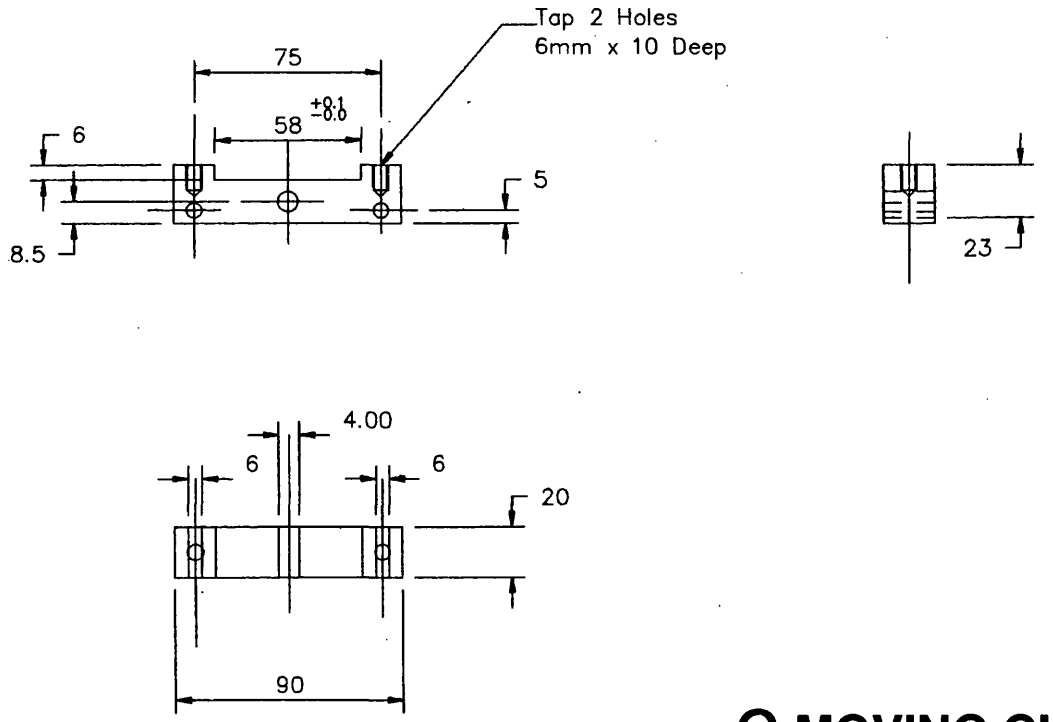

C MOVING CLAMP

unless otherwise specified
TOLERANCES are
one place (0) ±0.76 (±0.030)
two place (00) ±0.39 (±0.015)
three place (000) ±0.13 (±0.005)

DRAWN	DATE	SCALE	ISSUE
T.L.N.	14/11/91	N.T.S.	1

DESCRIPTION MOVING CLAMP

MATERIAL PERSPEX

DRAWING No WI 0174-3

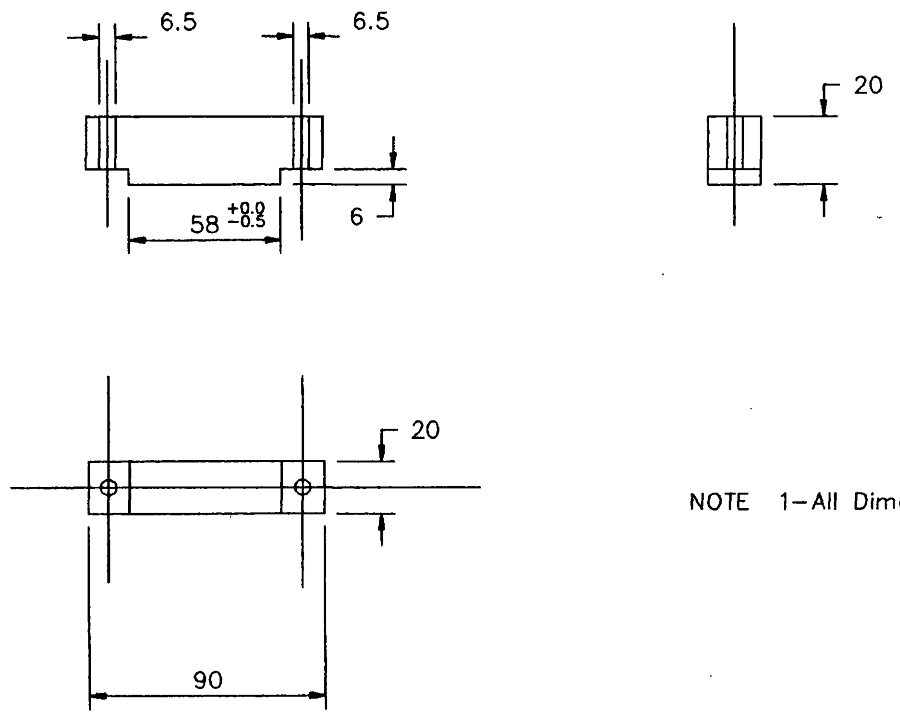

NOTE 1–All Dimensions in Millimeters

D TOP CLAMP

unless otherwise specified
TOLERANCES are
one place (0) ±0.76 (±0.030)
two place (00) ±0.39 (±0.015)
three place (000) ±0.13 (±0.005)

DRAWN	DATE	SCALE	ISSUE	DESCRIPTION TOPCLAMP	
T.L.N	14/11/91	N.T.S.	1	MATERIAL PERSPEX	DRAWING No WI 0174–4

GLASGOW UNIVERSITY — PHYSICS & ASTRONOMY

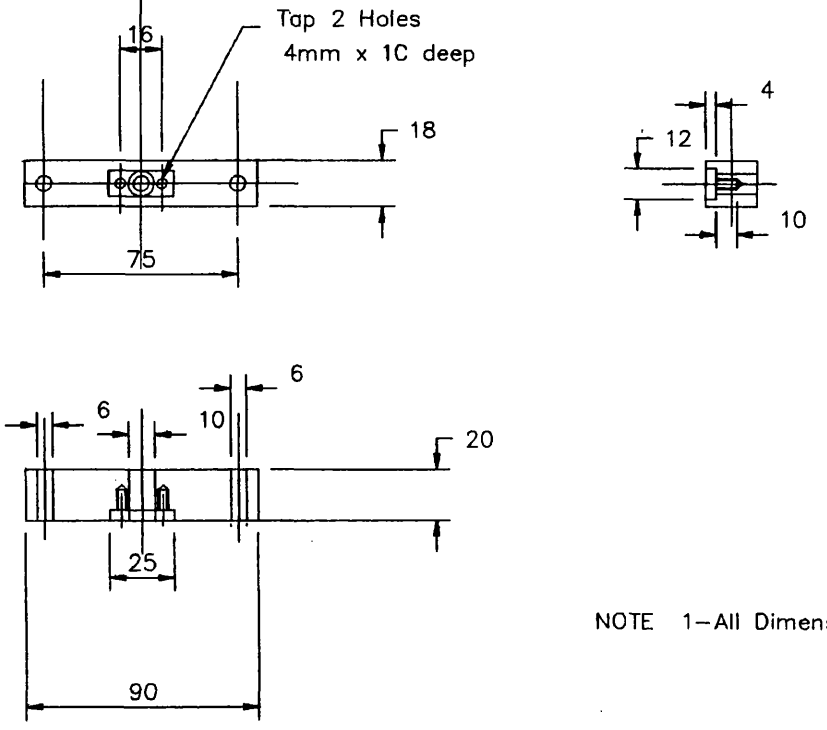

NOTE 1—All Dimensions in Millimeters

E TOP CLAMP OF MECHANISM HOLDER

unless otherwise specified TOLERANCES are						
one place (0) ±0.76 (±0.030)					DESCRIPTION	MECHANISM HOLDER
two place (00) ±0.39 (±0.015)						
three place (000) ±0.13 (±0.005)	DRAWN	DATE	SCALE	ISSUE	MATERIAL	DRAWING No
	T.L.N.	15/11/91	N.T.S	1	PERSPEX	W I 0174-5

GLASGOW UNIVERSITY *PHYSICS & ASTRONOMY*

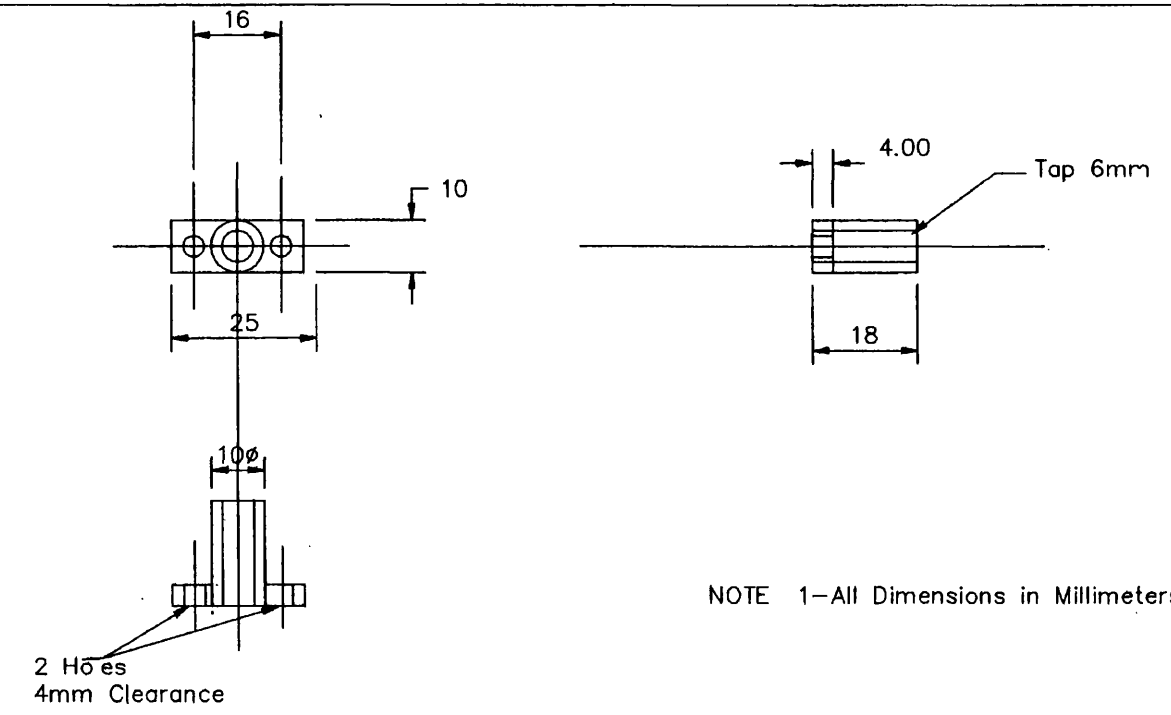

NOTE 1–All Dimensions in Millimeters

F GUIDE FOR METAL SCREW

unless otherwise specified TOLERANCES are					
one place (0) ±0.76 (±0.030)				DESCRIPTION DRIVE MECHANISM HOLDER	
two place (00) ±0.39 (±0.015)					
three place (000) ±0.13 (±0.005)	DRAWN	DATE	SCALE	ISSUE	MATERIAL	DRAWING No
	T.L.N	5/12/91	NTS	1	BRASS	W 1–0174–6

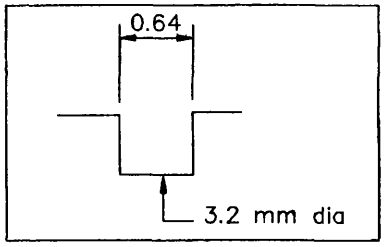

Groove Detail

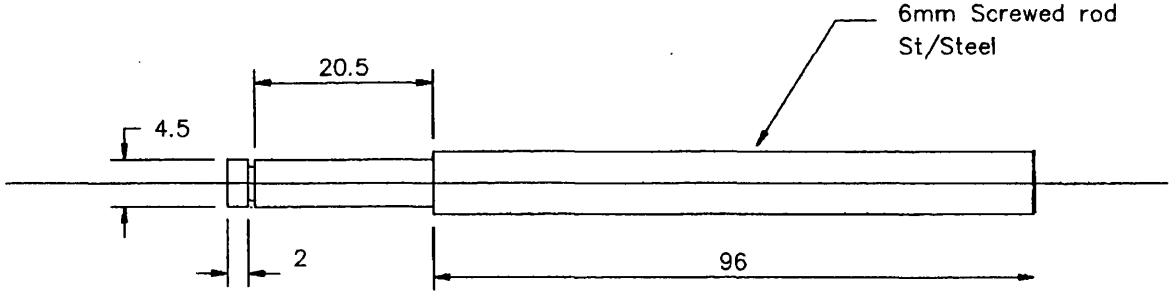

NOTE 1--ALL DIMENSIONS IN MILLIMETERS

G METAL SCREW TO WHICH HANDLE IS ATTACHED

unless otherwise specified TOLERANCES are					
one place (0) ±0.76 (±0.030)				DESCRIPTION DRIVE SCREW	
two place (00) =0.39 (±0.015)					
three place (000) =0.13 (±0.005)	DRAWN	DATE	SCALE	ISSUE	MATERIAL	DRAWING No W 1-0174-7
	T.L.N.	1/12/91	NTS	1	ST/STEEL SCREWED ROD	

The mean stretch achieved by the whole sheet was studied and the results shown in Figure 21. This figure shows that there were no significant differences in the length of individual squares at different positions on the sheet, as reflected by the small values obtained for standard errors. These results suggest uniformity of stretching of the silicone sheet both within and between batches of material.

3.3.3 Vsmc growth on silicone sheet

To determine whether vsmc grew well on the silicone sheet, an analysis of growth was performed. On day zero, 0.5 x 10^6 vsmc were plated down onto the untreated silicone sheeting of twenty pieces of cell stretching apparatus. The same number were placed into twenty untreated 75cm^2 tissue culture flasks. The number of cells present on 4 pieces of apparatus and in 4 flasks were evaluated daily for 5 days, at which time the vsmc in the tissue culture flasks reached confluence.
Even though more cells had been placed down onto the untreated silicone per cm^2, vsmc grew at a slower rate on untreated silicone than on untreated tissue culture flasks (Figure 22). On day 5, the flasks contained approximately 7 times the number of vsmc present on the silicone. Untreated silicone sheeting was therefore not a suitable substrate for vsmc growth. The efficacy of various cell adhesion-promoting agents to potentiate vsmc adhesion and growth on the silicone sheet was tested as follows. Silicone sheets were coated with either 0.01% collagen (type I), 25 μg/ml fibronectin, 2% gelatin solution, or 10 μg/ml poly-l-lysine, as described in section 2.5.2. Untreated silicone sheets were used as controls. After the appropriate treatment, vsmc were seeded at a density of 0.8 x 10^6 cells per piece of silicone sheeting, grown for 4 days and cell numbers determined. Figure 23 shows the number of cells on the silicone after 4 days in culture. Silicone coated with either collagen or gelatin contained approximately 0.6x10^6 cells, which was not significantly different from control values. Poly-lysine coated silicone contained approximately 1.2x10^6 cells, a small but significant increase over control. However, an approximate 5-fold increase in cell number was observed for vsmc grown on fibronectin-treated silicone. Fibronectin-coated silicone sheets provided

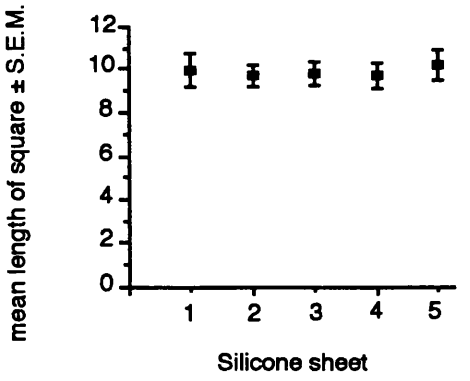

(a) 80mm (0%).

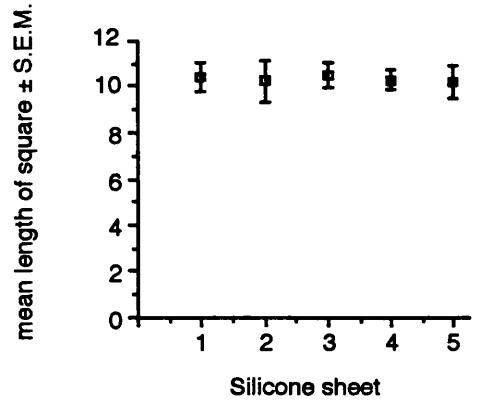

(b) 84mm (5%).

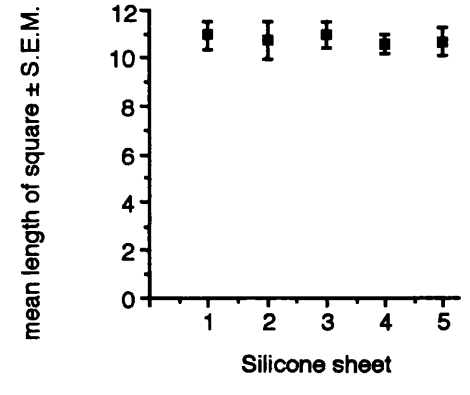

(c) 88mm (15%.)

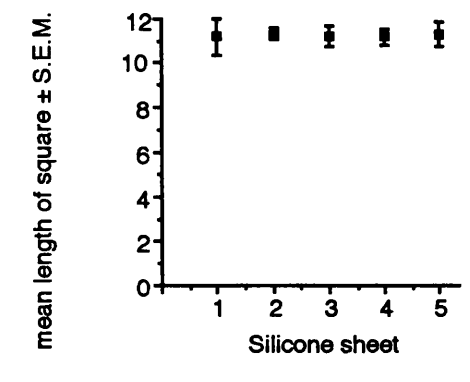

(d) 92mm (15%).

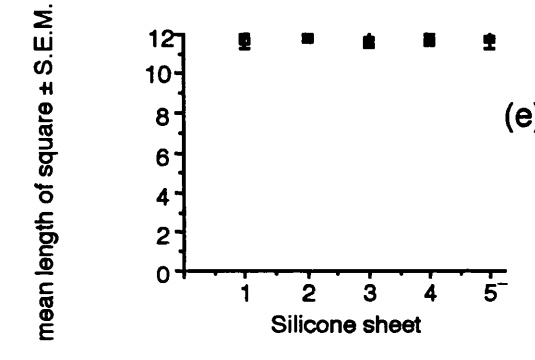

(e) 96mm (20%).

Figure 21. Properties of silicone sheet in response to stretch. A grid consisting of 40 squares was drawn onto 5 pieces of silicone, each from different batches, numbered 1, 2, 3, 4 and 5. The change in length of each individual square was measured as the length of the silicone sheet was increased from 80mm, to 84mm, 88mm, 92mm and 96mm. Results are expressed as mean length ± S.E.M.

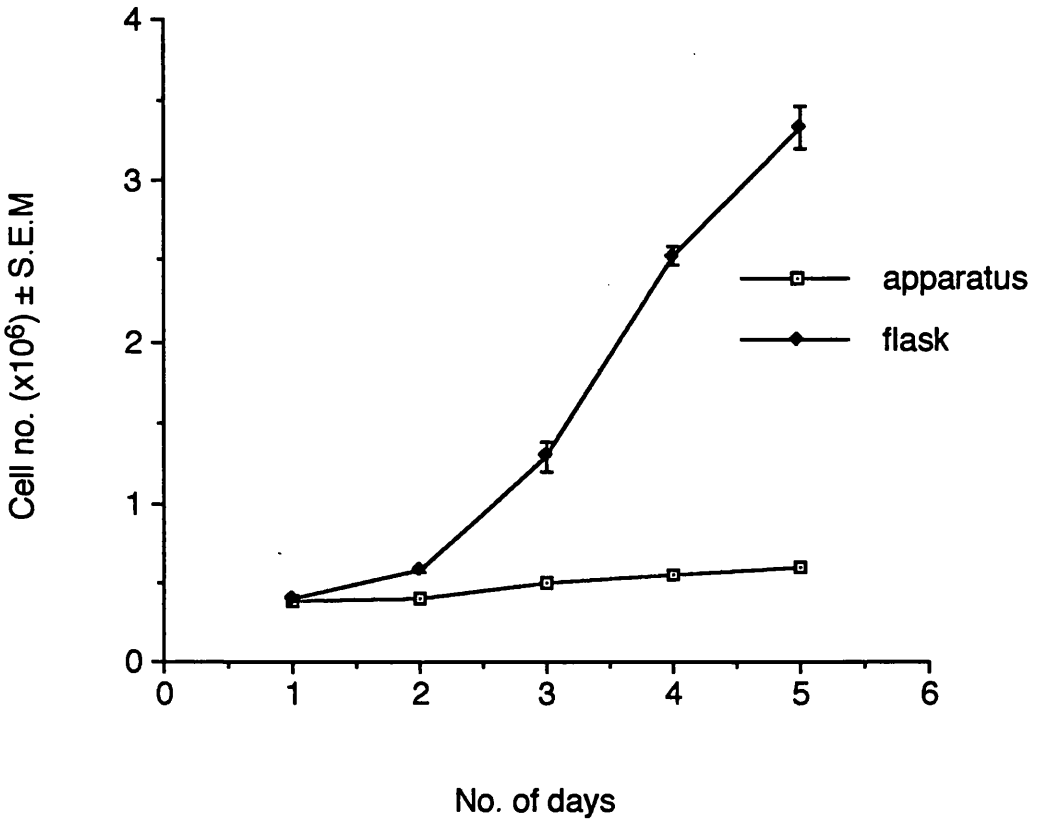

Figure 22. Growth of vsmc on untreated silicone sheet compared to untreated cell culture flasks. $0.5x10^6$ vsmc were plated down onto the silicone sheeting of 20 pieces of apparatus and the same density placed into 20, $75cm^2$ tissue culture flasks. This was regarded as day zero of the study. The number of cells present on 4 pieces of apparatus were evaluated daily, for 5 days, until the vsmc in the flasks had reached confluence.
Results are expressed as mean ± S.E.M; n=4.

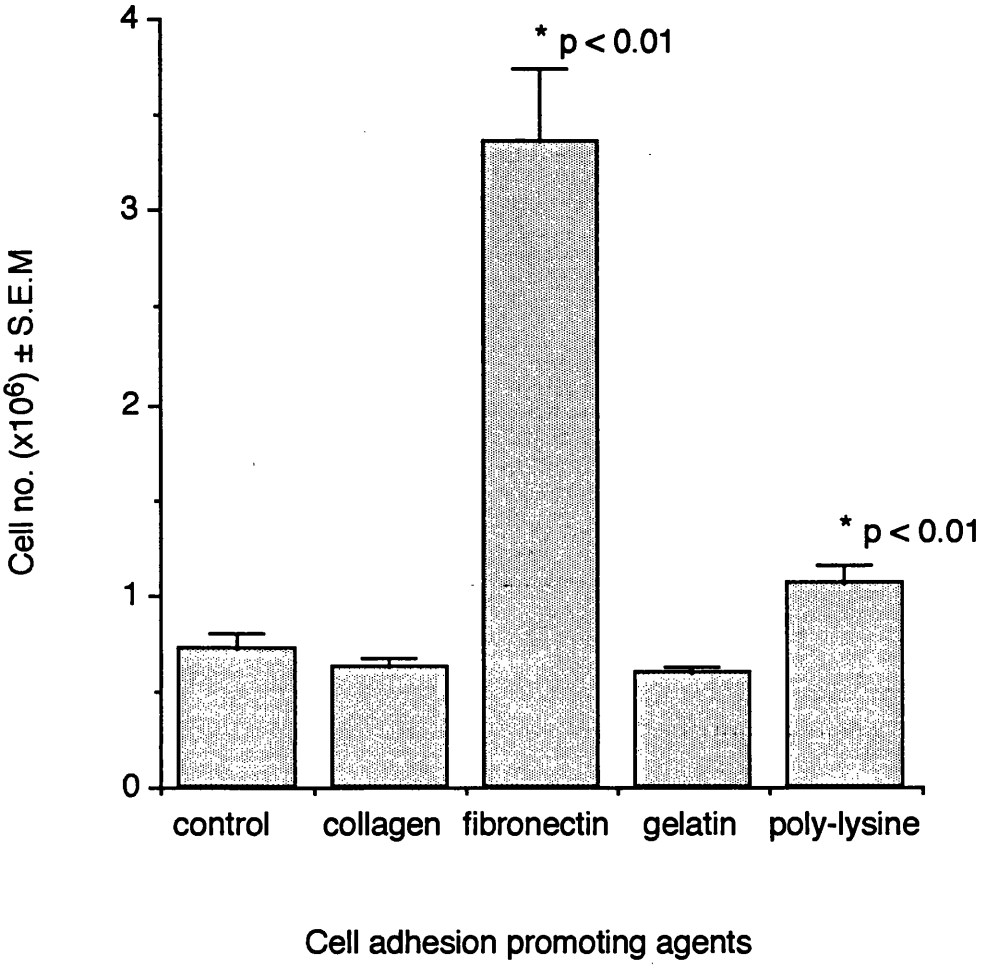

Figure 23. Effect of coating silicone sheet with cell adhesion-promoting agents, on vsmc growth. Silicone sheets were treated with collagen (0.01%), fibronectin (25μg/ml), gelatin (2%) or poly-lysine (10μg/ml). Vsmc were plated at a density of $0.8x10^6$ cells and grown on the silicone sheet as described in the methods (section 2.5.2). After 4 days in culture, cell numbers were determined using an Electronic Coulter counter. Values are expressed mean ± S.E.M; n=5.

the best substrate of those tested for vsmc growth. Plate 9 shows vsmc which grew to confluence on fibronectin-treated silicone. The growth of vsmc on fibronectin-treated silicone can be compared to that of vsmc growth on a tissue culture flask, by comparing Plate 9 with Plates 2&3 (Methods, section 2.3.2). These observations support the fact that fibronectin is a suitable substrate for vsmc growth.

To confirm that the vsmc had grown evenly over the fibronectin-treated silicone membranes, cells were grown to confluence on the silicone and then stained for protein using the protein stain coomassie blue, as described in section 2.5.4. Fibronectin-treated silicone without cells attached was also stained and used as a control. As shown in Plate 10b, an even blue staining was produced over the surface of the rectangular piece of silicone signifying that vsmc growth was evenly distributed across the silicone sheet. Silicone sheeting without vsmc attached did not stain with coomassie blue (Plate 10a).

3.3.4 Endothelial cell growth on silicone sheet

Studies on endothelial cell growth and the effects of stretching were also planned. Thus it was important to test silicone sheeting as a substrate for endothelial cell growth.

Bovine aortic endothelial cells at a density of 0.5×10^6 cells were plated down onto the untreated silicone sheeting of twenty pieces of cell stretching apparatus and the same number placed into twenty untreated $75cm^2$ tissue culture flasks at day zero of the study. The number of cells present on 4 pieces of apparatus and in 4 flasks was determined daily for 5 days at which time the endothelial cells present in the tissue culture flasks had reached confluence.

Figure 24 demonstrates that endothelial cells grew at a slower rate on silicone sheeting than in tissue culture flasks. On day 5, the flasks contained approximately 6 times the number of endothelial cells that were present on the silicone sheet. This was in agreement with the observations made for vsmc. The effects of the various cell adhesion promoting agents used in 3.3.3, were tested on endothelial cell growth . Figure 25 demonstrates that collagen, gelatin and poly-lysine-treated silicone, contained approximately 1.4×10^6 cells, which was only slightly

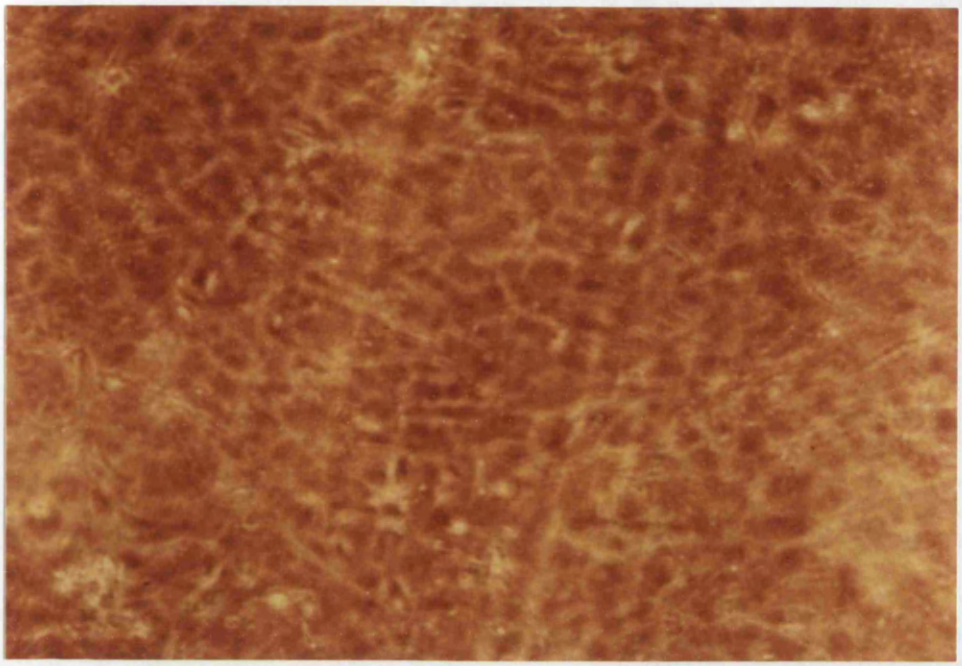

Plate 9. Photograph of confluent vsmc grown on fibronectin-treated silicone sheets.

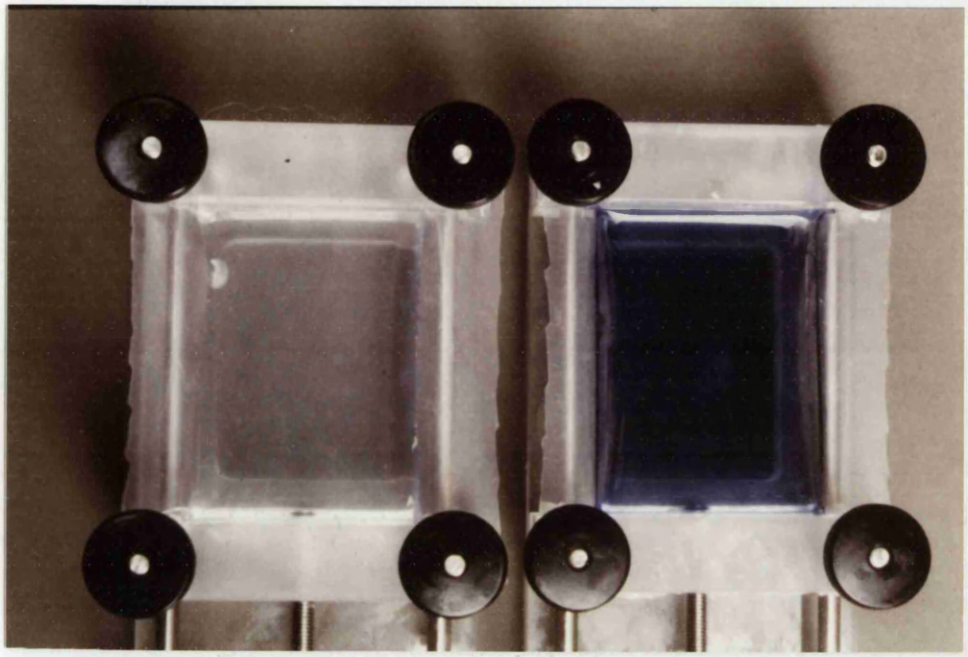

(a) (b)

Plate 10. Coomassie blue stained silicone with and without vsmc attached. Vsmc were plated at a density of 0.8 x 10^6 cells on fibronectin treated silicone sheets, grown to confluence and stained with coomassie blue as described in section 2.5.4 (10a). As controls, fibronectin treated silicone sheets without attached vsmc were also treated with coomassie blue (10b).

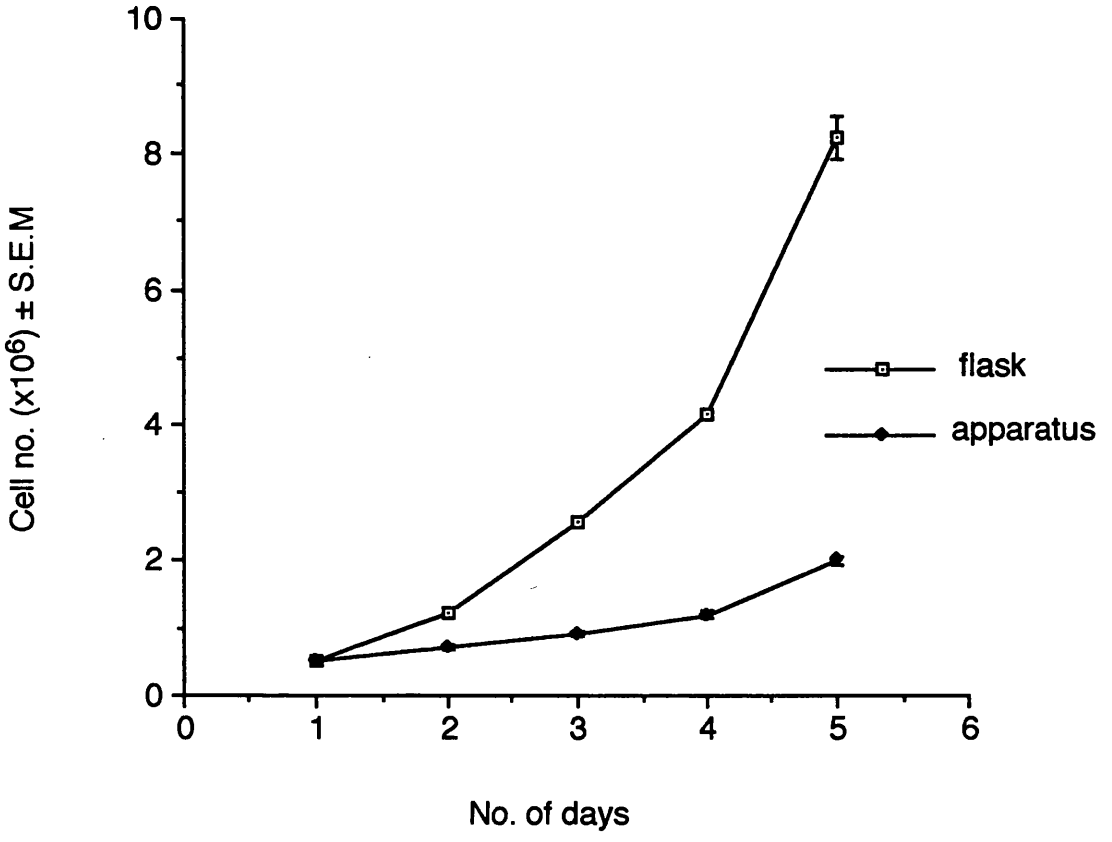

Figure 24. Growth of endothelial cells on silicone sheet compared to tissue culture flasks. Endothelial cells at a density of $0.5x10^6$ cells were plated down onto the silicone sheeting of 20 pieces of apparatus and the same density placed into 20, $75cm^2$ tissue culture flasks. This was regarded as day zero of the study. The number of cells present on 4 pieces of apparatus and in 4 flasks were evaluated daily for 5 days, until the endotheial cells in the flasks had reached confluence. Results are expressed as mean ± S.E.M; n=4.

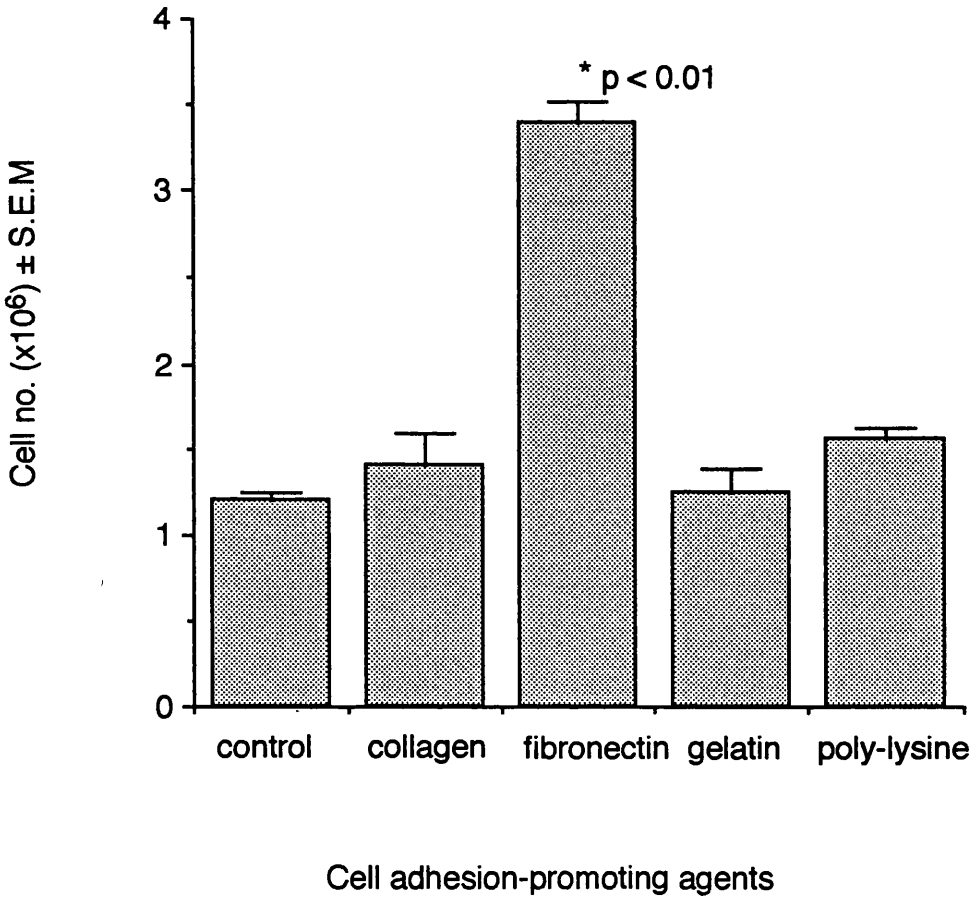

Figure 25. Effect of coating silicone sheet with cell adhesion-promoting agents on endothelial cell growth. Silicone sheets were treated with collagen (0.01%), fibronectin (25μg/ml), gelatin (2%) or poly-lysine (10μg/ml). Endothelial cells were plated at a density of $0.8x10^6$ cells and grown on the silicone as described in the methods (section 2.5.2). After 4 days in culture, cell numbers were determined using an electronic Coulter counter. Values are expressed as mean ± S.E.M; n=5.

greater than the control value of $1.2x10^6$ cells. The rate of endothelial cell growth on fibronectin-treated silicone was 3-fold greater than that of untreated silicone sheeting. These results revealed that fibronectin-treated silicone is also a good substrate for endothelial cell growth. Plate 11 shows endothelial cells which grew to confluence on fibronectin-treated silicone. When Plate 11 is compared to Plate 4 (section 2.3.4 of the methods), it can be seen that endothelial cells grow as well on fibronectin-treated silicone as they do in untreated tissue culture flasks.

3.3.5 Change in length of vsmc produced by a 20% stretch

The results obtained from analysing the change in length of squares drawn on silicone sheets suggested that the silicone sheet was stretched in a uniform manner throughout. However, it was important to show that vsmc did not become detached during stretching and that they remained tightly adhered and were stretched by the same amount as the silicone sheet.

Vsmc were plated sparsely onto the fibronectin-treated silicone (10×10^3 cells per piece of silicone sheet). This cell concentration allowed observation of a single cell. A single unstretched cell was photographed and then the silicone sheet was stretched by 20%. After stretching, the cell was photographed again. This was very difficult because each time the handle was turned, the cell moved out of the field of vision. Thus, the cell stretching apparatus had to be carefully moved to bring the cell back into focus.

A representative experiment is shown in Plates 12a&b. The length of the cell increased from 17.5μm (Plate 12a) to 21μm (Plate 12b) after stretching the silicone sheet by 20%. The mean change in length of a single vsmc was 22.7+/-1.63%. This was not significantly different from the stretch imparted to the silicone sheet.

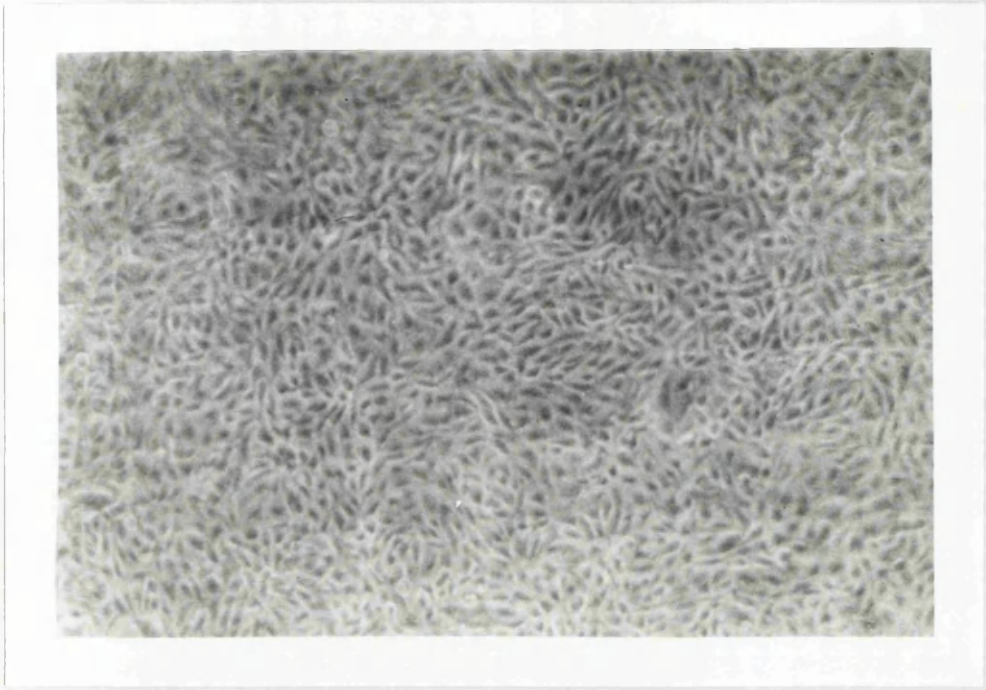

Plate 11. Photograph of confluent bovine aortic endothelial cells grown on fibronectin-treated silicone sheets.

(a)

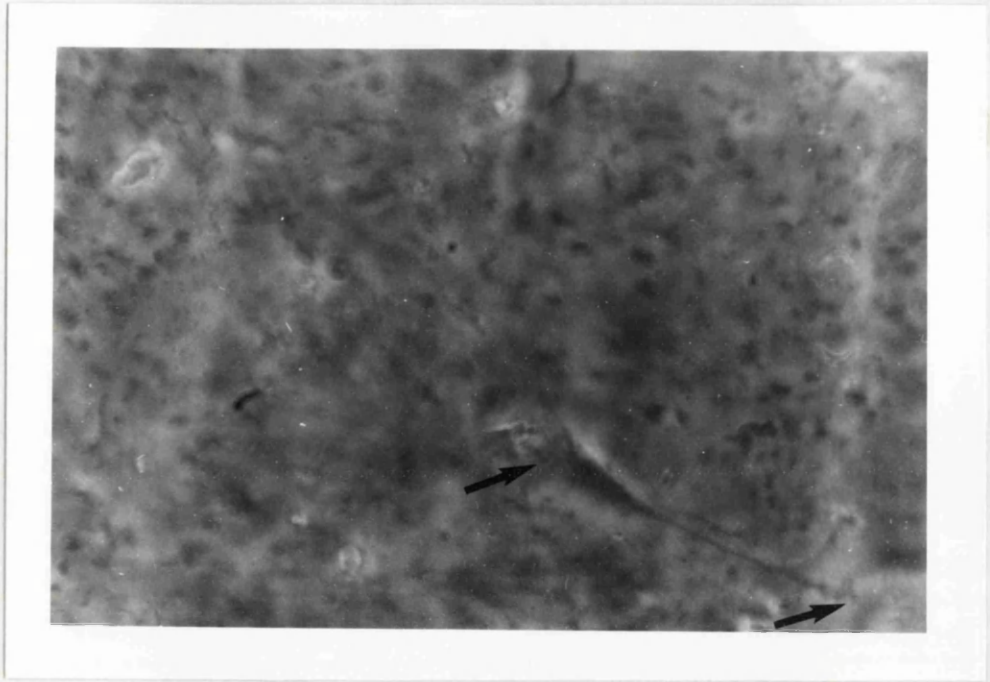

Distance= 17.5μm

(b)

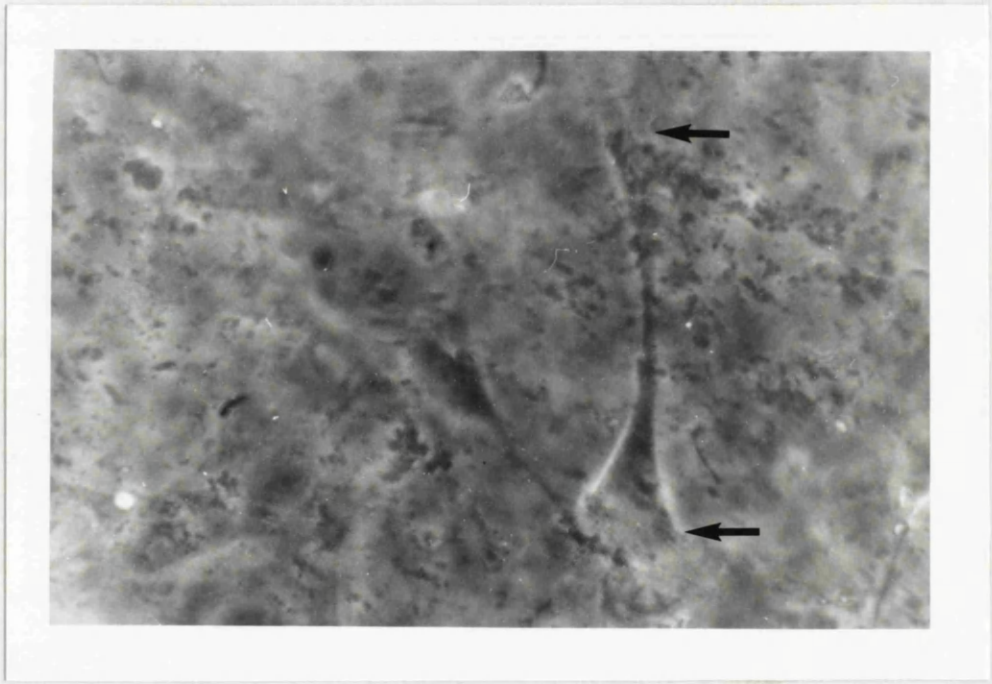

Distance=21μm

Plate 12. Photographs of a single vsmc unstretched (a) and after a 20% fixed stretch (b).

3.4 Final modifications

The system was further modified to allow microscopic examination of the original apparatus (Plate 7). The conventional inverted microscope has too short a focal length to view the cells on the silicone sheet. This problem was solved by reducing the thickness of the perspex base. The modified perspex base is shown in Plate 8.

3.5 Conclusions

A cell stretching apparatus was designed which resolved the major problems associated with previous systems, namely non-uniform stretch and limited range of stretch. The problem of restricted range of stretch was overcome by designing apparatus to achieve a stretch of 0-20%. The study conducted by Hebert et al. [230] suggests that this is a suitable range to examine. Thorough investigation showed that the silicone sheet was evenly stretched throughout the rectangular area.

Measuring a single cell in the unstretched position and after 20% stretch confirmed firm cell adhesion and a close correlation between silicone and cell stretch. Other groups studying the effects of stretch on cellular function did not confirm that the cells that were being stretched experienced a similar force to their subtrate. This is an important point which had to be confirmed.

Vsmc and endothelial cells grew well on silicone sheeting which had been treated with the cell adhesion-promoting agent, fibronectin. Staining had also shown that vsmc grew uniformly throughout the whole area of the rectangular piece of silicone.

Having checked all of the necessary requirements of the cell stretching apparatus and having verified that these had all been met in this system, it was now possible to examine the effect of stretch

on second messenger function. The results of which are discussed in the folowing chapter.

CHAPTER FOUR

RESULTS (B)

PROTO-ONCOGENE, PHOSPHOINOSITIDE AND VSMC GROWTH STUDIES

4.1 Proto-oncogene measurements

4.1.1 Vsmc

The aim was to use the system designed for stretching vsmc and endothelial cells in culture to study whether the forces existing in blood vessels play a role in the development of vascular hypertrophy. To examine whether stretch stimulates vsmc growth, proto-oncogene expression was measured. Proto-oncogenes are known to be expressed prior to cell proliferation and are therefore useful indicators of cell growth.

Vsmc which had been deprived of serum for 24h, were stretched by 20% for 0, 15, 30, 60, 180 or 360 min at 37°C. RNA was prepared from the cells, as described in section 2.8.10. RNA samples were processed for Northern analysis and the results obtained by autoradiography.

4.1.1.1 Expression of *c-fos* mRNA

Plate 13 is a photograph of a representative autoradiograph showing the effects of 20% stretch on *c-fos* mRNA expression. *c-fos* mRNA was undetectable in unstimulated cells. However, in response to a 20% stretch there was a rapid accumulation of *c-fos* mRNA, which was maximal at 15 min, still detectable at 30 min and then declined to basal levels. In parallel to these experiments, the effect of the growth factor, ANG II, on *c-fos* mRNA expression in vsmc was measured. Quiescent vsmc were treated with 1 μM ANG II for 0, 15, 30 60, 180 or 360 min and *c-fos* mRNA expression measured. Plate 14 shows that 1 μM ANG II produced maximum expression between 15 and 30 min and that expression returned to basal levels by 180 min. Therefore 20% stretch produced a similar time course of *c-fos* mRNA expression to that of a growth factor. From these results, we can conclude that stretch and growth factors such as ANG II can both stimulate *c-fos* mRNA expression over a similar time course. The work with ANG II was performed as part of a study (see publication list) to identify the ANG II receptor subtype which was responsible for the stimulation of proto-oncogene expression and phosphoinositide metabolism [36].

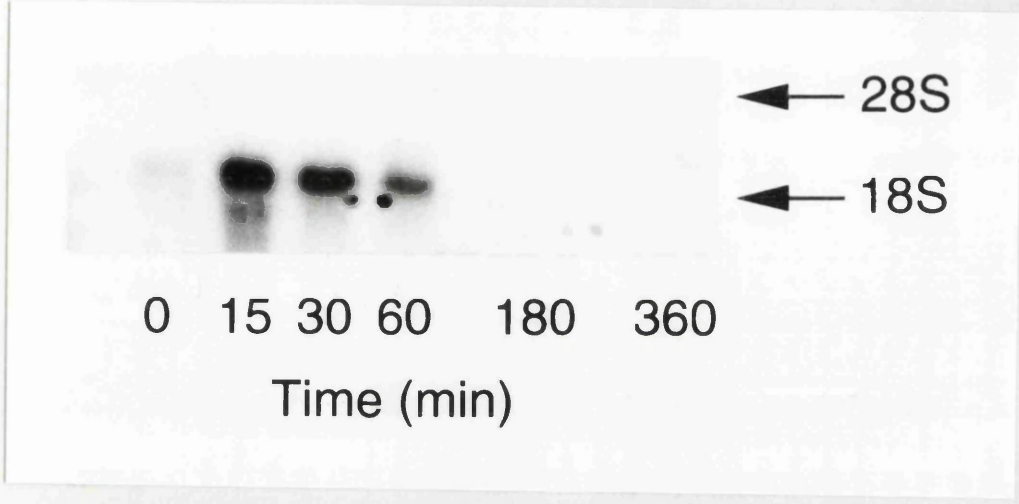

Plate 13. A representative autoradiograph showing the effects of a fixed stretch of 20% on *c-fos* mRNA induction, in vsmc. Vsmc were plated at a density of 0.8 x 10^6 cells and grown to confluence. Cells were serum deprived for 24h and then stretched by 20% for 0, 15, 30, 60, 180 or 360 min. RNA was extracted from the cells, run on agarose gels and blotted onto nylon membranes. The membranes were then hybridised with a *v-fos* cDNA probe, as described in section 2.8.10. The autoradiograph was exposed to x-ray film for 72h, at -70°C.

For each of the proto-oncogene studies discussed ,6 separate experiments were performed. For each experiment one representative data set are shown. In each experiment a control group in which no intervention was performed was studied. However, because no proto-oncogene expression was observed for the control group these photographs are not included in the results.

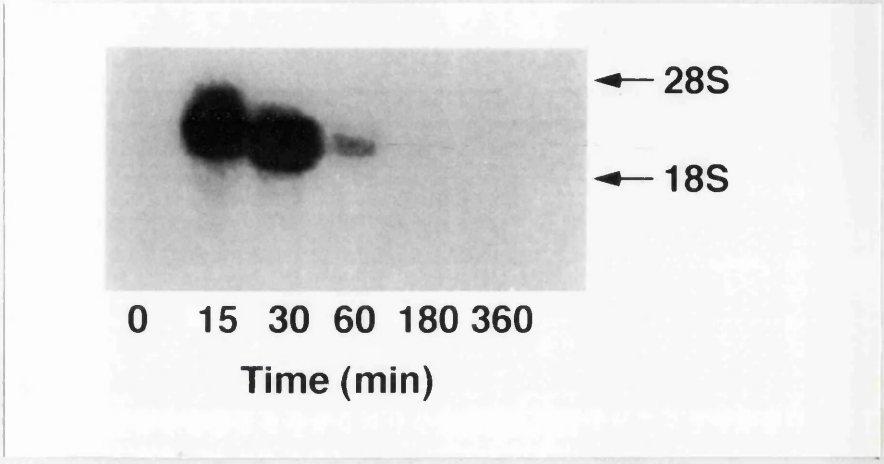

Plate 14. A representative autoradiograph showing the effects of 1 μm ANG II on *c-fos* mRNA induction, in vsmc. Vsmc were plated at a density of 0.8 x 10^6 cells and grown to confluence. Cells were serum deprived for 24h and then stretched by 20% for 0, 15, 30, 60, 180 or 360 min. RNA was extracted from the cells, run on agarose gels and blotted onto nylon membranes. The membranes were then hybridised with a *v-fos* cDNA probe, as described in section 2.8.10. The autoradiograph was exposed to x-ray film overnight, at -70°C.

Having studied the time course of *c-fos* mRNA expression in response to stretch and having established that a maximum *c-fos* expression was achieved usually by 15 min, the next step was to determine whether the concentration of the *c-fos* mRNA signal was dependent on the degree of stretch. Cells which had been deprived of serum for 24h were stretched by 0, 5, 10, 15 or 20%, for 15 min, at 37°C. Plate 15 is a photograph of a representative autoradiograph showing the results obtained in this study. The levels of *c-fos* mRNA were increased with increasing length of stretch and maximal levels were achieved by 15%. Thus the intensity of the *c-fos* mRNA signal was dependent on the degree of stretch.

4.1.1.2 Expression of *c-jun* mRNA

The protein product of the proto-oncogene *c-jun* plays an important role in the regulation of transcription, via the formation of the AP-1 complex (section 1.3.1.1). Therefore, the effect of 20% stretch on *c-jun* mRNA expression was studied. Quiescent vsmc were stretched by 20% for 0, 15, 30, 60, 180 or 360 min and *c-jun* mRNA expression measured (section 2.8.10). On several occasions, *c-jun* mRNA expression was observed in unstimulated cells, but *c-jun* mRNA expression was not induced in response to 20% stretch. *c-jun* mRNA expression in unstimulated vsmc has also been observed by other groups [231, 232, 233].

To determine whether ANG II could stimulate *c-jun* mRNA expression in vsmc, quiescent vsmc were treated with 1μM ANG II for 0, 15, 30 60, 180 or 360 min and *c-jun* mRNA expression measured. The results obtained from this group of experiments are shown in Plate 16. The mRNA for *c-jun* was undetectable in unstimulated vsmc. Maximum expression was seen between 30 and 120 min stimulation and at 180 min this declined to almost basal levels. The growth factor ANG II induced *c-jun* mRNA expression in vsmc but 20% stretch did not.

4.1.1.3 Expression of c-myc mRNA

The processes of proliferation and differentiation are known to be controlled by the proto-oncogene *c-myc* [46]. Thus, the effect of 20% stretch on these events was studied by examining *c-myc* mRNA expression, in quiescent vsmc. Vsmc were deprived of serum for 24h and then stretched by 20% for 0, 15, 30 or 60 min and *c-myc* mRNA

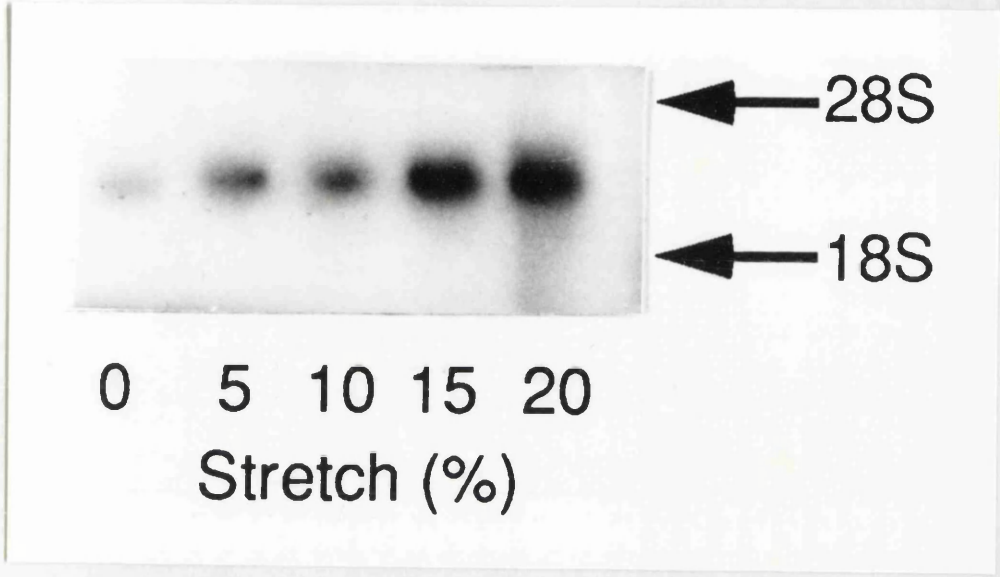

Plate 15. A representative autoradiograph showing the effects of a varied stretch on *c-fos* mRNA induction, in vsmc. Vsmc were plated at a density of 0.8 x 10^6 cells and grown to confluence. Cells were serum deprived for 24h and then exposed to a varied stretch of either 0, 5, 10, 15 or 20%, for 15 min. RNA was extracted from the cells, run on agarose gels and blotted onto nylon membranes. The membranes were then hybridised with a *v-fos* cDNA probe, as described in section 2.8.10. The autoradiograph was exposed to x-ray film for 48h, at -70°C.

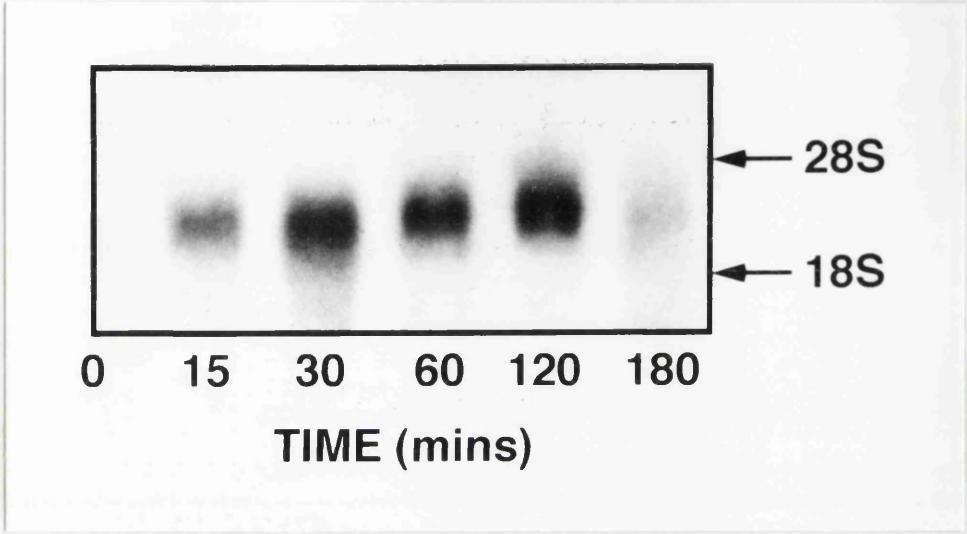

Plate 16. A representative autoradiograph showing the effects of 1 μM ANG II on *c-jun* mRNA induction, in vsmc. Vsmc were plated at a density of 0.8×10^6 cells and grown to confluence. Cells were serum deprived for 24h and then treated with 1 μM ANG II for 0, 15, 30, 60, 180 or 360 min. RNA was extracted from the cells, run on agarose gels and blotted onto nylon membranes. The membranes were then hybridised with a *c-jun* cDNA probe, as described in section 2.8.10. The autoradiograph was exposed to x-ray film overnight, at -70°C.

expression measured (section 2.8.10). 60 min was chosen as the end time point of the experiments because Naftilan et al. [34] had shown that *c-myc* mRNA expression in vsmc occurred rapidly in response to ANG II with maximum expression after 30 min. By studying fewer time points, more pieces of apparatus could be used for each time point which would increase the amount of RNA available for each of the time points studied. A basal *c-myc* mRNA expression was observed in unstimulated cells. However, in response to 20% stretch, this expression persisted over the 15, 30 and 60 min time points but did not increase above control levels (Plate 17).

To compare the effect of 20% stretch with that of a growth factor, the effect of 1μM ANG II on *c-myc* mRNA expression was investigated. Vsmc were deprived of serum for 24h and then treated with 1μM ANG II for 0, 15, 30 or 60 min and *c-myc* mRNA expression measured. Plate 18 shows that *c-myc* mRNA expression was detectable in unstimulated cells, which increased after 15 min stimulation and reached maximum levels between 30 and 60 min.

In conclusion, mechanical stretch increased *c-fos* mRNA with maximal expression occuring between 15 and 30 min. There was no evidence that stretch increased mRNA for either *c-jun* or *c-myc*. However, ANG II stimulated both *c-jun* and *c-myc* mRNA in vsmc.

4.1.2 Endothelial cells

Endothelial cells experience shear stresses but are also exposed to mechanical forces. The effect of stretch on proto-oncogene expression in bovine aortic endothelial cells was studied. The endothelial cell studies concentrated on the effects of 20% stretch on the expression of the proto-oncogenes *c-fos* and *c-jun* because of their importance in the regulation of transcription.

4.1.2.1 Expression of *c-fos* mRNA

Endothelial cells which had been deprived of serum for 24h, were stretched by 20% for 0, 15, 30, 60, 180, or 360 min, at 37°C. RNA was prepared from the cells, as described in section 2.8.10 and the samples processed for Northern analysis. Plate 19 is a photograph of a

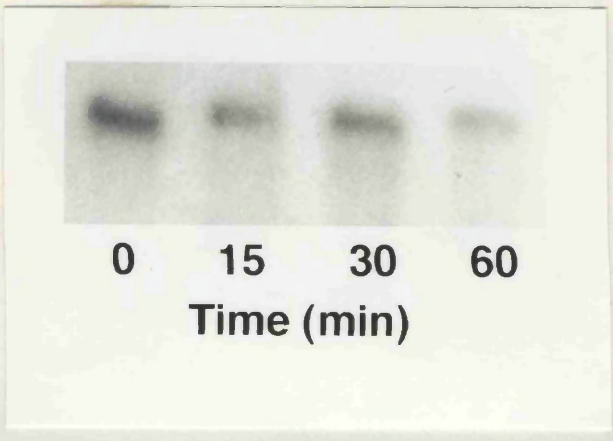

Plate 17. A representative autoradiograph showing the effects of a fixed stretch of 20% on *c-myc* mRNA induction, in vsmc. Vsmc were plated at a density of 0.8 x 10^6 cells and grown to confluence. Cells were serum deprived for 24h and then stretched by 20% for 0, 15, 30, 60, min. RNA was extracted from the cells, run on agarose gels and blotted onto nylon membranes. The membranes were then hybridised with a *c-myc* cDNA probe, as described in section 2.8.10. The autoradiograph was exposed to x-ray film for 72h, at -70°C.

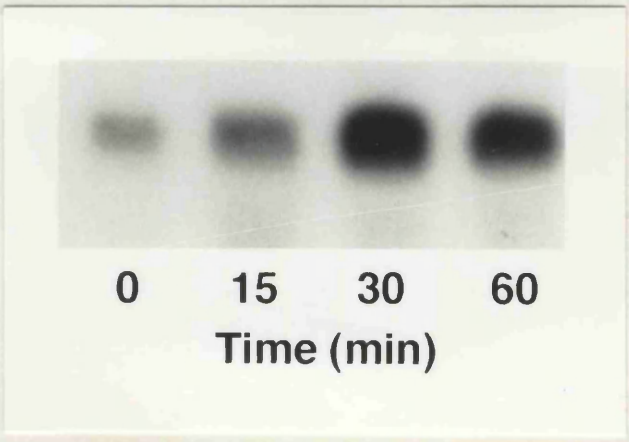

Plate 18. A representative autoradiograph showing the effects of 1 μM ANG II on *c-myc* mRNA induction, in vsmc. Vsmc were plated at a density of 0.8 x 10^6 cells and grown to confluence. Cells were serum deprived for 24h and then treated with 1 μM ANG II for 0, 15, 30, or 60 min. RNA was extracted from the cells, run on agarose gels and blotted onto nylon membranes. The membranes were then hybridised with a *c-myc* cDNA probe, as described in section 2.8.10. The autoradiograph was exposed to x-ray film overnight, at -70°C.

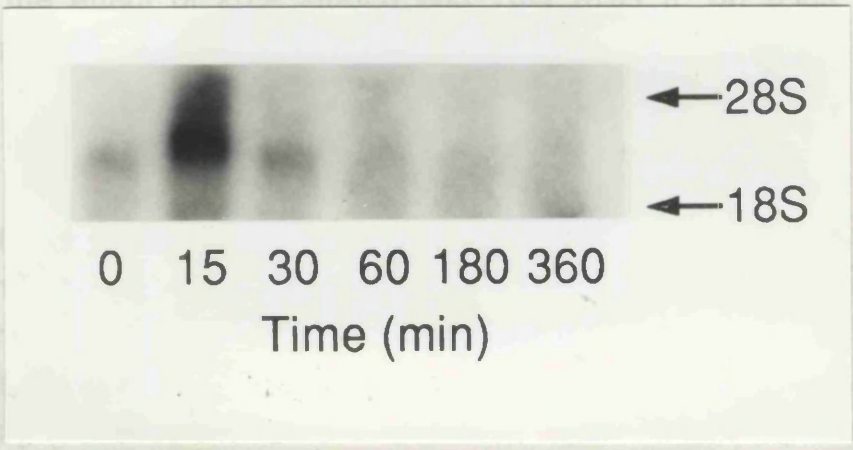

Plate 19. A representative autoradiograph showing the effects of a fixed stretch of 20% on *c-fos* mRNA induction, in endothelial cells. Endothelial cells were plated at a density of 0.8 x 10^6 cells and grown to confluence. Cells were serum deprived for 24h and then stretched by 20% for 0, 15, 30, 60, 180 or 360 min. RNA was extracted from the cells, run on agarose gels and blotted onto nylon membranes. The membranes were then hybridised with a *v-fos* cDNA probe as described in section 2.8.10. The autoradiograph was exposed to x-ray film overnight, at -70°C.

representative autoradiograph showing the effects of a 20% stretch on *c-fos* mRNA expression, in cultured endothelial cells. Low levels of c-*fos* mRNA signal was detected in unstimulated cells. However, 20% stretch for 15 min resulted in a rapid accumulation of *c-fos* mRNA, which declined to basal levels by 30 min and was undetectable by 60 min. This is a similar time course of *c-fos* mRNA expression as was observed when the effect of 20% stretch and 1μM ANG II, on *c-fos* mRNA expression in vsmc was investigated.

4.1.2.2 Expression *c-jun* mRNA

Endothelial cells which had been deprived of serum for 24h, were stretched by 20% for 0, 15, 30, 60, 180, or 360 min at 37°C. RNA was prepared and *c-jun* mRNA expression measured as described in section 2.8.10. Plate 20 is a photograph of a representative autoradiograph showing the effects of a 20% stretch on *c-jun* mRNA expression in cultured endothelial cells. Minimal levels of *c-jun* mRNA were detected in unstimulated cells, levels achieved maximum from 15 to 60 min and *c-jun* mRNA levels persisted to 360 min. 20% stretch did not induce *c-jun* mRNA expression in vsmc but the time course of *c-jun* mRNA expression produced by 1μM ANG II was very similar to that induced by 20% stretch in endothelial cells.

These studies have shown that mechanical stretch can stimulate *c-fos* and *c-jun* mRNA expression in endothelial cells.

4.2 Phosphoinositide metabolism

The effect of stretch on phosphoinositide turnover was studied.

Confluent vsmc were pre-labelled with ^{3}H-myo-inositol for 48h, subjected to 20% stretch for 20 min and total inositol phosphate production measured, according to the procedure of Berridge [226], as described in section 2.7.4. 20 min was chosen for the incubation time because vsmc treated with ANG II for 20 min showed a 1.8 fold increase in total inositol phosphate production [36]. Vsmc were treated with either 10% FCS, which was included as a positive control, 10^{-7}M ANG II, to compare the effects of stretch with that of a growth factor, or 20% stretch,

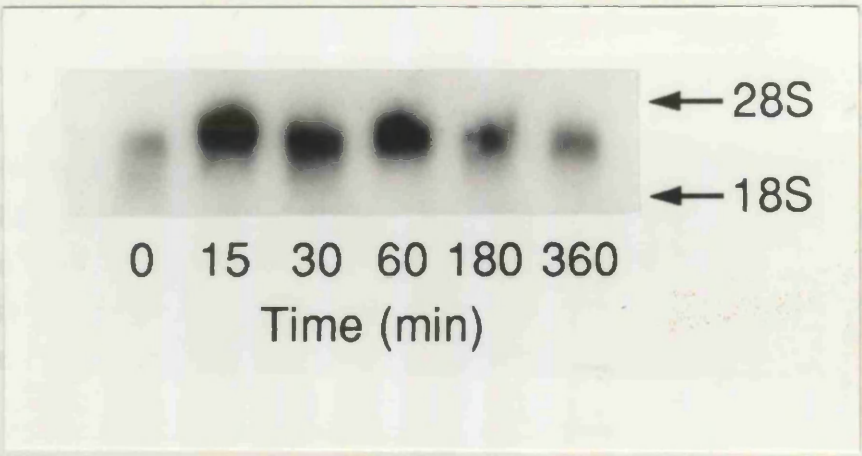

Plate 20. A representative autoradiograph showing the effects of a fixed stretch of 20% on *c-jun* mRNA induction, in endothelial cells. Endothelial cells were plated at a density of 0.8 x 10^6 cells and grown to confluence. Cells were serum deprived for 24h and then stretched by 20% for 0, 15, 30, 60, 180 or 360 min. RNA was extracted from the cells, run on agarose gels and blotted onto nylon membranes. The membranes were then hybridised with a *c-jun* cDNA probe as descbibed in section 2.8.10. The autoradiograph was exposed to x-ray film overnight, at -70°C.

for 20 min. The cells were then lysed and total inositol phosphate production was measured.

Figure 26 shows the results expressed as a % of control ± S.E.M. where control =100%. Incubation with 10% FCS resulted in a 7.7 fold increase in inositol phosphate levels released. This result had been anticipated because FCS contains many growth promoting substances and is therefore a good positive control. Incubation with 10^{-7}M ANG II resulted in a 2.3 fold increase in inositol phosphates released. After stretching cells by 20% for 20 min, a 3.2 fold increase in inositol phosphate levels was measured. Thus both 20% stretch and 10^{-7}M ANG II mediated inositol phosphate release in vsmc.

4.3 Growth response of vsmc to mechanical stretch

The experiments described above for rat mesenteric vsmc showed that stretch induced *c-fos* mRNA expression and increased inositol phosphate production but had no effect on *c-jun* or *c-myc* mRNA expression. The next group of experiments performed was to determine whether a fixed stretch could stimulate vsmc growth. This was achieved by examining the effect of stretch on vsmc number.

Vsmc were plated at a cell density of 0.4×10^6 cells/per piece of apparatus on day 0 of the study. The cells were fed with growth medium containing 20% serum. The following day (day 1) the number of cells present on 3 pieces of apparatus was counted, the medium removed from each of the remaining pieces of apparatus and replaced with growth medium containing 10% serum. 10 pieces of apparatus were stretched by 20% and the remaining 10 unstretched for control purposes. On day 2, the medium was removed and counted to determine whether any vsmc had become detached as a consequence of cell stretching. The number of vsmc present on the fibronectin-treated silicone was then determined for 3 stretched and 3 controls. This procedure was also repeated on day 3. On day 4 the number of cells present in the medium and on the fibronectin-treated silicone were determined for the remaining 4 stretched and 4 controls. Figures 27 & 28 show the results obtained for the fibronectin-treated silicone and medium, respectively.

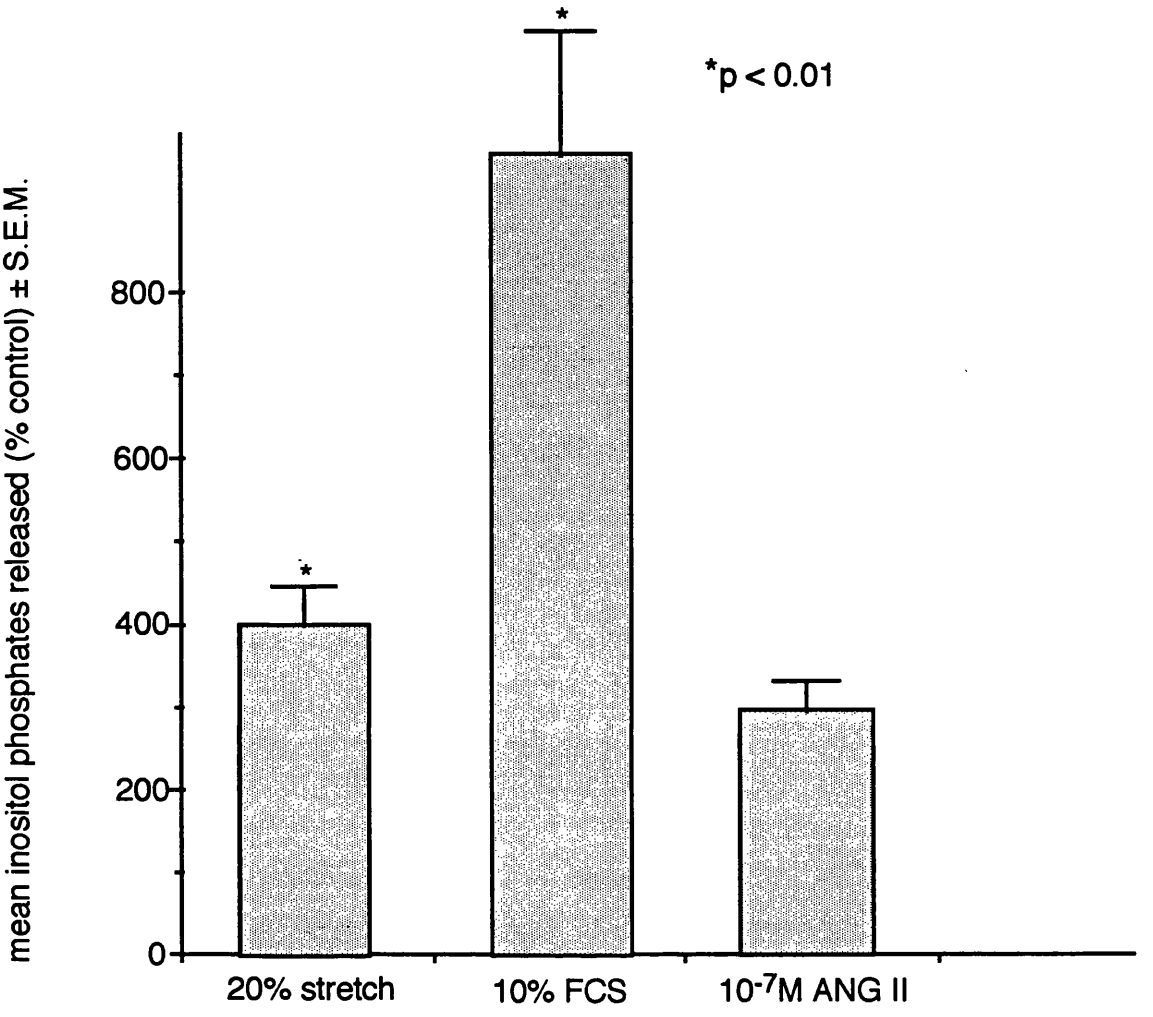

Figure 26. Effect of 20% stretch, 10% FCS and 10^{-7}M ANG II on phosphoinositide turnover, in vsmc. The cells were plated at a density of 0.8 x 10^6 cells, grown on fibronectin-coated silicone membranes and labelled with [^{3}H]-inositol.The cells were either stretched by 20%, or stimulated with 10% FCS, or 10^{-7}M ANG II. Total [^{3}H]-inositol phosphates released were measured. Results are expressed as a % of control ± S.E.M., where control =100%; n=6.

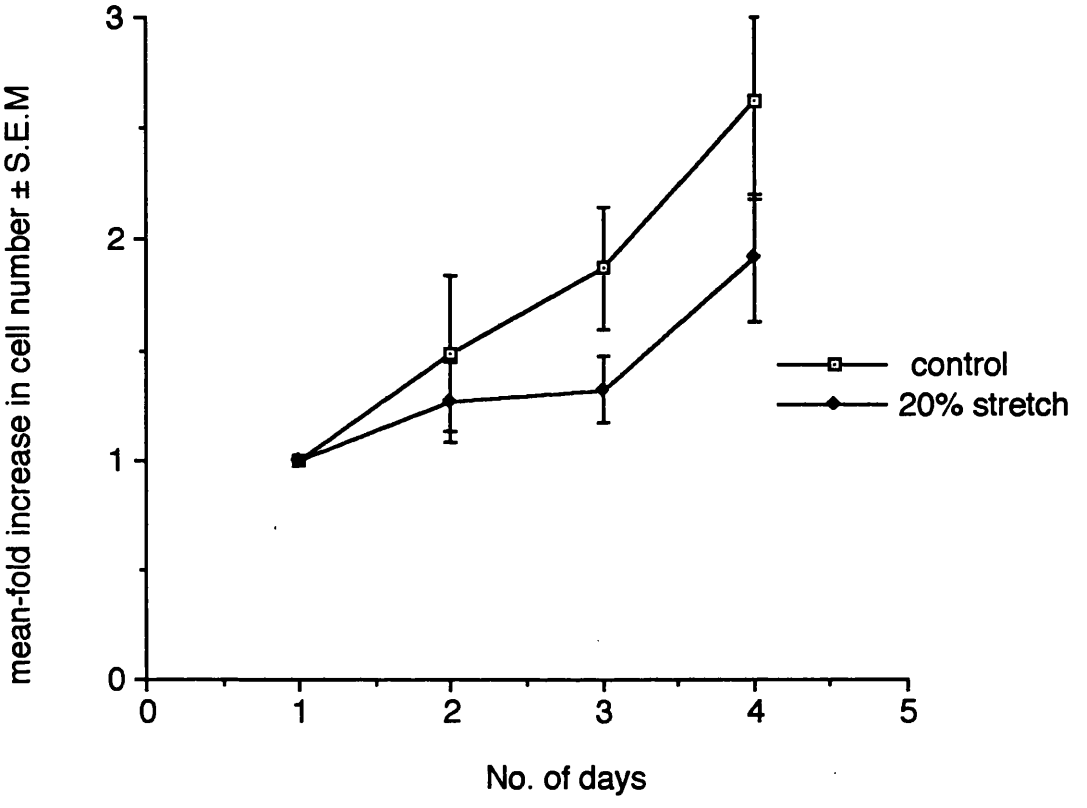

Figure 27. Effect of 20% stretch on vsmc growth. On day 0, cells were plated at a density of 0.4 x 10^6 cells / per piece of apparatus, in growth medium containing 20% serum. The following day the number of cells present on 3 pieces of apparatus was determined. 10 pieces of apparatus were then stretched by 20% and the remaining 10 left unstretched. The growth medium was replaced by medium containing 10% serum. Cell numbers were evaluated on days 2, 3 and 4. Results are expressed as mean-fold increase in cell number ± S.E.M; n=3.

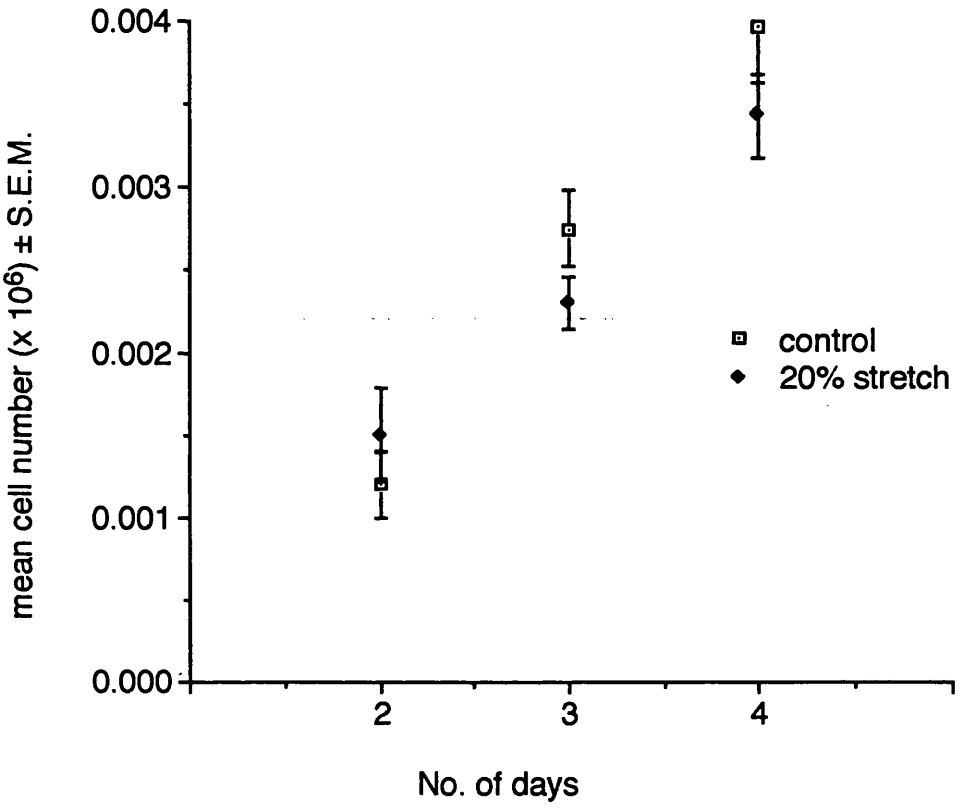

Figure 28. Effect of stretch on vsmc detachment. On day 0, vsmc were plated at a density of 0.4 x 10^6 cells / per piece of apparatus. On day 1, 10 pieces of apparatus were stretched by 20% and the remaining 10 used as controls. Over the following 3 days the growth medium was removed and the number of vsmc present in the medium of stretched and control vsmc was determined. n=3.

In Figure 27, results are expressed as a mean-fold increase in the number of cells present on the apparatus compared with day 1, ± S.E.M. Figure 27 shows that although the number of cells in the control group were higher than the stretch group on days 2, 3 and 4 , this did not reach statistical significance. Therefore no significant difference was observed in the rate of growth of stretched compared to control vsmc.

In Figure 28 results are expressed as mean cell number ± S.E.M. Very low cell counts were measured in the medium of control and stretched vsmc, suggesting that the vsmc had not become detached. No significant difference was observed for the number of vsmc present in the medium of stretched vsmc compared to control vsmc. Thus stretch did not cause cell detachment.

Although 20% stretch had produced an increase in *c-fos* mRNA expression and inositol phosphate production, 20% stretch alone did not produce a statistically significant increase in vsmc growth rate.

CHAPTER FIVE

DISCUSSION

5.1 The relevance of the present study to understanding the aetiology of hypertension

As discussed in the introduction, vascular hypertrophy (section 1.2) contributes to the development of essential hypertension. Vascular hypertrophy is characterised by an increase in the media:lumen ratio of the small resistance vessels (section 1.1.2.3), which produces an increased pressure in the systemic arterial circulation. Much research has been focussed on elucidating the aetiology of essential hypertension because it is also associated with increased risk of ischaemic heart disease and stroke.

At present, essential hypertension cannot be explained by impairment of a single parameter. It is accepted that a combination of factors are responsible for its development. Folkow [21] postulated that a hemodynamic component was involved in the development of vascular hypertrophy. This theory was extended to include the role of a non-hemodynamic growth-promoting component (Lever et al. [22]). Possible non-hemodynamic components include both vasoconstrictor peptides and peptide growth factors. The role of the non-hemodynamic factors (e.g ANG II) has been extensively studied. However, the hemodynamic component has been less well studied, especially *in vitro* and it was on this component that my project focussed.

The hemodynamic component consists principally of the forces of shear stress and pressure which are exerted on the vessel wall (Davies [135]). Endothelial cells and vsmc are subjected to the pressure component whereas only the endothelial cells experience the shear forces within the vessel. The radius of resistance vessels change with increased and decreased blood flow. When an increase in flow is required to facilitate maximum blood flow, the radius of the lumen will also be at its maximum diameter. This will be accompanied by a reduction in the radius of the media. As a result of this, the cells of the vessel wall will be mechanically deformed. When the vessel relaxes the cells will retain their original size and conformation. Thus, as cells are exposed to alterations in blood flow they will continuallly alter their size and shape. Under pathological conditions, the forces exerted would result in greater increases in mechanical perturbation of the cells. Therefore, to determine at the cellular and molecular level the signalling

mechanisms involved when cells are mechanically deformed, an *in vitro* system was developed to mimic these conditions.

5.2 The development of an *in vitro* system

The major advantage of an *in vitro* study is that a particular situation can be studied in isolation, in the absence of other humoral influences. There have been several attempts to develop an *in vitro* cell stretching system for various biological applications. Many of these designs encountered serious problems (section 1.6). In particular, they failed to ensure uniform stretch throughout the experimental tissue. Therefore, this project concentrated on designing a system which could produce an even stretch. Two versions were constructed and tested in terms of effects on growth and proto-oncogene expression.

5.3 First proto-type

The first design was based on the Petriperm dish. A vacuum could be used to vertically displace the base of the dish and this could be easily achieved in the incubator in an environment optimal for vsmc and endothelial cell growth. Previous studies had shown that a range of cell types could be grown in Petriperm dishes and it seemed likely that vsmc and endothelial cells would tightly adhere to the base of the dish and remain attached when the base of the dish was stretched. This proved to be the case. This was a simple system which could be engineered relatively quickly and could be produced economically in bulk. Growth and function in the system were evaluated as follows.

5.3.1 Growth

The first study assessed the effect of cell adhesion-promoting agents on vsmc and endothelial cell growth. Figure 16 shows that coating the dishes with gelatin and fibronectin resulted in a 2- and 2.4- fold increase in growth, respectively. Fibronectin was chosen for subsequent experiments because it was more effective in potentiating vsmc growth and because, unlike gelatin, fibronectin forms a monolayer. If the cell adhesion-promoting agent forms multilayers, when the base of the dish

is stretched, it is impossible to be sure that the cells attached to the cell adhesion agent are being stretched and not the cell adhesion-promoting agent alone. Fibronectin was also shown to produce a 1.5 fold increase in endothelial cell growth when compared to control cells (Figure 17). Both vsmc and endothelial cells grew well in Petriperm dishes coated with fibronectin.

As discussed earlier, the design of the system aimed to look at the effect of hemodynamic forces on cellular function, in the absence of other humoral influences. By introducing the use of fibronectin to the system these requirements remained satisfied because this extracellular adhesive glycoprotein is found *in vivo*, were it functions to mediate cell-matrix adhesion. This was also the function which it performed in this system. Therefore it was feasible to presume that fibronectin should not have any significant effects on the parameters which were to be examined in this study.

5.3.2 Proto-oncogene expression

The effect on *c-fos* mRNA expression caused by stretching vsmc by 20% for various times was measured. Plate 6 shows that *c-fos* mRNA was undetectable in unstimulated cells. In response to stretch there was a rapid accumulation of *c-fos* mRNA which reached maximum levels by 30 min, was still detectable at 180 min and returned to basal levels by 360 min. Plate 14 shows the results obtained when quiescent vsmc were treated with the growth factor, ANG II (1 μM). Expression of *c-fos* mRNA was undetectable in unstimulated cells. Maximum *c-fos* mRNA expression was achieved between 15 and 30 min and declined to basal levels after 60 min. These time courses of *c-fos* mRNA expression are in agreement with the observations made by Kawahara et al. [230] and Taubman et al. [231] for rat aortic vsmc. They observed maximum *c-fos* mRNA expression at 30 min in response to similar doses of ANG II. Thus, these results suggested that growth factors such as ANG II and mechanical stretch both induce *c-fos* mRNA expression via similar mechanisms. A stretching force does stimulate cell growth and therefore may contribute to the development of hypertrophy.

5.3.3 Problems with first proto-type

The above study provided evidence that mechanical stretch stimulates proto-oncogene expression. However, a maximum value of only 0.3% could be achieved using this system which was too small to imitate physiological conditions.

The minimal internal circumference (L_o) achieved when a vessel contracts is 0.4 L_o and the maximum when fully relaxed is 1.8L_o (Mulvany et al. [237]). Therefore, a 4.5 fold increase in internal circumference is achieved on relaxation of a contracted vessel. Such a dramatic change in the internal circumference of the vessel should cause the components of the vessel wall to experience large mechanical forces. Mulvany et al. [238] showed that in essential hypertensive patients the lumen diameter of vessels was reduced by 7% compared to normotensive patients. In combination, these facts suggest that although resistance vessels are extremely elastic in nature, changes in hemodynamic forces much smaller than maximal can initiate the process of vascular hypertophy, a factor which contributes to the development of hypertension. This conclusion is also suggested by the fact that a stretch of 0.3 % stimulated a growth response.

The major disadvantage of the Petriperm system was that the stretch achieved by the Petriperm dish was not uniform, being greatest in the central area of the base of the dish. To correct this and to increase the maximum stretch range an alternative system was devised.

5.4 Second prototype and final working model: performance criteria

The design of the new proto-type was based on the stretch frame which has been described in section 1.6.2. To develop an effective and reliable *in vitro* system was a time consuming and technically difficult task. However, with a knowledge of the essential features required of the system and the expertise of engineers, the new system was designed and constructed. Plate 8 shows the apparatus and its important features. Several types of silicone sheeting of varied thickness and elasticity from a range of manufacturers were tested, to find the most suitable. This system was based on the requirement that a thin piece of silicone sheeting exhibits elastic properties and is relatively easy to stretch

without having to exert too great a force. By turning the handle of the stretching apparatus the length of silicone could be increased. Since cells grown on the silicone sheet adhere tightly to their substrate, as the length of the silicone sheet is increased, the cells also experience a similar increase in their length.

Replicate measurements of areas from 5 grid marked silicone sheets showed that the degree of stretch was linear and uniform throughout the sheets over a range from 5% to 20% stretch (3.3.2), thus improving on the Petriperm dish model. Although both vsmc and endothelial cells grew better under culture flask conditions than on silicone sheeting, fibronectin caused a 5-fold and 3-fold improvement, respectively. Moreover, coomassie blue staining showed that vsmc grew uniformly throughout the rectangular area of the fibronectin-coated silicone sheeting (3.3.3).

It was important to establish that vsmc were stretched to the same extent as the silicone sheet substrate. Measurement of single cells before and after 20% stretching gave an average increase of 22.7 ± 1.63%. These performance criteria were judged to be good enough to proceed with the physiological study.

5.5 The effect of mechanical forces on proto-oncogene expression

The effect of stretch on proto-oncogene expression was studied in vsmc and endothelial cells. Preliminary experiments showed that an increase in *c-fos* mRNA expression was achieved with a stretching force of 0.3%. With the new apparatus a range of 0-20% was possible.

5.5.1 Proto-oncogene expression in vsmc in response to stretch

The expression of the proto-oncogenes *c-fos*, *c-jun* and *c-myc*, in response to stretch and to ANG II, were compared. These particular proto-oncogenes were chosen because as discussed in section 1.3.1.1 they are known to be involved in the process of cell proliferation.

Expression of *c-fos* mRNA was undetectable in control cells. Maximum expression was achieved after 15 min of 20% stretch, remained detectable at 30 min and declined to basal levels after 60 min

stimulation (Plate 13). The response of *c-fos* mRNA expression achieved is therefore dependent on the period of stretch. It was of interest to find out if the growth factor ANG II and stretch stimulate proto-oncogene expression via similar mechanisms. Plate 14 shows the effect of 1μM ANG II on proto-oncogene expression in vsmc. In unstimulated cells, *c-fos* mRNA expression was undetectable. Maximum *c-fos* mRNA expression was achieved at 15 and 30 min and the signal declined to basal levels after 60 min. The *c-fos* mRNA expression time course produced by 20% stretch was similar to that produced by 1μM ANG II.

These were very exciting results because they identified the existance of a relationship in the mechanism by which a mechanical force and a growth factor can stimulate vsmc growth. It is known that when proto-oncogene production is stimulated specific RNAses are simultaneously produced which degrade the proto-oncogene mRNA. These RNAses were identified by the fact addition of a protein synthesis inhibitor to the medium e.g cycloheximide, intensified the proto-oncogene mRNA response [34, 35, 37]. Therefore, for both mechanical stretch and ANG II to have stimulated proto-oncogene production with similar time courses of expression, the mechanism by which this occurrs must be very similar in nature.

The advantage of the new system was that it was possible to look at the effect of different lengths of stretch on particular cell signalling events during the same experiment, whereas other systems were restricted in the magnitude of stretch which could be achieved [183, 184, 215]. The value of this is illustrated in the experiments described in section 2.7.3. Using 15 min periods as the optimum response time, maximum *c-fos* mRNA expression resulted from a stretch of between 15 & 20%.

From the results obtained from the *c-fos* mRNA study, it was postulated that *c-jun* mRNA expression may also be induced. The protein products Fos and Jun interact with each other to form a heterodimeric transcription factor complex known as the AP-1 transcription factor. The AP-1 transcription factor binds to a consensus DNA sequence containing AP-1 sites and switches on the expression of late response genes involved in cell proliferation and differentiation (1.3.1.1). To determine whether this was the mechanism through which stretch could stimulate proliferation in vsmc, the effect of 20% stretch on *c-jun* mRNA expression was investigated.

In contrast to *c-fos*, *c-jun* mRNA expression was apparent in

unstretched cells but no further response was elicited by 20% stretch for up to 360 min. However, ANG II (1μm) did stimulate expression with a maximum expression achieved by 30 min, which persisted to 120 min (Plate 16). In this latter experiment *c-jun* mRNA expression was not detectable at time zero. Naftilan et al. [37] observed no *c-jun* mRNA expression in unstimulated vsmc. However, Schunkert et al. [234], Mollinedo et al. [235] and Viard et al. [236] have observed *c-jun* mRNA expression in unstimulated rat hearts, granulocytes and adrenocortical cells, respectively. This information suggests that *c-jun* mRNA may be expressed in some types of unstimulated cell, under some experimental conditions.

Another nuclear proto-oncogene of interest is that of *c-myc*, which is believed to play a role in the control of proliferation and differentiation [46]. To examine further the effect of a stretching force on cell growth the effect of 20% on *c-myc* mRNA expression was studied (2.7.1.1).

Although *c-myc* mRNA expression was observed under basal conditions over the 0-60 min time interval (Plate 17), no increase of expression occurred during stretching. A time interval of 0-60 min was chosen for this group of experiments because Naftilan et al. [34] observed maximum *c-myc* mRNA within 30 min of stimulation, with ANG II. In my ANG II experiments, unstimulated vsmc showed *c-myc* mRNA expression which increased significantly by 15 min and reached maximum levels between 30 min and 60 min (Plate 18). These results agreed with those of Naftilan et al. [34]. Thus mechanical stretch was unable to stimulate *c-myc* mRNA expression in quiescent vsmc in contrast to the actions of ANG II.

5.5.2 Proto-oncogene expression in endothelial cells in response to stretch

An increased rate of endothelial cell growth is important in the development of hypertension through its contributory role to vascular hypertrophy. An increased rate of endothelial cell proliferation should result in the increased production of the vasoconstrictor, endothelin. Endothelin stimulates vasoconstriction of blood vessels and therefore increases TPR. Therefore, the effect of stretch on expression of the proto-oncogenes *c-fos* and *c-jun,* in endothelial cells, was also investigated. These particular proto-oncogenes were chosen because of their involvement in the activation of the AP-1 transcription factor, an

important cell signalling event. In combination, the vsmc and endothelial studies allowed comparison of the time courses of expression of different proto-oncogenes, in two different cell types.

Plate 19 (section 4.1.2.1) shows that *c-fos* mRNA was present in unstimulated cells, in contrast to observations made for vsmc. It is difficult to say whether this is a common observation made for endothelial cells because limited studies have examined this effect. As for vsmc, a maximum signal was obtained after a 20% stretch for 15 min. This declined to basal levels by 30 min and was undetectable by 60 min. Thus vsmc and endothelial cells control *c-fos* mRNA expression in a similar manner.

If stretch stimulates endothelial cell growth does this occur via activation of the AP-1 transcription factor? To examine this question the effect of 20% stretch on *c-jun* mRNA expression, in endothelial cells, was investigated. Expression of *c-jun* mRNA was observed in unstimulated endothelial cells, as shown in Plate 20 (section 4.1.2.2). Maximum gene expression had occurred by 15 min and persisted at 60 min. Expression fell by 180 min but still remained above basal levels at 360 min. The time course of *c-jun* mRNA expression in endothelial cells was similar to that observed when ANG II was added to vsmc (Plate 16).

5.5.3 Summary of proto-oncogene studies

The proto-oncogene studies have shown that in vsmc, mechanical stretch stimulates *c-fos* mRNA expression in a similar time course to that of the growth factor ANG II. However, contrasting results were obtained for *c-jun* and *c-myc* mRNA expression. This suggests that mechanical stretch may not be involved in the development of vascular hypertrophy or that the expression of *c-jun* and *c-myc* mRNA are not pivotal in this process. If the latter is true this suggests that the formation of the AP-1 transcriptrion factor is not an important signalling event in the stimulation of vascular growth. From the available information it is not possible to say if this is the case.

The fact that mechanical stretch stimulates *c-fos* and *c-jun* mRNA expression in endothelial cells, in a time course similar to that observed for ANG II in vsmc, suggests that endothelial cells may play a vital role in vascular hypertrophy. Further studies are required to identify the precise role of endothelial cells in this process.

Thus, these results identify a precise difference in the role of vsmc and endothelial cells in the control of proto-oncogene expression and the subsequent stimulation of growth.

5.6 Phosphoinositide turnover in vsmc in response to stretch

Figure 5 of the introduction illustrates how a growth factor can stimulate the breakdown of PIP_2 which results in the production of IP_3 and DAG. A whole series of isomers of inositol phosphates are then produced via the action of various phosphatases. However, these phosphatases can be inhibited by lithium, which stabilises the isomers. This principle was exploited to measure the amount of inositol phosphates released in vsmc in response to 20% stretch. The inositol lipid pool was prelabelled with [^{3}H]-myo-inositol before the stretch was applied and the release of ^{3}H inositol phosphates measured.

From Figure 26, one can see that 20% stretch induced a 3.2 fold increase in inositol phosphate production, which was greater than the 2.3 fold increase observed for the growth factor ANG II. 10% FCS which was included as a positive control produced a 7.7-fold increase. The response to ANG II was of the same order to the 1.8 fold increase previously observed by our group[36]. This study had shown that both a growth factor and mechanical stretch could stimulate phosphoinositide turnover, an important early signalling event in many cellular processes, and that this possibly occurred via similar mechanisms.

In vivo, both hemodynamic and non-hemodnamic factors will coexist. Therefore, it will be of great interest to study the effect of stretch in combination with that of ANG II to reproduce this situation. Future work will also investigate the effect of stretch on inositol phosphate production in endothelial cells as well as determine the effect of different amounts of stretch on phosphoinositide turnover in both vsmc and endothelial cells.

5.7 Summary of proto-oncogene and phosphoinositide turnover studies

From the vsmc studies, it appears that mechanical stretch can produce changes in *c-fos* mRNA expression and inositol phosphate release,

typical of a growth factor, such as ANG II. However, this study found no evidence that mechanical stretch could stimulate *c-jun* and *c-myc* mRNA expression in vsmc. In contrast, endothelial cells increased both *c-fos* and *c-jun* mRNA expression when stretched; *c-myc* was not studied.

Mechanical stretch and the growth factor ANG II can both stimulate the hydrolysis of PIP_2, an important transmembrane signalling event known to be coupled to growth factor receptors [55]. This hydrolysis results in the production of the second messenger IP_3 responsible for the release of Ca^{2+} from intracellular stores. As shown in Figure 5, DAG is also a product of this hydrolysis which leads to the activation of the downstream regulatory enzyme PKC. PKC can then stimulate the expression of proto-oncogenes.

This study confirmed that both ANG II and mechanical stretch could stimulate *c-fos* mRNA expression in vsmc. ANG II also induced expression of *c-jun* and *c-myc* mRNA in vsmc, but mechanical stretch did not stimulate the expression of either of these proto-oncogenes. Therefore both early and later signalling events known to be involved in cell proliferation were shown to be stimulated via the growth factor action of ANG II or by mechanical stretch, in vsmc.

Although the ability of ANG II to stimulate proto-oncogene expression in endothelial cells was not investigated in this study, mechanical stretch was also shown to stimulate early signalling events in endothelial cells.

5.8 Vsmc growth

The process of vascular growth can arise as a result of hypertrophy, and/or hyperplasia or remodelling of the vasculature (section 1.2). Therefore, to further examine the role of mechanical stretch in this process, its effect on vsmc growth rate was investigated. The effect of stretching vsmc on growth rate was determined by the simple expedient of estimating vsmc numbers in control and stretched cells. Stretching by 20% for 1, 2, or 3 days caused no significant increase in cell numbers compared with control. Of considerable practical value, no more cells were released into the supernatant medium in stretched than unstretched preparations. This indicates that the fibronectin-coated silicone sheeting provides a good substrate for cell growth and adhesion

(Figure 28).

Although *c-fos* mRNA expression and phosphoinositide turnover were stimulated in vsmc in response to mechanical stretch, under the conditions used in this study, vsmc growth was increased but not statistically significant. It is possible to suggest that the inability of mechanical stretch to stimulate *c-jun* mRNA expression and thus activate the AP-1 transcription factor may be partially responsible for this effect.

A range of results have been observed when the rate of cell growth in response to mechanical stretch has been studied which largely depends on whether the cells are receiving a fixed stretch or a cyclic stretch, the cell type being studied, the system used to stretch the cells, the amount by which they are stretched and the time interval over which they are stretched. None of the following studies can be directly compared with my study because of the difference in experimental conditions.

Previous studies which looked at the effect of mechanical stretch on growth rate observed a variety of results. Brunette et al. [184] observed an increase in DNA synthesis in epithelial cells which received a fixed stretch of 4.2% and Sumpio et al. [186] observed a decrease in smc number and a decrease in DNA synthesis in response to a 24% cyclic strain over 7 days. However, Liu et al. [187] exposed fetal rat lung cells to 48h of an intermittent stretch pattern of 5% elongation, 60 stretches/min, for 15 min of each hour and observed both an increase in DNA synthesis and a 10% increase in cell number.

5.9 The relevance of a fixed stretch

The cell stretching system which was designed produced a single fixed stretch. The fact that this stimulated second messenger system activity is very encouraging evidence that hemodynamic factors play an important role in the development of vascular hypertrophy. Under pathological conditions, mechanical forces will cause the cells of the vessel wall to experience multiple stretch regimens of varied frequency and duration. In such situations, an amplified effect on second messenger events might be expected. Perhaps a single stretch is not sufficient stimulus to induce any significant difference in expression of the proto-oncogenes *c-jun* and *c-myc* , or to significantly affect the rate of vsmc growth. However, it is reasonable to begin by studying a single stretching event because the

mechanical forces experienced *in vivo* are in fact multiple single stretching events. Moreover, a single fixed stretch did stimulate *c-fos* mRNA expresion and phosphoinositide turnover in vsmc. Studying a single fixed stretch also allows decision as to whether the initial single stretching force experienced by the vessel triggers cell signalling mechanisms or whether continuous stretching is responsible for this effect.

5.10 Pulsatile system

To further investigate the effect of a mechanical load on signalling mechanisms involved in cell proliferation, a pulsatile system has been developed. The first proto-type of the pulsatile system is shown in Plate 21. The cell stretching apparatus is connected to a motor which displaces the handle of the stretching apparatus over a variable frequency of 0-60 cycles/min. Its performance is being assessed at present. Important factors which are to be checked is whether the silicone sheeting can withstand multiple stretches because this could introduce creasing of the silicone. The behaviour of the cells grown on the silicone, in response to a pulsatile force will also be studied.

5.11 Overall conclusions

The achievements of this project were the development an *in vitro* cell stretching system capable of mimicking the hemodynamic forces to which cells are exposed in the vessel wall and the preliminary investigation of the effect of mechanical forces on second messenger signalling events involved in cell proliferation. The final working model of the system satisfied the requirements of such a system and produced useful information on the biochemical and cell physiological effects of mechanical stretch. A single fixed stretch induced specific proto-oncogene expression in both vsmc and endothelial cells and stimulated PIP_2 hydrolysis in vsmc. The parallel experiments involved with the growth factor ANG II showed that mechanical stretch and ANG II had similar effects on these second messenger events. Differences observed between growth factor action and hemodynamic factors may be resolved

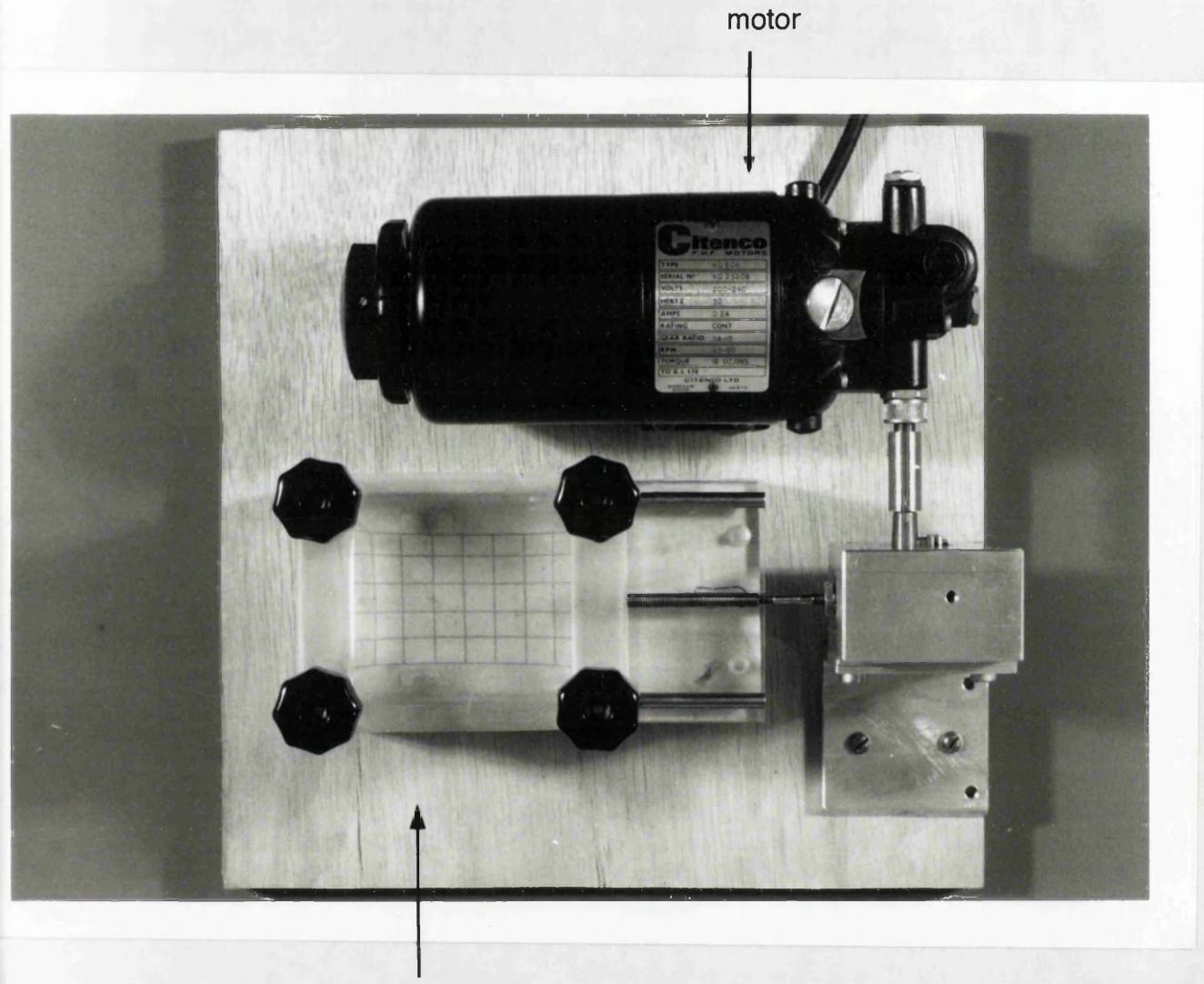

Plate 21. Pulsatile stretching system

by looking at a cyclical stretch in preference to a fixed stretch and this is the direction in which this work should proceed.

CHAPTER SIX

REFERENCES

(1) Bowman WC & Rand MJ. Textbook of pharmacology. 2nd ed. Blackwell Scientific publications, 1988.

(2) Ylitalo P, Vapaatao H, Metsa-Ketela T, Pitkajarvi T. Dependence of plasma renin activity on prostaglandin excretion in essential hypertension. Acta Physiol Scand 1978; 102(1): 120-22.

(3) Batumen V. Lead nephropathy, gout, and hypertension. Am J Med Sci 1993; 305(4): 241-47.

(4) Singh RB, Mori H. Risk factors for coronary heart disease: synthesis of a new hypothesis through adaptation. Med Hypotheses 1992; 39(4): 334-41.

(5) Krieger JE, Dzau VJ. Molecular biology of hypertension. Hypertension 1991; 18 (suppl I): I3-I17.

(6) Meerson FZ. The myocardium in hyperfunction, hypertrophy and heart failure. Circ Res 1969; 25 (suppl II): II 1-163

(7) Linzbach AJ. Heart failure from the point of view of quantitative anatomy. Am J Cardiol 1960; 5: 370-82.

(8) Frohlich ED, Chobanian AV, Devereux RB, et al. The heart in hypertension. New Eng J Med 1992; 14: 998-1008.

(9) Wolinsky H. Response of the rat aortic media to hypertension. Morphological and chemical studies. Circ Res 1970; 26: 507-22.

(10) Weiner H. Lessons taught by experimental high blood pressure research [editorial]. Psychosom Med 1976; 38(5): 297-99.

(11) Fernandez D, Crane WA. New cell formation in rats with accelerated hypertension due to partial aortic constriction. J Path 1970; 100: 307-16.

(12) Bevan RD, van Marthens E, Bevan JA. Hyperplasia of vascular smooth muscle in experimental hypertension in the rabbit. Circ Res 1976; 38 (suppl II): II 58-62.

(13) Mulvany MJ, Hansen PK, Aalkjaer C. Direct evidence that the greater contractility of resistance vessels in spontaneously hypertensive rats is associated with a narrow lumen, a thickened media, and an increased number of smooth muscle cell layers. Circ Res 1978; 43: 854-64.

(14) Owens GK, Schwartz SM. Alterations in vascular smooth muscle mass in the spontaneously hypertensive rat. Circ Res 1982; 51: 280-289.

(15) Warshaw DM, Mulvany MJ, Halpern W. Mechanical and morphological properties of arterial resistance vessels in young and old spontaneously hypertensive rats. Circ Res 1979; 45: 250-59.

(16) Yamori Y, Igawa T, Kanbe T, Nara Y, Tagami M. Enhanced growth rate of cultured smooth muscle cells from spontaneously hypertensive rats. Heart-vessels 1988; 4 (2): 94-99.

(17) Nissen R, Cardinale GJ, Undenfriend S. Increased turnover of arterial collagen in hypertensive rats. Proc Natl Acad Sci USA 1978; 75(1):451-53.

(18) Brayden JE, Halpern W, Brann LR. Biochemical and mechanical properties of resistance arteries from normotensive and hypertensive rats. Hypertension 1983; 5: 17-25.

(19) Mulvany MJ. Determinants of vascular hemodynamic characteristics. Hypertension 1984; 6 (suppl III): III 13-18.

(20) Mulvany MJ. Vascular growth in hypertension. J Cardiovasc Pharmacol 1992; 20 (suppl 1): S7-11.

(21) Folkow B. Vascular changes in hypertension - a review and recent animal studies. In: Berglund G, Hansson L and Werkö (eds.),

Pathophysiology and Management of Arterial Hypertension. L Lidgren and Söner, Mölndal, Sweden 1975; 95-113.

(22) Lever AF, Beattie E, Brown W, et al. Effects of angiotensin II, growth factors and inhibitors of the renin-angiotensin system on arterial pressure and cardiovascular structure. J Hypertens 1986; 4: 515-24.

(23) Mulvany MJ. Editorial review. The fourth Sir George Pickering memorial lecture: The structure of the resistance vasculature in essential hypertension. J Hypertens 1987; 5: 129-36.

(24) Greenberg S, Curro FA. Venous smooth muscle function during the development of genetic hypertension. Bibl Anat 1977;16 (Part II): 304-306.

(25) Takeshita A, Mark AL, Eckberg DL, Abboud FM. Effect of central venous pressure on arterial baroreflex control of heart rate. Am J Physiol 1979; 236(1): H42-47.

(26) Nilsson H, Folkow B. Structurally reduced compliance of the venous capacitance vessels in SHR. Acta Physiol Scand 1980; 110 (2): 215-217.

(27) Safar ME, London GM. Venous system in essential hypertension. Clin Sci 1985; 69 (5): 497-504.

(28) Nordborg C, Johansson BB. The ratio between thickness of media and internal radius in cerebral, mesenteric and renal arterial vessels in SHR. Clin Sci 1979; 57: 27S-29S.

(29) Yamori Y, Horie R, Tanase H, et al. Possible role of nutritional factors in the incidence of cerebral lesions in stroke- prone spontaneously hypertensive rats. Hypertension 1984; 6 (1): 49-53.

(30) Lever AF. Slow pressor mechanisms in hypertension: A role for hypertrophy of resistance vessels. J Hypertens 1986; 4: 515-24.

(31) Dusing R, Gobel B, Weisser B, Dittrich D, Kraemer S, Vetter H. Mechanism and significance of arteriolar media hypertrophy/

hyperplasia in arterial hypertension. Role of the Na^+/H^+ antiport. Klin Wochenschr 1988; 66 (23): 1151-59.

(32) Campbell-Boswell M, Robertson AL. Effects of angiotensin II and vasopressin on human smooth muscle cells *in vitro*. Exp Mol Pathol 1981; 32: 265-76.

(33) Lyall F, Morton JJ, Lever AF, Cragoe EJ. Angiotensin II activates Na^+/H^+ exchange and stimulates growth in cultured vascular smooth muscle cells. J Hypertens 1988: 6 (suppl IV): S438-41.

(34) Naftilan AJ, Pratt RE, Dzau VJ. Induction of platelet-derived growth factor A-chain and *c-myc* gene expressions by angiotensin II in cultured rat vascular smooth muscle cells. J Clin Invest 1989; 83: 1419-24.

(35) Naftilan AJ, Pratt RE, Eldridge CS, Lin HL, Dzau VJ. Angiotensin II induces *c-fos* expression in smooth muscle via transcriptional control. Hypertension 1989; 13: 706-11.

(36) Lyall F, Dornan ES, McQueen J, Boswell F, Kelly M. Angiotensin II increases proto-oncogene expression and phosphoinositide turnover in vascular smooth muscle cells via the angiotensin II AT_1 receptor. J Hypertens 1992; 10: 1463-69.

(37) Naftilan AJ, Gilliland GK, Elsbridge CS, Kraft AS. Induction of the proto-oncogene *c-jun* by angiotensin II. Mol Cell Biol 1990; 10: 5536-40.

(38) Shi Y, Glynn JM, Guilbert LJ, Cotter TG, Bissonnette RP, Green DR. Role for *c-myc* in activation-induced apoptotic cell death in T cell hybridomas. Science 1992; 257 (5067): 212-14.

(39) Askew DS, Ashmun RA, Simmons BC, Cleveland JL. Constitutive *c-myc* expression in an IL-3-dependent myeloid cell line suppresses cell cycle arrest and accelerates apoptosis. Oncogene 1991; 6 (10): 1915-22.

(40) Landschulz WH, Johnson PF, McKnight SL. The leucine zipper: a hypothetical structure common to a new class of DNA binding proteins. Science 1988; 240: 1759-64.

(41) Angel P, Imagawa M, Chiu R, et al. Phorbol ester-inducible genes contain a common *cis* element recognised by a TPA-modulated *trans* -acting factor. Cell 1987; 49: 729-39.

(42) Lee W, Mitchell P, Tjian R. Purified transcription factor AP-1 interacts with TPA-inducible enhancer elements. Cell 1987; 49: 741-52.

(43) Bohmann D, Bos TJ, Admon A, Nishimura T, Vogt PK, Tjian R. Human proto-oncogene *c-jun* encodes a DNA binding protein with structural and functional properties of transcription factor AP-1. Science 1987; 238: 1386-92.

(44) Lamph WW, Wamsley P, Sassone-Corsi P, Verma IM. Induction of proto-oncogene JUN/AP-1 by serum and TPA. Nature 1988; 334: 629-31.

(45) Marcu KB. Regulation of expression of the *c-myc* proto-oncogene. Bioessays 1987; 6: 28-32.

(46) Coppola JA, Cole MD. Constitutive *c-myc* oncogene expression blocks mouse erythroleukemia cell differentiation but not commitment. Nature 1986; 320: 760-63.

(47) Komuro I, Kurabayashi M, Takaku F, Yazaki Y. Expression of cellular oncogenes in the myocardium during the developmental stage and pressure-overloaded hypertrophy of the rat heart. Circ Res 1988; 62: 1075-79.

(48) Jackson T, Allard MF, Sreenan CM, Doss LK, Bishop SP, Swain JL. The *c-myc* proto-oncogene regulates cardiac development in transgenic mice. Mol Cell Biol 1990; 10: 3709-16.

(49) Freeman RS, Donoghue DJ. Protein kinases and proto-oncogenes: Biochemical regulators of the eukaryotic cell cycle. Biochemistry 1991; 30: 2293-302.

(50) Yamashita T, Yamamoto K, Kikuchi A, et al. Purification and characterisation of c-Ki-ras p21 from bovine brain crude membranes. J Biol Chem 1988; 263 (32): 17181-8.

(51) Claycomb WC, Lanson NA Jr. Proto-oncogene expression in proliferating and differentiating cardiac and skeletal muscle. Biochem J 1987; 247: 701-6.

(52) Ross R. Platelet-derived growth factor. Lancet 1989; 1 (8648): 1179-82.

(53) Macara IG. Oncogenes and cellular signal transduction. Physiol Rev 1989; 69: 797-820.

(54) Hunter T. A thousand and one protein kinases. Cell 1987; 50: 823-829.

(55) Liscovitch M. Crosstalk among multiple signal-activated phospholipases. TIBS 1992; 17: 393-98.

(56) Exton JH. Signalling through phosphatidylcholine breakdown. J Biol Chem 1990; 265: 1-4.

(57) Billah MM, Anthes JC. The regulation and cellular functions of phosphatidylcholine hydrolysis. Biochem J 1990; 269: 281-91.

(58) Asaoka Y, Nakamura S, Yoshida K, Nishizuka Y. Protein kinase C, calcium and phospholipid degradation. TIBS 1992; 17: 414-17.

(59) Angel P, Karin M. The role of Jun, Fos and the AP-1 complex in cell-proliferation and transformation. Biochim Biophys Acta 1991; 1072 (2-3): 129-57.

(60) Paul M, Ganten D. The molecular basis of cardiovascular hypertrophy: the role of the renin-angiotensin system. J Cardiovasc Pharmacol 1992; 19 (suppl 5): S51-8.

(61) Peach MJ. Molecular actions of angiotensin. Biochem Pharmacol 1981; 30: 2745-51.

(62) Vallotton MB. The renin-angiotensin system. Trends Pharmacol Sci 1987; 8: 69-74.

(63) Dzau VJ. Tissue renin-angiotensin system: physiologic and pharmacologic implications. Circulation 1988; 77 (suppl I): I 1-3.

(64) Naruse M, Naruse K, Inagaki T, Inagami T. Immunoreactive renin in the mouse adrenal gland. Localisation in the inner cortical regions. Hypertension 1984; 6: 275-80.

(65) Brecher AS, Shier DN, Dene H, et al. Regulation of adrenal renin messenger ribonucleic acid by dietary sodium chloride. Endocrinology 1989; 124: 2907-13.

(66) Re R, Fallon JT, Dzau V, Quay SC, Haber E. Renin synthesis by canine aortic smooth muscle cells in culture. Life Sci 1981; 30: 99-106.

(67) Lilly LS, Pratt RE, Alexander RW, et al. Renin expression by vascular endothelial cells in culture. Circ Res 1985; 57: 312-18.

(68) Griffin SA, Brown WCB, MacPherson F, et al. Angiotensin II causes vascular hypertrophy in part by a non-pressor mechanism. Hypertension 1991; 17: 626-35.

(69) Owens GK. Influence of blood pressure on development of aortic medial smooth muscle hypertrophy in spontaneously hypertensive rats. Hypertension 1987; 9: 178-87.

(70) Powell JS, Clozel JP, Muller RKM, et al. Inhibitors of angiotensin-converting enzyme prevent myointimal proliferation after vascular injury. Science 1989; 245: 186-88.

(71) Harrap SB, Nicolaci JA, Doyle AE. Persistent effects on blood pressure and renal haemodynamics following chronic angiotensin converting enzyme inhibition with perindopril. Clin Exp Pharmacol Physiol 1986; 13: 753-65.

(72) Berk BC, Vekshtein V, Gordon HM, Tsuda T. Angiotensin II-stimulated protein synthesis in cultured vascular smooth muscle cells. Hypertension 1989; 13: 305-14.

(73) Geisterfer AAT, Peach MJ, Owens GK. Angiotensin II induces hypertrophy, not hyperplasia, of cultured rat aortic smooth muscle cells. Circ Res 1988; 62: 749-56.

(74) Bobik A, Grinpukel S, Little PJ, Grooms A, Jackman G. Angiotensin II and noradrenaline increase PDGF-BB receptors and potentiate PDGF-BB stimulated DNA synthesis in vascular smooth muscle. Biochem Biophys Res Commun 1990; 166: 580-88.

(75) Araki S, Kawahara Y, Kariya K, et al. Stimulation of platelet-derived growth factor-induced DNA synthesis by angiotensin II in rabbit vascular smooth muscle cells. Biochem Biophys Res Commun 1990; 168(1): 350-57.

(76) Griendling KK, Berk BC, Ganz P, Gimbrone MA, Alexander RW. Angiotensin II stimulation of vascular smooth muscle phosphoinositide metabolism. State of the art lecture. Hypertension 1987; 9 (suppl III): III-181-5.

(77) Yanagisawa M, Kurihara H, Kimura S, et al. A novel potent vasoconstrictor peptide produced by vascular endothelial cells. Nature 1988; 332: 411-15.

(78) Shubeita HE, McDonough PM, Harris AN, et al. Endothelin induction of inositol phospholipid hydrolysis, sacromere assembly, and cardiac gene expression in ventricular myocytes. A paracrine mechanism for myocardial cell hypertrophy. J Biol Chem 1990; 265: 20555-62.

(79) Takuwa N, Takuwa Y, Yanagisawa M, Yamashita K, Masaki T. A novel vasoactive peptide endothelin stimulates mitogenesis through inositol lipid turnover in Swiss 3T3 fibroblasts. J Biol Chem 1989; 264: 7856-61.

(80) Muldoon LL, Pribnow D, Rodland KD, Magun BE. Endothelin-1 stimulates DNA synthesis and anchorage-independent growth of Rat-1 fibroblasts through a protein kinase C-dependent mechanism. Cell Regul 1990; 1(4): 379-90.

(81) Lonchampt MO, Goulin J, Pinelis V, Chabrier PE, Braquet P. Effect of endothelin on the proliferation of aortic smooth muscle cells in normotensive and spontaneously hypertensive rats. Arch Mal Coeur Vaiss 1990; 83(8): 1309-11.

(82) Muldoon LL, Rodland KD, Forsythe ML, Magun BE. Stimulation of phosphatidylinositol hydrolysis, diacylglycerol release, and gene expression in response to endothelin, a potent new agonist for fibroblasts and smooth muscle cells. J Biol Chem 1989; 264: 8529-36.

(83) Komuro I, Kurihara M, Sugiyama T, Takaku F, Yazaki Y. Endothelin stimulates *c-fos* and *c-myc* expression and proliferation of vascular smooth muscle cells. FEBS Letts 1988; 238: 249-52.

(84) Dubin D, Pratt RE, Cooke JP, Dzau VJ. Endothelin, a potent vasoconstrictor is a vascular smooth muscle mitogen. J Vasc Med Biol 1989; 1: 150-4.

(85) Bobik A, Grooms A, Millar JA, Mitchell A, Grinpukl S. Growth factor activity of endothelin on vascular smooth muscle. Am J Physiol 1990; 258: C409-15.

(86) Hirata Y, Takagi Y, Fukuda Y, Maruma F. Endothelin is a potent mitogen for rat vascular smooth muscle cells. Atheroscler 1989; 78: 225-8.

(87) Scott-Burden T, Resink TJ, Buhler FR. Enhanced growth and growth factor responsiveness of vascular smooth muscle cells from hypertensive rats. J Cardiovasc Pharmacol 1989; 14 (suppl 6): S16-21.

(88) Harris EI, Millar JA. DNA biosynthetic responses to mitogens in cultured vascular smooth muscle cells (VSMC) from SHR, WKY, GH and N rats {Abstract}. 6th International Symposium on Rats with Spontaneous Hypertension and Related Studies, Lyon, 1989.

(89) Saltis J, Agrotis A, Bobik A. TGF-β_1 potentiates growth factor-stimulated proliferation of vascular smooth muscle cells in genetic hypertension. Am J Physiol 1992; 263: C420-28.

(90) Ko YD, Sachinidis A, Graack GH, et al. Inhibition of angiotensin II and platelet-derived growth factor-induced vascular smooth muscle cell proliferation by calcium entry blockers. Clin Investig 1992; 70(2): 113-17.

(91) Katayose D, Ohe M, Yamauchi K, et al. Increased expression of PDGF A- and B-chain genes in rat lungs with hypoxic pulmonary hypertension. Am J Physiol 1993; 265 (2 Pt 1): L100-6.

(92) Pfeifle B, Ditschuneit HH, Distschuneit H. Binding and biological actions of insulin like growth factors on human arterial smooth muscle cells. Horm Metab Res 1982; 14: 409-14.

(93) Banksota NK, Taub R, Zellner K, Olsen P, King GL. Characterisation of induction of proto-oncogene *c-myc* and cellular growth in human vascular smooth muscle cells by insulin and IGF-1. Diabetes 1989; 38: 123-9.

(94) Cercek B, Fishbein MC, Forrester JS, Helfant RH, Fagin JA. Induction of insulin-like growth factor-I messenger RNA iin rat aorta after balloon denudation. Circ Res 1990; 66(6): 1755-60.

(95) Clemmons DR. Variables controlling the secretion of a somatomedin-like peptide by cultured porcine smooth muscle cells. Circ Res 1985: 56: 418-26.

(96) Murphy LJ, Ghahary A, Chakrabarti S. Insulin regulation of IGF-1 expression in rat aorta. Diabetes 1990; 39: 657-62.

(97) Lever AF, Harrap SB. Essential hypertension: a disorder of growth with origins in childhood? J Hypertens 1992; 10: 101-20.

(98) Sarzani R, Brecher P, Chobanian AV. Growth factor expression in aorta of normotensive and hypertensive rats. J Clin Invest 1989; 83: 1404-8.

(99) Bowen-Pope DF, Majesky MW, Ross R. Growth factors for vascular smooth muscle cells. In: Campbell JH, Campbell GR eds. Vascular smooth muscle in culture. vol 1. Boca Raton, Florida: CRC Press 1987 71-92.

(100) Gospodarowicz D, Ferrara N, Haaparanta T, Neufeld G. Basic fibroblast growth factor: expression in cultured bovine vascular smooth muscle cells. Eur J Cell Biol 1988; 46: 144-51.

(101) Thomas KA. Fibroblast growth factors. FASEB J 1987; 1: 434-40.

(102) Gajdusek CM, Carbon S. Injury-induced release of basic fibroblast growth factor from bovine aortic endothelium. J Cell Physiol 1989; 139: 570-9.

(103) Novak-Hofer I, Thomas G. Epidermal growth factor-mediated activation of an S6-kinase in Swiss mouse 3T3 cells. J Biol Chem 1985; 260: 10314-19.

(104) Scott-Burden T, Resink TJ, Baur U, Burgin M, Buhler FR. Epidermal growth factor responsiveness in smooth muscle cells from hypertensive and normotensive rats. Hypertension 1989; 13: 295-304.

(105) Berk BC, Brock TA, Webb RC, et al. Epidermal growth factor, a vascular smooth muscle mitogen, induces rat aortic contraction. J Clin Invest 1985; 75: 1083-6.

(106) Sporn MB, Roberts AB, Wakefield LM, Assoian RK. Transforming growth factor-beta: biological function and chemical structure. Science 1986; 233: 532-34.

(107) Gronwald RG, Seifert RA, Bowen-Pope DF. Differential regulation of expression of two platelet-derived growth factor receptor subunits by transforming growth factor-beta. J Biol Chem 1989; 264: 8120-5.

(108) Chen JK, Hoshi H, McKeehan WL. Heparin-binding growth factor type one and platelet-derived growth factor are required for the optimal expression of cell surface low density lipoprotein receptor binding activity in human adult arterial smooth muscle cells. In Vitro Cell Dev Biol 1988; 24: 199-204.

(109) Stenmark KR, Orton EC, Reeves JT, et al. Vascular remodelling in neonatal pulmonary hypertension. Role of the smooth muscle cell. Chest 1988; 93: 1275-1335.

(110) de Bold AJ, Borenstein HB, Veres AT, Sonnenberg H. A rapid and potent natriuretic response to intravenous injection of atrial myocardial extract in rats. Life Sci 1981; 28: 89-94.

(111) Currie MG, Geller DM, Cole BR, et al. Bioactive cardiac substance. Potent vasorelaxant activity in mammalian atria. Science 1983; 221: 71-3.

(112) Bloch KD, Seidman JG, Naftilan JD, Fallon JT, Seidman CE. Neonatal atria and ventricles secret atrial natriuretic factor via tissue-specific secretory pathways. Cell 1986; 47: 695-702.

(113) Wei YF, Rodi CP, Day ML, et al. Developmental changes in the rat atriopeptin hormonal system. J Clin Invest 1987; 79: 1325-29.

(114) Saito Y, Nakao K, Arai H, et al. Relationship between ventricular expression of atrial natriuretic peptide gene and hemodynamic parameter in old myocardial infarction. J Cardiovasc Pharmacol 1989; 13 (suppl 6): S1-4.

(115) Drexler H, Hanze J, Finckh M, Lu W, Just H, Lang RE. Atrial natriuretic peptide in a rat model of cardiac failure. Atrial and ventricular mRNA, atrial content, plasma levels, and effect of volume loading. Circulation 1989; 79: 620-33.

(116) Gu J, D'Andrea M, Seethapathy M. Atrial natriuretic peptide and its messenger ribonucleic acid in overloaded and overload-released ventricles of rat. Endocrinology 1989; 125: 2066-74.

(117) Izumo S, Nadal-Ginard B, Mahdavi V. Proto-oncogene induction and reprogramming of cardiac gene expression produced by pressure overload. Proc Natl Acad Sci USA 1988; 85: 339-43.

(118) Matsubara H, Mori Y, Yamamoto J, Inada M. Diabetes-induced alterations in atrial natriuretic peptide gene expression in Wistar-Kyoto and spontaneously hypertensive rats. Circ Res 1990; 67: 803-13.

(119) Montorsi P, Tonolo G, Polonia J, Hepburn D, Richards AM. Correlates of plasma atrial natriuretic factor in health and hypertension. Hypertension 1987; 10: 570-76.

(120) Franco-Saenz R, Somani P, Mulrow PJ. Effect of atrial natriuretic peptide (8-33-Met ANP) in patients with hypertension. Am J Hypertens 1992; 5: 266-75.

(121) MacIver DH, Green NK, Gammage MD, et al. Effect of experimental hypertension on phosphoinositide hydrolysis and proto-oncogene expression in cardiovascular tissues. J Vasc Res 1993; 30: 13-22.

(122) Izzard AS, MacIver DH, Cragoe EJ, Heagerty AM. Intracellular pH in rat resistance arteries during the development of experimental hypertension. Clin Sci 1991; 81: 65-72.

(123) Mulvagh SL, Michael LH, Perryman MB, Roberts R, Schneider MD. A hemodynamic overload *in vivo* induced cardiac expression of the cellular oncogene *c-myc*. Biochem Biophys Res Commun 1987; 147: 627-36.

(124) Izumo S, Lompre A-M, Matsuoka R, et al. Myosin heavy chain messenger RNA and protein isoform transitions during cardiac hypertrophy. Interaction between hemodynamic and thyroid hormone-induced signals. J Clin Invest 1987; 79: 970-77.

(125) Schwartz SM, Campbell GR, Campbell JH. Replication of smooth muscle cells in vascular disease. Circ Res 1986; 58: 427-44.

(126) Schiaffino S, Samuel JL, Sassoon D, et al. Non-synchronous accumulation of alpha-skeletal actin and beta-myosin heavy chain mRNAs during early stages of pressure-overload-induced cardiac hypertrophy demonstrated by *in situ* hybridisation. Circ Res 1989; 64: 937-48.

(127) Imamura S, Matsuoka R, Hiratsuka E, Kimura M, Nishikawa T, Takao A. Local response to cardiac overload on myosin heavy chain gene expression and isozyme transition. Circ Res 1990; 66: 1067-73.

(128) Lansman JB, Hallam TJ, Rink TJ. Single stretch-activated ion channels in vascular endothelial cells as mechanotransducers. Nature 1987; 325: 811-13.

(129) Olesen SP, Chapman DE, Davies PT. Haemodynamic shear stress activates a potassium current in vascular endothelial cells. Nature 1988; 331: 168-70.

(130) Kent RL, Hoober JK, Cooper G. Load responsiveness of protein synthesis in adult mammalian myocardium: Role of cardiac deformation linked to sodium influx. Circ Res 1989; 64: 74-85.

(131) Komuro I, Kaida T, Shibazaki Y, et al. Stretching cardiac myocytes stimulates proto-oncogene expression. J Biol Chem 1990; 265: 3595-98.

(132) Bauters C, Moalic JM, Bercovici J, et al. Coronary flow as a determinant of *c-myc* and *c-fos* proto-oncogene expression in an isolated adult rat heart. J Mol Cell Cardiol 1988; 20: 97-101.

(133) Mann DL, Kent RL, Cooper G. Load regulation of the properties of adult feline cardiocytes: growth induction by cellular deformation. Circ Res 1989; 64: 1079-90.

(134) von Harsdorf R, Lang RE, Fullerton M, Woodcock EA. Myocardial stretch stimulates phosphatidylinositol turnover. Circ Res 1989; 65: 494-501.

(135) Davies PF. How do vascular endothelial cells respond to flow. News Physiolog Sci 1989; 4: 22-5.

(136) Ohno M, Gibbons GF, Lopez F, Cooke JP, Dzau VJ. Shear stress induces transforming growth factor-β1 (TGF-β_1) expression via a flow-activated potassium channel. William Harvey Research Conference 1992: The endothelium in cardiovascular disease.

(137) Reich KM, Frangos JA. Effect of flow on prostaglandin E_2 and inositol trisphosphate levels in osteoblasts. Am J Physiol 1991; 261: C428-432.

(138) Mo M, Eskin SG, Schilling WP. Flow-induced changes in Ca^{2+} signaling of vascular endothelial cells: effect of shear stress and ATP. Am J Physiol 1991; 260: H1698-1707.

(139) Ando J, Ohtsuka A, Korenaga R, Kamiya A. Effect of extracellular ATP level on flow-inuced Ca^{2+} response in cultured vascular endothelial cells. Biochem Biophys Res Commun 1991; 179 (3): 1192-99.

(140) Shen J, Luscinskas FW, Forbes Dewey C, Gimbrone MA. Fluid shear stress modulates cystolic free calcium in vascular endothelial cells. Am J Physiol 1992; 262 : C384-90.

(141) Bodin P, Bailey D, Burnstock G. Increased flow-induced ATP release from isolated vascular endothelial cells but not smooth muscle cells. Br J Pharmacol 1991; 103 (1): 1203-5.

(142) Mitsumata M, Nerem RM, Alexander RW, Berk B. Shear stress inhibits endothelial cell proliferation by growth arrest in the Go/G1 phase of the cell cycle. William Harvey Research Conference 1992: The endothelium in cardiovascular disease.

(143) Levesque MJ, Nerem RM, Sprague EA. Vascular endothelial cell proliferation in culture and the influence of flow. Biomaterials 1990; 11: 702-7.

(144) Hsieh HJ, Li NQ, Frangos JA. Shear stress increases endothelial platelet-derived growth factor mRNA levels. Am J Physiol 1991; 260: H642-6.

(145) Davies PF, Remuzzi A, Gordon EJ, Dewey CF, Gimbrone MA. Turbulent fluid shear stress induces vascular endothelial cell turnover *in vitro*. Proc Natl Acad Sci 1986; 83: 2114-7.

(146) Drenckahn D, Groschel-Stewart U, Kendrick-Jones J, Scholey J. Antibody to thymus myosin: its immunological characterisation and use for immunocytochemical localisation of myosin in vertebrate nonmuscle cells. Eur J Cell Biol 1983; 30: 100-11.

(147) Gabbiani G, Gabbiani F, Lombardi D, Schwartz SM. Organisation of actin cytoskeleton in normal and regenerating arterial endothelial cells. Proc Natl Acad Sci USA 1983; 80: 2361-4.

(148) Franke RP, Grafe M, Schnittler H, Seiffge D, Mittermayer C. Induction of human vascular endothelial stress fibres by fluid shear stress. Nature 1984; 307: 648-9.

(149) Fischel R, Shai S, Norc K, Bernstein K, Berk B. Endothelial cell angiotensin converting enzyme expression is upregulated by fluid shear stress. FASEB J 1991; 5: 5.

(150) Richardson JB. The mechanics of fracture healing. MD Thesis 1989, University of Aberdeen.

(151) Frangos JA, Eskin SG, McIntire LV, Ives CL. Flow effects on prostacyclin production by cultured human endothelial cells. Science 1985; 227: 1477-79.

(152) Frangos JA, Ives CL, Eskin SG, McIntyre LV. Effect of pulsatile flow on prostacyclin production by endothelial cells. FASEB J 1991; 73: 291.

(153) Rubanyi GM, Romero JC, Vanhoutte PM. Flow-induced release of endothelium-derived relaxing factor. Am J Physiol 1986; 250: H1145-49.

(154) Grabowski EF, Jaffe EA, Weksler BB. Prostacyclin production by cultured endothelial cell monolayers exposed to step increases in shear stress. J Lab Clin Med 1985; 105: 36-43.

(155) Sharefkin JB, Diamond SL, Eskin SG, McIntire LV, Dieffenbach CW. Fluid flow decreases preproendothelin mRNA levels and suppresses endothelin-1 peptide release in cultured human endothelial cells. J Vasc Surg 1991; 14: 1-9.

(156) Yoshizumi M, Kurihara H, Sugiyama T, et al. Hemodynamic shear stress stimulates endothelin production by cultured endothelial cells. Biochem Biophys Res Commun 1989; 161: 859-64.

(157) Taylor WR, Harrison DG, Nerem RM, Peterson TE, Alexander RW. Characterisation of the release of endothelium-derived nitrogen oxides by shear stress. FASEB J Abstracts 1991; Part (III): 7879.

(158) Kelm M, Feelisch M, Deussen A, Strauer BE, Schrader J. Release of endothelium derived nitric oxide in relation to pressure and flow. Cardiovasc Res 1991; 25: 831-6.

(159) Buga GM, Gold ME, Fukuto JM, Ignarro LJ. Shear stress-induced release of nitric oxide from endothelial cells grown on beads. Hypertension 1991; 17: 187-93.

(160) Hutcheson IR, Griffith TM. Release of endothelium-derived relaxing factor is modulated both by frequency and amplitude of pulsatile flow. Am J Physiol 1991; 261: H257-62.

(161) Cucina A, Sterpetti AV, Morena AR, Santoro D'Angelo L, Cavallaro A. Shear stress increases the release of IL-1 and L-6 by bovine aortic endothelial cells. William Harvey Research Conference 1992: The endothelium in cardiovascular disease.

(162) Sprague EA, Steinbach BL, Nerem RM, Schwartz CJ. Influence of a laminar steady-state fluid-imposed wall shear stress on the binding, internalisation and degradation of low density lipoproteins by cultured arterial endothelium. Circulation 1987; 76 : 648-56.

(163) Davis MJ, Meininger GA, Zawieja DC. Stretch-induced increases in intracellular calcium of isolated vascular smooth muscle cells. Am J Physiol 1992; 263: H1292-9.

(164) Taniguchi J, Guggino WB. Membrane stretch: a physiological stimulator of Ca^{2+} activated K^{+} channels in thick ascending limb. Am J Physiol 1989; 26: F347-52.

(165) Kirbrer MT, Ordway RW, Clapp LH, Walsh JV, Singer JJ. Both membrane stretch and fatty acids directly activate large conductance Ca^{2+}-activated K^{+} channels in vascular smooth muscle cells. FEBS 1992; 297: 24-8.

(166) Craelius W, El-Sherif N, Palant CE. Stretch-activated ion channels in cultured mesangial cells. Biochem Biophys Res Commun 1989; 159: 516-21.

(167) Ypey DL, Weidema AF, Hold KM, et al. Voltage, calcium and stretch activated ionic channels and intracellular calcium in bone cells. J Bone Min Res 1992; 7(2): S377-87.

(168) Bear C. A nonselective cation channel in rat liver cells is activated by membrane stretch. Am J Physiol 1990; 258: C421-8.

(169) Kulik TJ, Bialecki RA, Colucci WS, Rothman A, Glennon ET, Underwood RH. Stretch increases inositol trisphosphate and inositol tetrakisphosphate in cultured pulmonary vascular smooth muscle cells. Biochem Biophys Res Commun 1991; 180: 982-7.

(170) Komuro I, Katoh Y, Kaida T, et al. Mechanical loading stimulates cell hypertrophy and specific gene expression in cultured rat cardiac myocytes. J Biol Chem 1991; 266 (2): 1265-8.

(171) Rosales OR, Sumpio BE. Changes in cyclic strain increase inositol trisphosphate and diacylglycerol in endothelial cells. Am J Physiol 1992; 262: C956-62.

(172) Brophy CM, Mills I, Rosales O, Isales C, Sumpio BE. Phospholipase C: a putative mechanotransducer for endothelial cell response to acute hemodynamic changes. Biochem Biophys Res Commun 1993: 190; 576-81.

(173) von Harsdorf R, Lang R, Fullerton M, Smith AI, Woodcock EA. Right atrial dilatation increases inositol-(1, 4, 5) trisphosphate accumulation. FEBS Letts 1988; 233: 201-5.

(174) Rosales OR, Shin T, Sumpio BE. Pulsatile stretch induces protein kinase C translocation. FASEB J Abstracts 1991; Part (II): 3749.

(175) Katusic ZS, Shepherd JT, Vanhoutte PM. Endothelium-dependent contraction to stretch in canine basilar arteries. Am J Physiol 1987; 252: H671-73.

(176) Wirtz HRW, Dobbs LG. Calcium mobilisation and exocytosis after one mechanical stretch of lung epithelial cells. Science 1990; 250: 1266-69.

(177) Armstrong RB, Duan C, Delp D, Hayes DA, Glenn GM, Allen GD. Elevations in rat soleus muscle [Ca^{2+}] with passive stretch. J Appl Physiol 1993; 74(6): 2990-7.

(178) Sadoshima J, Jahn L, Takahashi T, Kulik TJ, Izumo S. Molecular characterisation of the stretch-induced adaptation of cultured cardiac cells. J Biol Chem 1992; 267; 15: 10551-60.

(179) Komuro I, Katoh Y, Kaida T, et al: Mechanical loading stimulates cell hypertrophy and specific gene expression in cultured rat cardiac myocytes. J Biol Chem 1991; 266 (2): 1265-68.

(180) Mann DL, Kent RL, Cooper IV G. Load regulation of the properties of adult feline cardiocytes: Growth induction by cellular deformation. Circ Res 1989; 64: 1079-90.

(181) Banes AJ, Gilbert J, Taylor D, Monbureau O. A new vacuum-operated stress-providing instrument that applies static or variable duration cyclic tension or compression to cells *in vitro*. J Cell Sci 1985; 75: 35-42.

(182) Goldspink G, Scutt A, Martindale J, Jaenicke T, Turay L, Gerlach GF. Stretch and force generation induce rapid hypertrophy and myosin isoform gene switching in adult skeletal muscle. Biochem Soc Trans 1991; 19: 368-73.

(183) Hasegawa S, Sato S, Saito S, Suzuki Y, Brunette DM. Mechanical stretching increases the number of cultured bone cells synthesising DNA and alters their pattern of protein synthesis. Calcif Tissue Int 1985; 37: 431-6.

(184) Brunette DM. Mechanical stretching increases the number of epithelial cells synthesising DNA in culture. J Cell Sci 1984; 69: 35-45.

(185) Sumpio BE, Banes AJ. Response of porcine aortic smooth muscle cells to cyclic tensional deformation in culture. J Surg Res 1988; 44: 696-701.

(186) Sumpio BE, Banes AJ, Levin LG, Jonson G. Mechanical stress stimulates aortic endothelial cells to proliferate. J Vasc Surg 1987; 6: 252-6.

(187) Liu M, Skinner SJM, XU J, Han RNN, Tanswell AK, Post M. Stimulation of fetal rat lung cell proliferation in vitro by mechanical stretch. Am J Physiol 1992; 263: L376-83.

(188) Nishioka S, Fukuda K, Tanaka S. Cyclic stretch increases alkaline phosphatase activity of osteoblast-like cells: a role for prostaglandin E_2. Bone and Mineral 1993; 21: 141-50.

(189) Vandenburgh HH, Swasdison S, Karlisch P. Computer-aided mechanogenesis of skeletal muscle organs from single cells *in vitro*. FASEB J 1991; 5: 2860-2867.

(190) Antonio J, Gonyea WJ. Role of muscle fiber hypertrophy and hyperplasia in intermittently stretched avian muscle. J Appl Physiol 1993; 74 (4): 1893-8.

(191) Betz E, Roth J, Schlote W. Proliferation of smooth muscle cells in long-term local electrical stimulation of the carotid arteries. Folia angiol 1980: 28; 27-31.

(192) Dartsch PC, Hammerle H. Orientation response of arterial smooth muscle cells to mechanical stimulation. Eur J Cell Biol 1986; 41: 339-46.

(193) Terracio L, Miller B ,Borg TK. Effects of cyclic mechanical stimulation of the cellular components of the heart: *in vitro* . In Vitro Cell Dev Biol 1988; 24: 53-8.

(194) Samuel JL, Vandenburgh HH. Mechanically induced orientation of adult rat cardiac myocytes *in vitro.* In Vitro 1990; 26: 905-14.

(195) Pender N, McCulloch C. Quantitation of actin polymerisation in two human fibroblast sub-types responding to mechanical stretching. J Cell Sci 1991; 100: 187-93.

(196) Harris RC, Harason MA, Badr KF. Continuous stretch-relaxation in culture alters rat mesangial cell morhology, growth characteristics, and metabolic activity. Lab Invest 1992; 66: 548-54.

(197) Mills I, Letsou G, Rabban J, Sumpio B, Gewirtz H. Mechanosensitive adenylate cyclase activity in coronary vascular smooth muscle cells. Biochem Biophys Res Commun 1990; 171: 143-47.

(198) Letsou GV, Rosales O, Maitz S, Vogt A, Sumpio BE. Stimulation of adenylate cyclase activity in cultured endothelial cells subjected to cyclic stretch. J Cardiovasc Surg 1990; 31: 634-9.

(199) Iba T, Mills I, Sumpio BE. Intracellular cyclic AMP levels in endothelial cells subjected to cyclic strain *in vitro.* J Surg Res 1992; 52: 625-30.

(200) Upchurch GR, Banes AJ, Wagner WH, et al. Differences in secretion of prostacyclin by venous and arterial endothelial cells grown *in vitro* in a static versus a mechanically active environment. J Vasc Surg 1989; 10: 292-8.

(201) Sumpio BE, Banes AJ. Prostacyclin synthetic activity in cultured aortic endothelial cells undergoing cyclic mechanical deformation. Surgery 1988; 104: 383-9.

(202) Carosi JA, Eskin SG, Mcintire LV. Cyclical strain effects on production of vasoactive materials in cultured endothelial cells. J Cell Physiol 1992; 151: 29-36.

(203) Vandenburgh HH, Hatfaludy S, Sohar I, Shansky J. Stretch-induced prostaglandins and protein turnover in cultured skeletal muscle. Am J Physiol 1990; 259: C232-40.

(204) Sumpio BE. Molecular biology of the vascular system: fundamental concepts and the tools. J Vasc Surg 1992; 15(5): 906-907.

(205) Harder DR, Sanchez-Ferrer C, Kauser K, Stekiel WJ, Rubanyi GM. Pressure releases a transferable endothelial contractile factor in cat cerebral arteries. Circ Res 1989; 65: 193-8.

(206) Ohno M, Ochiai M, Taguchi J, et al. Stretch may enhance the release of endothelium-derived relaxing factor in rabbit aorta. Biochem Biophys Res Commun 1990; 173: 1038-42.

(207) Hishikawa K, Nakaki T, Suzuki H, Saruta T, Kato R. Transmural pressure inhibits nitric oxide release from human endothelial cells. Eur J Pharmacol 1992; 215: 329-31.

(208) Iba T, Shin T, Sonoda T, Rosales O, Sumpio BE. Stimulation of endothelial secretion of tissue-type plasminogen activator by repetitive stretch. J Surg Res 1991; 50: 457-60.

(209) Sumpio BE, Banes AJ, Link WG, Johnson G. Enhanced collagen production by smooth muscle cells during repetitive mechanical stretching. Arch Surg 1988; 123: 1233-6.

(210) Sumpio BE, Banes AJ, Link GW, Iba T. Modulation of endothelial cell phenotype by cyclic stretch: inhibition of collagen production. J Surg Res 1990; 48: 415-20.

(211) Riser BL, Cortes P, Zhao X, Bernstein J, Dumler F, Narins RG. Intraglomerular pressure and mesangial stretching stimulate extracellular matrix formation in the rat. J Clin Invest 1992; 90: 1932-43.

(212) Leung DYM, Seymour G, Mathews MB. Cyclic stretching stimulates synthesis of matrix components by arterial smooth muscle cells *in vitro*. Science 1976; 191: 475-7.

(213) Sottiurai VS, Kollros P, Seymour G, Zarins CK, Matthews MB. Morphologic alteration of cultured arterial smooth muscle cells by cyclic stretching. J Surg Res 1983; 35: 490-7.

(214) Wang N, Butler JP, Ingber DE. Mechanotransduction across the cell surface and through the cytoskeleton. Science 1993; 260: 1124-27.

(215) Gardner DG, Wirtz H, Dobbs LG. Stretch-dependent regulation of atrial peptide synthesis and secretion in cultured atrial cardiocytes. Am J Physiol 1992; 263: E239-44.

(216) Page E, Goings GE, Power B, Upshaw-Earley J. Basal and stretch-augmented natriuretic peptide secretion by quiescent rat atria. Am J Physiol 1990; 28: C801-18.

(217) Schiebinger RJ, Greening KM. Interaction between stretch and hormonally stimulated atrial natriuretic peptide secretion. Am J Physiol 1992; 262: H78-83.

(218) Kinnunen P, Vuolteenaho O, Uusimaa P, Ruskoaho H. Passive mechanical stretch releases atrial natriuretic peptide from rat ventricular myocardium. Circ Res 1992; 70: 1244-1253.

(219) Newman TM, Severs NJ. Stretch and anesthetic dependency of atrial natriuretic peptide release demonstrated by an ultrastructural assay. J Cell Physiol 1993; 155: 240-7.

(220) Vandenburgh HH, Hatfauldy S, Karlisch P, Shansky J. Skeletal muscle growth is stimulated by intermittent stretch-relaxation in tissue culture. Am J Physiol 1989; 256: C674-C682.

(221) Hatfauldy S, Shansky J, Vandenburgh HH. Metabolic alterations induced in cultured skeletal muscle by stretch-relaxation activity. Am J Physiol 1989; 256: C175-C81.

(222) Daifotis AG, Weir EC, Dreyer BE, Broadus AE. Stretch-induced parathyroid hormone-related peptide gene expression in the rat uterus. J Biol Chem 1992; 267: 23455-8.

(223) Yamamoto M, Harm SC, Grasser WA, Thiede MA. Parathyroid hormone-related protein in the rat urinary bladder: A smooth muscle relaxant produced locally in response to mechanical stretch. Proc Natl Acad Sci USA 1992; 89: 5326-30.

(224) Stacy GP, Jobe RL, Taylor K, Hansen DE. Stretch-induced depolarisations as a trigger of arrhythmias in isolated canine left ventricles. Am J Physiol 1992; 263: H613-21.

(225) Franz MR, Cima R, Wang D, Profitt D, Kurz R. Electrophysiological effects of myocardial stretch and mechanical determinants of stretch-activated arrythmias. Circulation 1992; 86: 968-78.

(226) Berridge MJ, Downes CP, Hanley MR. Lithium amplifies agonist-dependent phosphatidylinositol responses in brain and salivary glands. Biochem J 1982; 206: 587-95.

(227) Curran T, Peters G, van Beveren C, Teich NM, Verma IM. FBJ Murine Osteosarcoma virus: Identification and molecular cloning of biologically active proviral DNA. J Virol 1982; 44(2): 674-82.

(228) Hayashi K, Makino R, Kawamura H, Arisawa A, Yoneda K. Characterisation of rat *c-myc* and adjacent regions. Nucleic Acid Res 1987; 15: 6419-36.

(229) Angel P, Allegretto EA, Okino ST, et al. Oncogene *jun* encodes a sequence-specific *trans* -activator similar to AP-1. Nature 1988; 332: 166-71.

(230) Hebert MT, Marshall JM. Direct observations of effects of baroreceptor stimulation on mesenteric circulation of the rat. J Physiol 1988; 400: 29-44.

(231) Schunkert H, Jahn L, Izumo S, Apstein CS, Lorell BH. Localisation and regulation of *c-fos* and *c-jun* proto-oncogene induction by systolic wall stress in normal and hypertrophied rat hearts. Proc Natl Acad Sci USA 1991; 88: 11480-84.

(232) Mollinendo F, Vaquerizo MJ, Naranjo JR. Expression of *c-jun*, *jun B* and *jun D* proto-oncogenes in human peripheral-blood granulocytes. Biochem J 1991; 273: 477-79.

(233) Viard I, Hall SH, Jaillard C, Berthelon MC. Regulation of *c-fos*, *c-jun* and *jun-B* messenger ribonucleic acids by angiotensin II and corticotrophinin ovine and bovine adrenocortical cells. Endocrinology 1992; 130: 1193-1200.

(234) Kawahara Y, Sunako M, Tsuda T, et al. Angiotensin II induces expression of the *c-fos* gene through protein kinase C activation and calcium ion mobilisation in cultured vascular smooth muscle cells. Biochem Biophys Res Commun 1988; 150: 52-9.

(235) Taubman MB, Berk BC, Izumo S, et al. Angiotensin II induces *c-fos* mRNA in aortic smooth muscle. J Biol Chem 1989; 264: 526-30.

(236) Mulvany MJ. Determinants of vascular hemodynamic characteristics. Hypertens 1984; 6: [suppl III]: III13-18.

(237) Mulvany MJ, AAlkjaer C. Structure and function of small arteries. Physiol Rev 1990; 70: 921-61.

PUBLICATION LIST

(1) Lyall F, Dornan ES, McQueen J, Boswell F, Kelly M. Angiotensin II increases proto-oncogene expression and phosphoinositide turnover in vascular smooth muscle cells via the angiotensin II AT_1 receptor. J Hypertens 1992; 10: 1463-69.

(2) Lyall F, Deehan MR. Effects of pressure overload on vascular smooth muscle cells. Biomechanics and cells; Society for experimental biology seminar series 54, Cambridge University Press 1994, Lyall F, El Haj AJ (eds),: 23-36.

(3) Lyall F, Deehan MR, Greer IA, Boswell F, Brown WC, McInnes GT. Mechanical stretch increases proto-oncogene expression and phosphoinositide turnover in vascular smooth muscle cells. J Hypertens 1994; in press.

GLASGOW UNIVERSITY LIBRARY